FOURTH QUARTERLY REPORT

LANDSAT II INVESTIGATION PROGRAMME

No. 28230

N77-20536

REPORT NO. 568   MARCH 1977

Goddard

PHYSICS AND ENGINEERING LABORATORY

DSIR

NEW ZEALAND

FOURTH QUARTERLY REPORT

LANDSAT II INVESTIGATION PROGRAMME

No. 28230

N77-20536

REPORT NO. 568   MARCH 1977

Principal Investigator:

    Dr Mervyn C. Probine   (Programme No. 28230)

Co-Investigators:

    Dr Richard P. Suggate   (Programme No. 2823A)

    Mr Michael G. McGreevy   (Programme No. 2823B)

    Mr Ian   F. Stirling   (Programme No. 2823C)

CONTENTS

This is the penultimate report of the present contract.
It is therefore pleasing to see the increasing maturity of the
programme showing through in the number of studies that are
complete, or almost complete. Furthermore, it is pleasing to
note that the number of active participants, and institutions,
is continuing to increase as the potential of the technology
becomes better known, and more widely appreciated.

However, the programme has not been without its problems.
To the best of our knowledge no imagery has been acquired over
New Zealand since the end of May 1976. During the 1976/77 New
Zealand summer there was an unusually extensive and continuous
cloud cover which, in many cases, coincided with the times of
satellite passes. Failure to acquire imagery, for this reason,
has been disappointing for many reasons; but it has been
particularly damaging in two specific areas:

1. A major wheat survey to be undertaken for the
    Department of Agriculture has produced no
    satellite results in spite of intensive "ground
    truth" preparations.

2. We have so far not obtained complete satellite
    coverage of the country, and we therefore lack
    the images to complete the mapping programme.

I understand that heavy demand for imagery, coupled with the
failure of one "on board" recorder, is making it difficult for
NASA to provide further imagery over this country. However, in
the short time remaining before the completion of this contract,
I would urge that further effort be made to provide as much
imagery as climatic conditions will allow. A suggestion for more
reliable selection of "cloud free" conditions is made on page 72
of the report.

The organisation of this presentation follows the pattern
of past reports. Investigations aimed at developing the
technology of remote sensing are detailed in Part I; and
investigations relating to specific applications by user groups
are detailed in Parts II to VII.

In Part I there is a very full report by the PEL Remote
Sensing Group on the effect of the atmosphere on spectral
signatures. Dr Michael Duggin of the CSIRO, Australia, was a
collaborator in this programme. There are also significant new
results on an image rectification method suitable for small
computers, and work on ship detection using LANDSAT imagery (which,
so far as we know, breaks completely new ground). Applications also
described include forest inventory studies, snow field assessment,
initial work on crop stress analysis, and new work on applications
of tidal estuary investigations.

In Parts II to IV the continuing programmes of the Co-investigators are outlined; and, in addition, Parts V to VII contain descriptions of specific new programmes which have developed out of the main programme. These include, in Part V, forest service investigations on windthrow in forests, classification of forest types, mapping of snow areas, and fire damage monitoring in forests; in Part VI the use of imagery for mapping vegetation and landform is described by the Ministry of Works and Development; and, finally, in Part VII Professor Ross Cochrane describes further work by his department on applications to land use studies.

Interest in off-shore monitoring from satellites has been stimulated by both Dr Ellis's visit to NASA late last year, and by the New Zealand Prime Minister's recent announcement that this country will declare a 200 mile economic management zone around our shores later this year.

The increasing interest in the LANDSAT series of satellites, and the growing realisation of the potential of the SEASAT series, is bringing the decision closer on whether we should, or should not, purchase the facilities for "real time" local reception of satellite imagery.

Once again it is a pleasure to record our thanks to our NASA colleagues for continued help and co-operation. In the face of all of the help we have received so far, it is somewhat embarrassing to have to request further assistance. However, additional imagery to fill the gap in coverage from May 1976 to March 1977, is a very pressing need. In defence of this further request, I can only plead that it would be a pity to terminate the contract with incomplete coverage of the country and point to the fact (as is revealed in this report) that imagery acquired so far is being used to good effect by the New Zealand team.

Dr Mervyn C. Probine
Principal Investigator

and

Assistant Director-General, DSIR

21 March 1977

4

PART I

DEVELOPMENT OF REMOTE SENSING TECHNOLOGY

IN NEW ZEALAND

Investigation No.:   28230

Principal Investigator: Dr Mervyn C. Probine

Agency: Physics and Engineering Laboratory
                            Department of Scientific and
                                Industrial Research

Address: Private Bag
                            Lower Hutt
                            New Zealand

Telephone No.:   Wellington 666-919

Authors: Dr P.J. Ellis
                            Dr M.J. McDonnell
                            Dr I.L. Thomas
                            Mr A.D. Fowler

                            Dr A.J. Lewis   (Research Visitor -
                                                   Louisiana, U.S.A.)

                            Dr M.J. Duggin   (Division of Mineral
                                                   Physics, CSIRO,
                                                   Australia)

                            Mr N.   Ching   (New Zealand Forest
                                                   Service)

                            Mr C.T. Nankivell   (Technical Trainee)

CONTENTS

CONTENTS (Cntd)

1. INTRODUCTION

By arrangement with NASA, the publication of this report has been delayed by three months to cover the New Zealand summer period, which is normally the most favourable period for satellite and aircraft data acquisition. During this time, a major project for the remote sensing section was to have been an attempt to survey the cereal crops of mid-Canterbury from LANDSAT imagery. To this end, ground truth surveys of Leeston, Southbridge and Darfield areas were made, covering over four hundred fields with information of crop type, variety, soil conditions and treatment.

Unfortunately, no images of any part of New Zealand have been acquired, to our knowledge, since 31 May 1976. The problem seems to have been largely caused by a year of exceptionally high cloud cover, which on many occasions was synchronised with the satellite overpasses. The high rainfall resulted in very good cereal crop, which was harvested at least a month later than normal. The only imagery acquired before harvest was a multispectral aircraft survey (Section 2.2).

Most of the topics in this report are therefore related to LANDSAT imagery acquired before May 1976. It is now planned to conduct a retrospective ground truth survey of the extended test areas, to correlate with LANDSAT images taken in August and October 1975. Resulting from a visit to the EROS Data Centre (PJE), a variety of enhanced images of the October scene are available, processed by the "Image 100" interactive analyser. Some preliminary work with these images is discussed in Section 3.5 (ILT).

Other projects, such as the Eyrewell windthrow analysis, continue from work described in the previous reports. The tendency is for the "user" group to take over the interpretative phase of these projects, and the report on Eyrewell is to be found in the contribution from the New Zealand Forest Service (Part V).

Technique development at P.E.L. continues with emphasis on CCT processing. Programs are now available to users on one of the national networks (Section 2.4 ILT), and a complete package of geometric correction programs is being completed using the P.E.L. in-house facility (Section 2.5 MMcD). A scanning microdensitometer should be completed very shortly to enable aircraft imagery to be digitised and processed by computer.

The Water and Soil Division of the Ministry of Works and Development has appointed a full-time co-ordinator for its remote sensing activities, Douglas Hicks, whose contribution appears in part VI. A close liaison has already been established with the P.E.L. section, and we look forward to a continuing and fruitful collaboration. The main contributor from the Department of Lands and Survey, Douglas McK. Scott, has returned to Scotland, and we welcome Bob Child, who is now the co-ordinator for that Department.

New Zealand has a long coastline and an extensive offshore region. Both of these are becoming increasing subjects of study. The Pauatahanui inlet survey (Section 3.6) is one of a series of intensive studies of estuarine areas being conducted or planned.

Interest in offshore monitoring from satellites has recently been stimulated by discussions with NASA personnel in Washington, Goddard Space Flight Centre and Pasadena (PJE). (PEL Overseas Visit Report No. 72.) As a result, the P.E.L. group decided to see if the resolution of LANDSAT images permitted objects such as ships to be detected, using CCT data. The success of this experiment is detailed in Section 3.2 (MMcD and AJL).

It is becoming increasingly evident that future use of "operational" satellite imagery in New Zealand will depend on the ready availability and frequency of the data, and this in turn implies "real time" reception from a local satellite receiving station. The total lack of LANDSAT II imagery over the last year has served to emphasise the situation, although this absence of data can be used to make a case against the use of satellites, and in favour of a "reliable" in-house system based on aircraft. For this reason we feel that every effort should be made to improve the flow of data from LANDSAT, if its cost-effectiveness is to be demonstrated in this country, and the case for direct reception is to be convincingly made.

To try to alleviate this problem, some suggestions concerning cloud-cover criteria and satellite scheduling are made in Section 5.1.

2. TECHNIQUES

2.1 Photographic Processing

Methods described in previous reports continue to be used to provide imagery for Co-investigators and other user groups. Much of this work involves the colour compositing of 70 mm LANDSAT products in the colour additive viewer. With the advent of the new laser generated 1:1,000,000 scale transparencies from EROS, there arises the problem of producing colour composites from these improved products. The necessity for such composites will be reduced when the remote sensing section commissions a "colorwrite" machine, capable of producing colour composites directly from CCTs. However, where CCTs are not available, colour composites may still have to be made from photographic products, and methods of doing this are being investigated.

2.2 Aircraft Programme

Over the past reporting period effort has been directed at commencing a single crop (wheat) inventory of the Canterbury Plains area between the Waimakariri and Rakaia Rivers. It was hoped to mount joint ground truth/aircraft underflying with the satellite coverage predicted for the later stages of the growing cycle (late southern spring) and the late maturation phase of the cycle (mid-southern summer). Unfortunately the wet weather, whilst leading to unusually well developed crop stands, has also prevented any satellite coverage of the area and has also cancelled the scheduled spring flying programme.

Previously all our studies on the agricultural application of remote sensing had taken place in the Darfield area which has a good mixture of pasture and cropping activities. In commencing this extended inventory programme it was desirable to employ another test site in the same general area, but having different soil/stress etc. influences on the resultant spectral signature, and a higher percentage of cereal crops. In consultation with the New Zealand Ministry of Agriculture and Fisheries it was decided to use the strips along either side of the road from Leeston to the Rakaia River as this second test site.

This area was selected as the scheduled flight line would cut quite different soil types when compared to those underlying the Darfield test site yet both sites support the same type of wheat crop. The soils in the Darfield test site area are classified as "Associated dry-subhygrous yellow-brown shallow and stony soils". These soils, being reasonably water porous, are more successfully used for pasture production than cereal cropping. (All soil data has been taken from Soil Bureau, D.S.I.R., Bulletin No. 27 (1968).) The Leeston to Rakaia River flight line moves from coverage of crops on "Gley" to "Waimakariri" and "Templeton" "Recent" soils. These Gley soils tend to hold more water and organic material than the soils around Darfield, or the adjacent Recent soils in the Leeston area. The Leeston area also supports a more intensive/extensive cropping programme than that in the Darfield test region.

Both regions were covered with MSS multi-spectral aerial photography in early February - just before the wheat harvesting had reached its peak. The results of this and of the retrospective survey mentioned in the introduction will be covered in the next report.

On 9 February five MSS sorties were flown over Pauatahanui Inlet some 15 miles NNE of Wellington. These flights were staged to capture tidal levels, sediment motions, tidal flushing action, vegetation categories, and erosion potentials of a small tidal basin adjacent to a spreading urban development. The study period was chosen to span the spring low to high tidal cycle. The aerial survey programme complemented simultaneous studies undertaken by the Soil Bureau and Oceanographic Institute Divisions of D.S.I.R. together with the Ministry of Works and Development and the Victoria Universit (Wellington). Again these results will be commented upon in the next report.

2.3 Atmospheric Work

2.3.1 Introduction

Studies are being conducted in New Zealand and Australia, on the atmosphere and its effect on spectral signatures in the LANDSAT bandpasses. The project is a joint one with Minerals Research Division, CSIRO, Australia. In this reporting period, however, we discuss only the measurements made with New Zealand equipment at test sites in both countries. A brief introduction to this work is to be found in the First Quarterly Report (NTIS-N76-20606). The methods outlined are described here in more detail, with results of measurements made over a two year period.

This Section covers the calibration of the radiometer used to make ground based measurements of global and solar irradiance. The laboratory calibration, combined with solar irradiance data, taken over several hours on a clear day, enables the spectral irradiance of the Sun at the top of the atmosphere to be determined. Comparison of these values for each LANDSAT bandpass with values derived from published data, serves as a check of the validity of all these measurements, and the techniques involved.

In this report, only the solar irradiance data, measured with a collimated detection viewing the Sun directly, is considered. Derived parameters include the atmospheric extinction coefficient and beam transmission, and data from Australian and New Zealand test sites is compared with similarly derived data from the Northern Hemisphere.

2.3.2 Objectives

The objectives of this ongoing programme can be summarised.

(a) To calibrate the LANDSAT radiometer in the irradiance mode, in the laboratory using a standard lamp, and to use the instrument to determine the solar spectral irradiances in the LANDSAT bandpass at the top of the atmosphere. Comparison can then be made with published values.

(b) To record global and solar irradiance data over a period of years at test sites in Australia and New Zealand, and hence to establish the typical values and short and long term fluctuations.

(c) To compare measured quantities such as beam transmittance with similar quantities measured by observers in the Northern Hemisphere.

(d) To apply the recorded atmospheric data to the correction of MSS band imagery.

2.3.3 Radiometer Calibration

2.3.3.1 Spectral Response of Instrument

An "ideal" LANDSAT radiometer would have a uniform response to incident power within each of the MSS defined bandpasses of 100 nm and 300 nm width, and zero response to all other wavelengths. In practice, the limitations of filter manufacture and the spectral dependence of detector responsivity will combine to produce an overall "instrument response" which is not ideal. This means that, in general, the instrument output reading will depend on the spectral distribution of the incident radiation, as well as on its absolute value within the passband.

An expression for instrument output is easily derived. We define $S(\lambda)$ as the incident power density per unit bandwidth at the radiometer, from a spectrally varying source at wavelength λ.

$AR(\lambda)$ is the instrument response per unit bandwidth at wavelength λ, with $R(\lambda)$ as the peak normalised response function and A as a constant gain factor.

In a narrow band $\Delta\lambda$, centered on λ, the instrument output is given by:

$$V (\Delta\lambda) = A S(\lambda) R(\lambda) \Delta\lambda$$

Over all wavelengths, the instrument output is therefore:

$$V = A \int_{0}^{\infty} S(\lambda) R(\lambda) d\lambda \qquad \dots\dots 2.3.1$$

Thus the output recorded by the radiometer depends upon the product of $S(\lambda)$ and $R(\lambda)$, which must both be known if the output is to be meaningful in absolute terms.

It is convenient here to define three quantities. The "effective irradiance" is defined as the incident power density which contributes to the instrument output reading, that is, within the actual bandpass of the radiometer.

The "equivalent square bandwidth" is the width of a "square bandpass" response function which is equal in area to the area under the actual peak normalised response curve.

The "square MSS bandpass" is a response of unity within the 100 nm or 300 nm passbands and zero at all other wavelengths.

A common practice is to assume a "square MSS bandpass", and to interpret all incident power from spectrally varying sources in terms of this "square" response. This gives rise to errors if the "unknown" source has a different spectral distribution to that which has been used to calibrate the instrument. This arises directly from equation 2.3.1, since a change in $S(\lambda)$ will produce a different response, depending on whether $R(\lambda)$ is "square" or "actual".

The output errors illustrated in this report (Table 2.3.1) are small compared to those which can occur in radiometric measurements of terrestrial targets, which generally have more rapidly varying spectral radiance within the MSS bandpass. This leads one to question the accuracy of absolute radiance data, particularly when comparing results from different radiometers.

2.3.3.2 Laboratory Calibration of Instrument

All the measurements described in this report were made with a LANDSAT radiometer manufactured by Gamma Scientific.

The wavelength response of each MSS band was first determined in the PEL Photometry Section, using a quartz iodine source, double prism monochromator and calibration thermopile. Plots of the peak normalised response functions are shown in Figure 2.3.1. The results indicate that a spectral "leak" exists on the long wave side of MSS band 4, and the energy contribution due to this leak amounts to 5.8% of the scale reading when viewing a standard lamp.

The instrument was then calibrated in the irradiance mode, that is, using the cosine receptor, against a standard lamp with a known spectral distribution of output power. The lamp itself was checked for total irradiance against an NPL sub-standard source, and found to be within 0.5% of its rated value.

The results are shown in Table 2.3.1. The column labelled (2) shows the irradiance at the radiometer entrance aperture within the "square MSS bandpasses", and not necessarily contributing to the instrument reading.

2.3.4 Global and Solar Irradiance

2.3.4.1 Atmospheric Model and Derivation of Parameters

The nomenclature used in papers on atmospheric work varies widely between authors. In an attempt to come closer to a "standard" terminology, we have adopted the definitions of Thekaekara (1972) for irradiance (E) and for zenith angle (Z).

The global (spectral) irradiance on a horizontal surface a ground level is given by:

$$E_G(\lambda) = E_O(\lambda) \cos Z \exp(-\alpha(\lambda)m) + E_{SKY}(\lambda) \quad \ldots. \; 2.3.2$$

$E_O(\lambda)$ = solar spectral irradiance per unit bandwidth at the top of the atmosphere

Z = solar zenith angle

$\alpha(\lambda)$ = atmospheric extinction coefficient at wavelength λ

m = airmass - defined as the ratio of total number of attenuating particles in the observer's line

of sight, to the total number of
attenuating particles in the vertical
column

$E_{SKY}(\lambda)$ = global irradiance per unit bandwidth due
to radiation emanating from the sky.

Equation 2.3.2 is based on a simplified "flat Earth" model
which takes no account of the Earth's curvature, and assumes a
homogeneous layered atmosphere.

The quantity $E_G(\lambda)$ is the global irradiance per unit band-
width at the wavelength λ. We can define the quantities $E_{(\ )}(\Delta\lambda)$,
and $\alpha(\Delta\lambda)$, as the irradiance and extinction coefficient within
a specified bandwidth $\Delta\lambda$.

Global irradiance $E_G(\Delta\lambda)$ is measured directly with a radio-
meter having a bandwidth response $\Delta\lambda$, and a horizontal Lambertian
receiving surface (cosine receptor).

Solar irradiance $E_s(\Delta\lambda)$, is defined as the irradiance in
bandwidth $\Delta\lambda$, originating directly from the Sun, together with
contributions along the Sun/detector path, and falling on a
detector surface which is normal to the Sun's rays. We find that
$E_s(\Delta\lambda)$ is most easily measured with a tracking radiometer and
collimating tube which admits radiation from the Sun's disc and
has a limiting field of view of not more than 3°.

Solar irradiance is described by a simpler expression than
equation 2.3.2, since E_{SKY} is removed and the cosine term no
longer applies.

$$E_s(\Delta\lambda) = E_o(\Delta\lambda) \exp(-\alpha(\Delta\lambda) m) \qquad \dots. 2.3.3$$

If $E_s(\Delta\lambda)$ is measured for a number of different zenith angles
that is, at different times of the day, it is possible to deduce
the value of α and the instrument reading which corresponds to
$E_o(\Delta\lambda)$.

This assumes that airmass m is a known function of solar
zenith angle Z. For values of Z which do not exceed a specified
limit:

$$m = \sec Z \qquad \dots. 2.3.4$$

The limiting values of Z are considered in the next section. The
assumption is also made that the Solar constant and atmospheric
transmission do not change during the period of the measurements.

We have chosen to insert the measured values of $E_s(\Delta\lambda)$ into
a computer program which finds the least squares fit of expression
2.3.3 to these values. The zenith angle is computed from the time
and date of measurement, Sun declination and observer's latitude.

Equally, by taking logarithms of 2.3.3, we have:

$$\text{Ln } E_s(\Delta\lambda) = \text{Ln } E_0(\Delta\lambda) - \alpha(\Delta\lambda)\, m \qquad \dots\, 2.3.5$$

The values of $\text{Ln } E_s(\Delta\lambda)$ can be plotted against $m (\simeq \sec Z)$, and a straight line fit gives α (slope), and E_0 from the intercept on the irradiance axis.

This method of deriving α and E_0 is well known, and is used by a number of authors (Shaw et al. 1973, Rogers 1974). Indeed, it is the basis of the "Smithsonian long method" of determining the Solar constant (Johnson 1954).

2.3.4.2 The Effect of Large Zenith Angles

The range of zenith angles which are considered to satisfy equation 2.3.4 varies widely with author:

Limiting range of Z = 0° - 62° (Thekaekara 1972)

         "   = 0° - 80° (Shaw et al. 1973)

         "   = 0° - 60° (Rogers 1974)

         "   = 0° - 70° (Johnson 1954)

A more accurate expression for m at large zenith angles is given by the empirical relation due to Bemporad:

$$m = \sec Z - 0.001867\,(\sec Z-1) - 0.002875\,(\sec Z-1)^2 -$$

$$0.0008083\,(\sec Z-1)^3 \qquad \dots\, 2.3.6$$

The atmospheric transmission factor along the line of sight is given by:

$$\tau_s = \exp(-\alpha(\Delta\lambda)\, m) \qquad \dots\, 2.3.7$$

Generally, it is the error in τ_s, caused by an error in estimating m, which is of interest, and this error is also a function of the extinction coefficient. Figure 2.3.2 is a plot of τ_s against m for various values of $\alpha(\Delta\lambda)$. m is calculated from 2.3.4 and from 2.3.6. It can be seen that for all values of extinction coefficient, τ_s differs by < 0.5% at a zenith angle of 75° for the two calculations of m.

Shaw et al. (1973) and Rogers (1974) make irradiance measurements out to zenith angles 84.2° (m = 10) and 81.7° (m = 7) respectively. The difficulty of making accurate measurements at these large zenith angles can be appreciated when it is realised that the airmass changes from 7 to 10 for a Sun angle change of only 2.5°, corresponding to a time change of ten minutes.

Because of the necessity for stability of atmospheric transmission during the determination of E_0 and α, we have avoided the

ends of the day, and limited our measurements to a period of six hours centered on Solar noon, and to values of airmass not exceeding four.

2.3.4.3 Results of Measurements at Test Sites

For accurate measurement of the solar spectral irradiance at the top of the atmosphere ($E_O(\Delta\lambda)$), the criterion of stable atmospheric transmission over the measurement period has proved to be difficult to realise in practice. Of the test sites at Wellington, Pauatahanui, Wainuiomata, Darfield and Menindee, only at Wellington, and at the Australian test site at Menindee, New South Wales, have results of sufficient accuracy been obtained.

Global and solar irradiance measurements have been made at about twenty minute intervals over a six hour period centered on solar noon. A sample of the computer output from the least squares fit program is shown in Figure 2.3.3.

For all test sites, each set of measurements has been subjected to the least squares fit program. Because atmospheric fluctuations increase the standard deviation and reduce the confidence in the derived values E_O and α, only five data sets have been selected for the estimation of E_O. These all have standard deviations of less than 0.7. The derived values of E_O shown in Table 2.3.2 are the result of applying the laboratory calibration to the computer radiometer reading for E_O.

All the solar irradiance values given in Table 2.3.2 are for "effective irradiance" as defined in Section 2.3.3.1.

Once calibrated, the radiometer can be used to measure the short term variations in extinction coefficient using equation 2.3.3 and the known values of E_O. Figures 2.3.4 and 2.3.5 are plots of diurnal variations of extinction coefficient in New Zealand and Australia.

2.3.5 Derived and Predicted Values of Solar Irradiance at the Top of the Atmosphere

Before a comparison of solar irradiance $E_O(\Delta\lambda)$, as derived from our measurements, can be made with $E_O(\Delta\lambda)$ predicted from the published data (Thekaekara 1972), it is necessary to correct the published figures for annual variations due to the Earth's elliptic orbit.

The Earth/Sun distance at any time of the year can be computed to sufficient accuracy, and as a fraction of the mean value, by an iterative procedure involving a simple form of Kepler's equation:

$$E - e \sin E = 2\pi(t - T) \qquad \dots\dots 2.3.8$$

$$\text{and} \quad r/r_{mean} = 1 - e \cos E \qquad \dots\dots 2.3.9$$

E   =   eccentric anomaly

e   =   orbit eccentricity

(t - T)   =   time after perihelion in years

The ratio of irradiance E_O at time (t - T) to the mean value is calculated by:

$$E_O = E_O \text{ (mean) } \{\frac{r_{mean}}{r}\}^2 \qquad \dots 2.3.10$$

The maximum variations occur at the perihelion (Solar constant = 1399 W/m^2) and at the aphelion (Solar constant = 1309 W/m^2) in accordance with the values cited by Thekaekara (1972).

Column 4 in Table 2.3.2 gives the "effective irradiance" at the top of the atmosphere, corrected for orbit ellipticity, and calculated from the published data.

2.3.6 Comparison of Beam Transmittance Measurements in Southern and Northern Hemisphere

Beam transmittance τ_B is defined here as the transmission through a vertical column of the atmosphere.

Thus $\tau_B = \exp(-\alpha(\Delta\lambda))$

Rogers (1974) gives average, maximum and minimum values of τ_B derived from 10 sets of field measurements in the Eastern U.S.A. and these are reproduced in Table 2.3.3 (c). Table 2.3.3 (a) gives the same parameters for three sets of New Zealand data, and 2.3.3 (b) shows three sets of Australian data.

2.3.7 Summary and Conclusions

2.3.7.1 Radiometer Calibration

In this report, we have endeavoured to point out some of the problems involved in calibrating a radiometer, and in defining that calibration, either in the irradiance or radiance mode. Discrepancies between the "actual" spectral response of the instrument and the "calibration bandpass", often assumed to be square and of nominal width, can give rise to errors in measuring the irradiance of a source of unknown spectral distribution, or the radiance of target of unknown spectral distribution.

We have described a calibration procedure in which the spectral response of the instrument in each MSS band is carefully measured and the response function is then multiplied by the calibration source function, to give a curve whose area is proportional to

the instrument reading. In this way, the instrument is calibrated for the "effective" irradiance incident upon the detector.

The laboratory calibration has been checked by the iterative fitting of a simple atmospheric model to measurements taken over five days in New Zealand and Australia. This fitting procedure automatically derives the Solar irradiance at the top of the atmosphere, within the instrument bandwidth, and in terms of the instrument scale reading.

The average of these five sets of derived values converted into $\mu w/cm^2/Bw$ using the laboratory calibration, have then been compared with values calculated from the published figures of extra-terrestrial Solar spectral irradiance.

Our measurements give extra-terrestrial irradiances which differ from the published figures by the following amounts (expressed as a percentage):

MSS band 4: - 9.4%	MSS band 5: + 6.4%
MSS band 6: + 0.4%	MSS band 7: - 4.6%

In view of the large number of variables involved in these measurements, we feel that these discrepancies are smaller than might have been expected. However, we consider that further investigations should be made to identify the differences, particularly the "cross over" between bands 4 and 5.

Part of the problem is to be found in the variability of the atmosphere over the test sites, leading to a large standard deviation between the data and the fitted curve. This points to the necessity for making more "clear day" measurements, and is an argument in favour of setting up a recording radiometer which track the Sun and provides near continuous data during the day.

2.3.7.2 Atmospheric Extinction

The results of atmospheric extinction measurements, illustrate in Figures 2.3.4 and 2.3.5, show clearly the greater opacity of the atmosphere in MSS band 4, due mainly to Rayleigh scattering. MSS band 7, however, contains a broad based water vapour absorption band, centered at about 930 nm, and this results in a consistently higher extinction coefficient in this band. The short term fluctuations are also greater in band 7, probably due to the movement of water vapour "cells" near the ground.

The large fluctuations in band 7, and the high extinction coefficients for the Menindee test site were slightly puzzling, since this test site in Western New South Wales is in a semi-desert area. The measurements, however, were made in extremely hot conditions on the bank of an irrigation canal, and this could account for a high atmospheric water vapour content in the immediat vicinity of the instrument.

2.3.7.3 Comparison of Beam Transmittance in Two Hemispheres

Comparison of the results of Rogers (1974) with the New Zealand and Australian figures shows some significant features. The average transmittances in the visible and first I/R bands are higher for the New Zealand and Australian test sites compared to those for the Eastern U.S.A. test site.

Rogers' results show a consistent increase in atmospheric transmittance from MSS 4 to MSS 7. Our results indicate that MSS 7 is more severely affected by atmospheric water vapour.

2.3.7.4 Future Work

We believe that measurements should continue at selected test sites, and that effect of variables such as atmospheric pressure, humidity, and instrument stability with temperature should be more fully investigated.

The objectives (d) in section 2.3.2 remain to be achieved as part of our ongoing programme.

2.3.7.5 References

Johnson (1954) - "Physical Meteorology", Chapter 4. John Wiley & Sons. 1954.

Rogers (1974) - "Investigation of techniques for correcting ERTS data for solar and atmospheric effects". Final report - Goddard Space Flight Centre - Contract No. NAS 5-21863.

Shaw et al. (1973) - "Investigations of atmospheric extinction using direct solar radiation measurements made with a multiple wavelength radiometer". G.E. Shaw, J.A. Reagan and B.M. Herman. J. App. Meteorology, 12, March 1973 pp 374-380.

Thekaekara (1972) - "Proposed specification for the solar constant and air mass zero solar spectral irradiance". NASA SP-298. Space Simulation. 1972.

Source	Instrument Reading mV	Equivalent Square Bandwidth nm	(1) Effective Irradiance at Instrument $\mu w/cm^2/Bw$	(2) Irradiance in "Square" MSS Bands $\mu w/cm^2/Bw$	Ratio (1)/(2)	MSS CH. NO.
S1	20.6	72.8	366.1	503.5	0.727	4
"	37.8	104.5	984.9	912.5	1.079	5
"	57.3	124.4	1487.1	1194.3	1.245	6
"	85.1	264.6	3539.3	4075.1	0.869	7
S2			12815	17701	0.724	4
"			15570	15150	1.028	5
"			15342	12373	1.240	6
"			24221	24912	0.972	7

Notes: 1-Source S1: Standard Lamp No. 178A at 2854° K

2-Source S2: Mean Solar Irradiance at top of Atmosphere

3-"Effective Irradiance", "Irradiance in Square MSS Bands" are defined in Section 2.3.3.1.

Table 2.3.1

Response of radiometer to a standard lamp, and calculated values of mean solar irradiance, within the actual instrument bandpasses, and the nominal "Square" MSS Bands.

Test Site Location - Date	Extinction Coefficient α	Derived Value of E_O $\mu w/cm^2/Bw$	E_O from Published Data $\mu w/cm^2/Bw$	MSS Channel Number
Menindee - Lake Tandou 23 Nov 1975	0.130 0.120 0.055 *	11570 17156 15201 *	13161 15990 15775 *	4 5 6 7
Menindee - Lake Tandou 24 Nov 1975	0.158 0.103 0.093 0.143	11803 16619 15559 23544	13166 15996 15762 24884	4 5 6 7
Menindee - Lake Tandou 25 Nov 1975	0.179 0.126 0.135 *	11974 16882 16249 *	13170 16002 15766 *	4 5 6 7
Wellington P.E.L. 23 July 1975	0.175 0.114 0.081 0.093	11304 15995 14788 22429	12424 15095 14874 23482	4 5 6 7
Pauatahanui Boat House 9 Feb 1977	0.182 0.117 0.112 0.122	12354 17447 16449 23927	13147 15973 15739 24848	4 5 6 7
	Average Values of E_O	(11801 (16820 (15649 (23300	13014 15811 15583 24405	1 2 3 4

Table 2.3.2

Values of extinction coefficient and E_O derived for computer fit of Equation 2.3.3, compared to E_O obtained from published data (Thekaekara 1972).

* Standard deviation too large in these channels.

MSS Band	Average	Maximum	Minimum	Standard Deviation
4	0.853	0.867	0.827	0.010
5	0.903	0.915	0.883	0.009
6	0.920	0.934	0.895	0.007
7	0.896	0.915	0.829	0.016

(a) Compiled from three   (WELLINGTON   23 July 1975
     sets of data at New   (DARFIELD   3 Aug 1975
     Zealand test sites   (PAUATAHANUI   9 Feb 1977

MSS Band	Average	Maximum	Minimum	Standard Deviation
4	0.845	0.860	0.831	0.007
5	0.884	0.899	0.860	0.009
6	0.901	0.920	0.880	0.010
7	0.866	0.903	0.807	0.018

(b) Compiled from three   (MENINDEE   21 Nov 1975
     sets of data at an   ("   24 Nov 1975
     Australian test site   ("   25 Nov 1975

MSS Band	Average	Maximum	Minimum	Standard Deviation
4	0.799	0.856	0.697	0.051
5	0.852	0.901	0.770	0.048
6	0.885	0.940	0.812	0.051
7	0.899	0.975	0.843	0.052

(c) Compiled from 10 sets of data in Eastern USA test
     site over the period January-June 1973 (Rogers
     1974).

Table 2.3.3

Comparison of Beam Transmittance Measurements in Southern
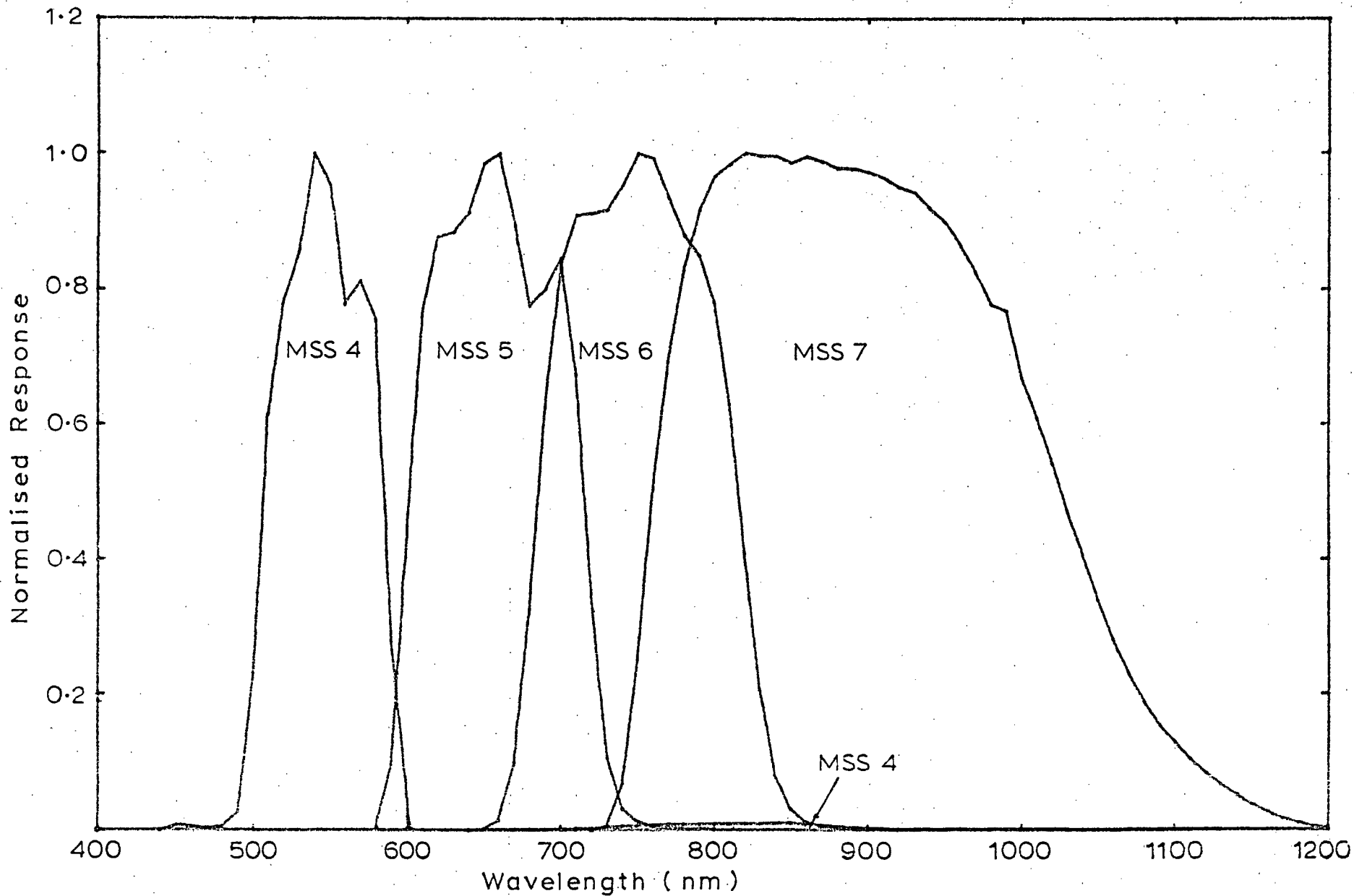and Northern Hemisphere.

FIG. No 2·31   PLOT of PEAK NORMALISED SPECTRAL RESPONSE
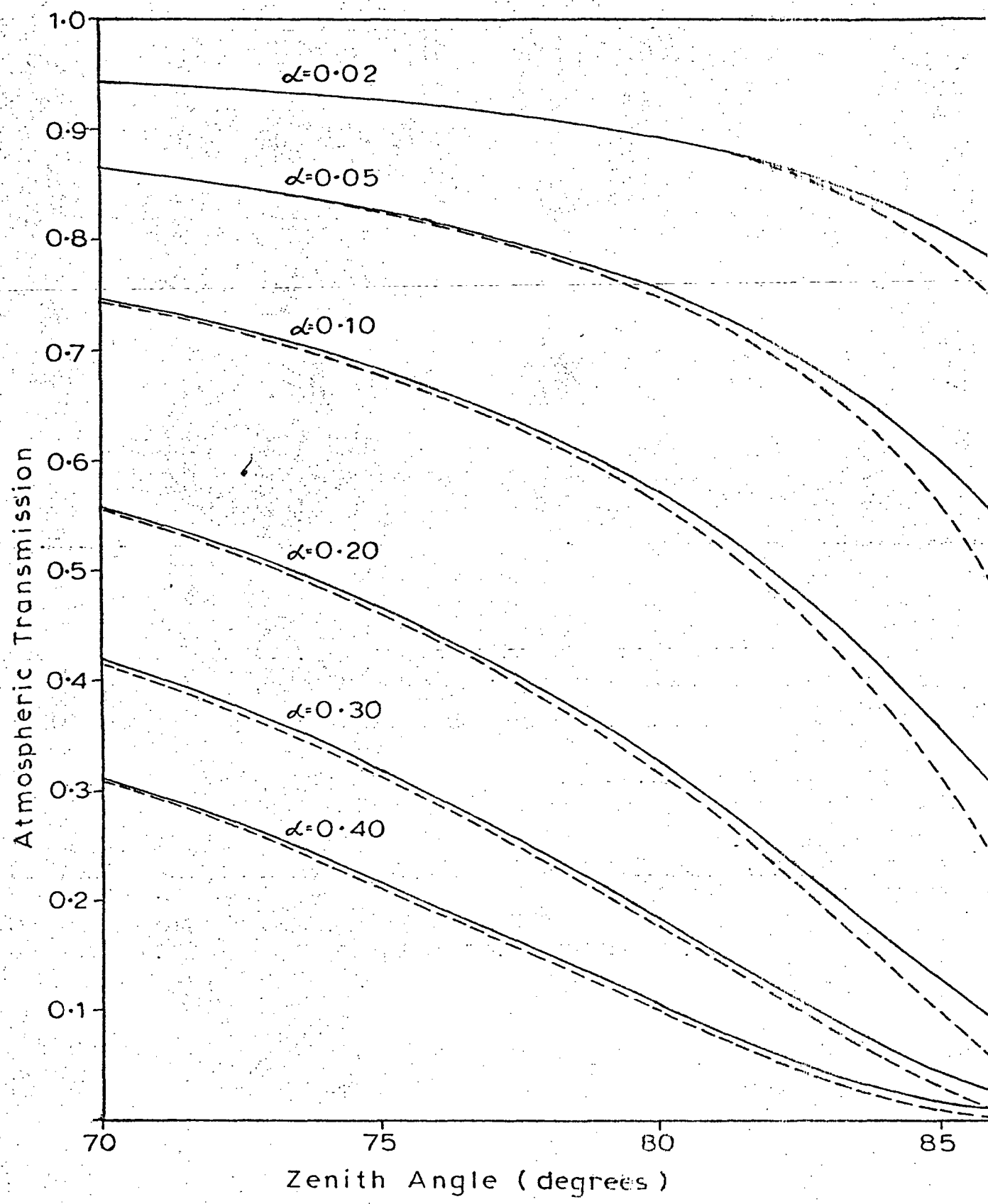FUNCTIONS of GAMMA RADIOMETER

FIG. No. 2·3·2   Plot of Atmospheric Transmission against Zenith Angle for Different Values of Extinction Coefficient α

FIG. No

MENINDEE - LAKE TANDOU--****--24 NOVEMBER 1975
MSS CHANNEL NO. 1

MEASURED TIMES AND VALUES
****

LOCAL TIME HOURS	ZENITH ANGLE DEGREES	AIRMASS SEC Z	LOG IRRADIANCE	IRRADIANCE
9.26667	54.8078	1.73514	3.91801	50.3
9.68333	49.547	1.54125	3.95124	52
9.95	46.1794	1.44425	3.9634	52.9
10.25	42.393	1.35413	3.97968	53.5
10.5	39.2588	1.2915	3.99083	54.1
10.7833	35.7234	1.23176	4.00186	54.7
11.1	31.8164	1.17683	4.01277	55.3
11.5667	26.2028	1.11453	4.02356	55.9
11.8333	23.1224	1.08735	4.02714	56.1
12.25	18.6401	1.05536	4.03424	56.5
12.5167	16.1238	1.04095	4.03424	56.5
12.9167	13.2777	1.02747	4.03069	56.3
13.1667	12.3709	1.02377	4.02356	55.9
13.65	13.0954	1.0267	4.02714	56.1
14.2167	17.305	1.04741	4.02892	56.2

****

NUMBER OF ITERATIONS = 12
THE ATTENUATION CONSTANT IS .158599
SOLAR IRRADIANCE I IS 66.4144

THESE ARE THE TABULATED VALUES OF I EXP(-J/G(T))

LOCAL TIME HOURS	ZENITH ANGLE DEGREES	AIRMASS SEC Z	LOG IRRADIANCE	IRRADIANCE
8	70.6441	3.01717	3.71739	41.157
8.5	64.4359	2.31738	3.82838	45.988
9	58.1674	1.89595	3.89522	49.1668
9.5	51.8627	1.61931	3.93909	51.372
10	45.5485	1.42795	3.96944	52.955
10.5	39.2588	1.2915	3.99108	54.1135
11	33.0438	1.19296	4.00671	54.9659
11.5	26.9902	1.12223	4.01793	55.5859
12	21.2696	1.0731	4.02572	56.0208
12.5	16.2697	1.04172	4.0307	56.3002
13	12.8864	1.02584	4.03322	56.4422
13.5	12.5226	1.02437	4.03345	56.4554
14	15.3948	1.03722	4.03141	56.3404
14.5	20.1578	1.06525	4.02697	56.0905
15	25.7724	1.11046	4.0198	55.6898
15.5	31.7756	1.17631	4.00935	55.1112
16	37.9661	1.26843	3.99474	54.3118
16.5	44.2453	1.39595	3.97452	53.2245
17	50.5576	1.57405	3.94627	51.7421
17.5	56.8666	1.82952	3.90575	49.6875

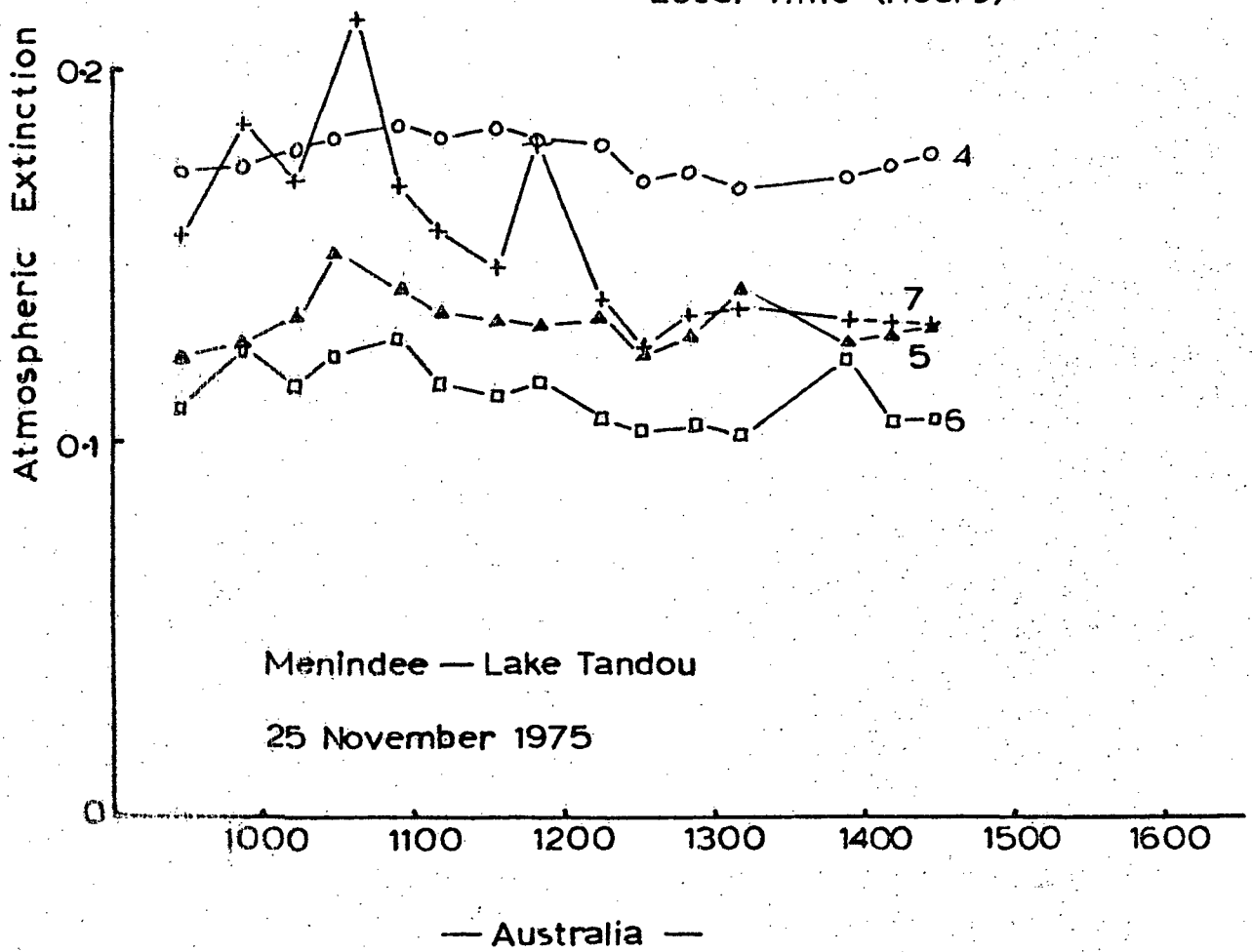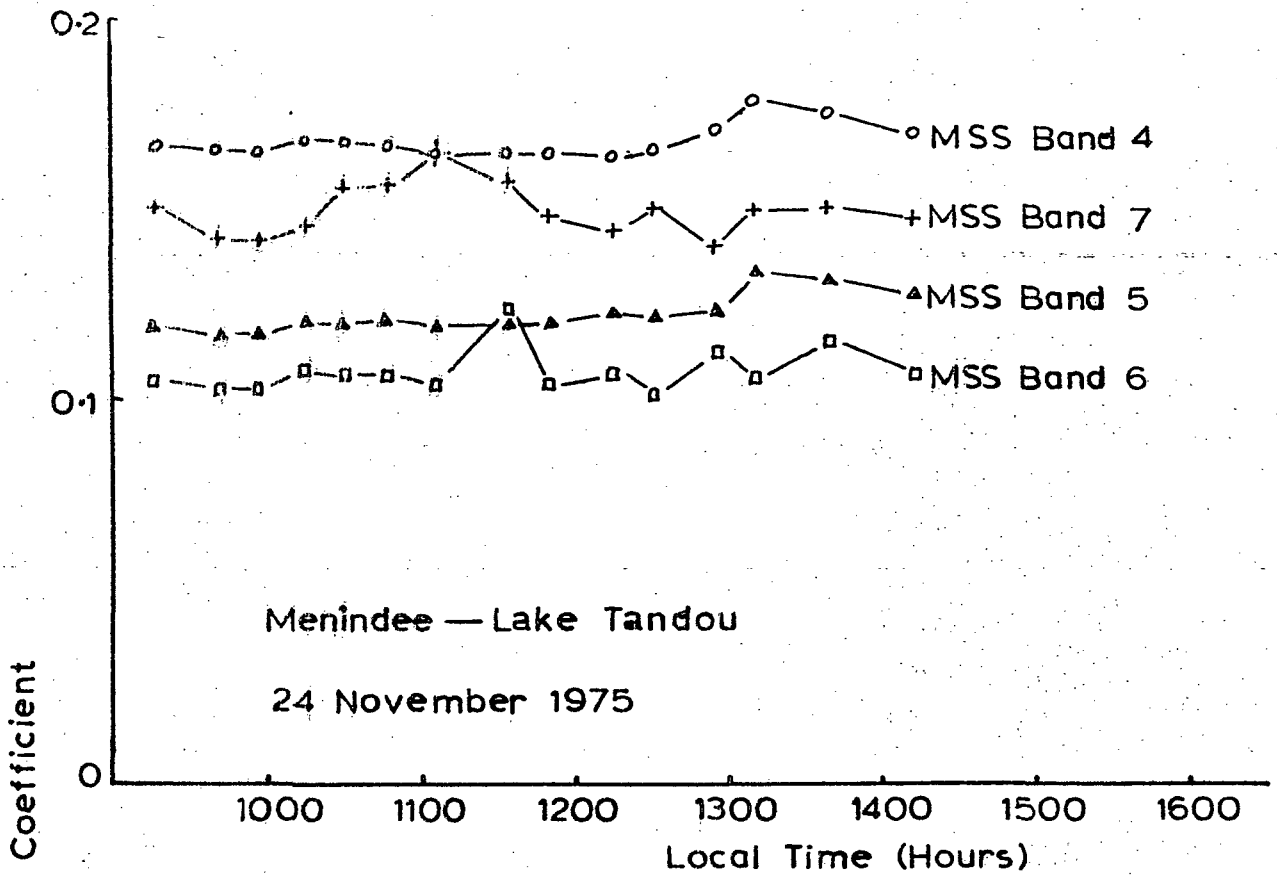EXPECTED (COMPUTED) NOON VALUE = 56.4653
STANDARD DEVIATION = .225519

Figure 2.3.3   Sample output from least squares fit of
equation 2.3.3 to measured data.
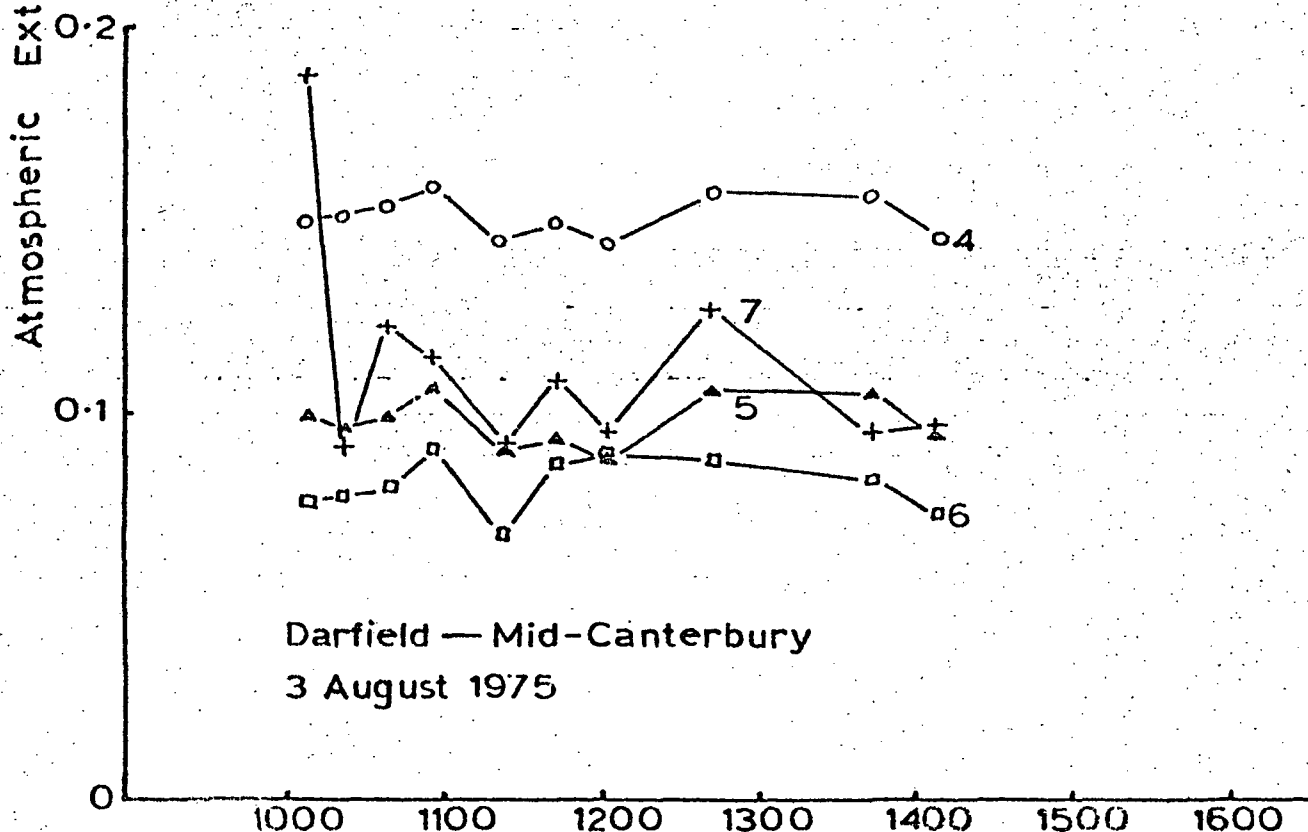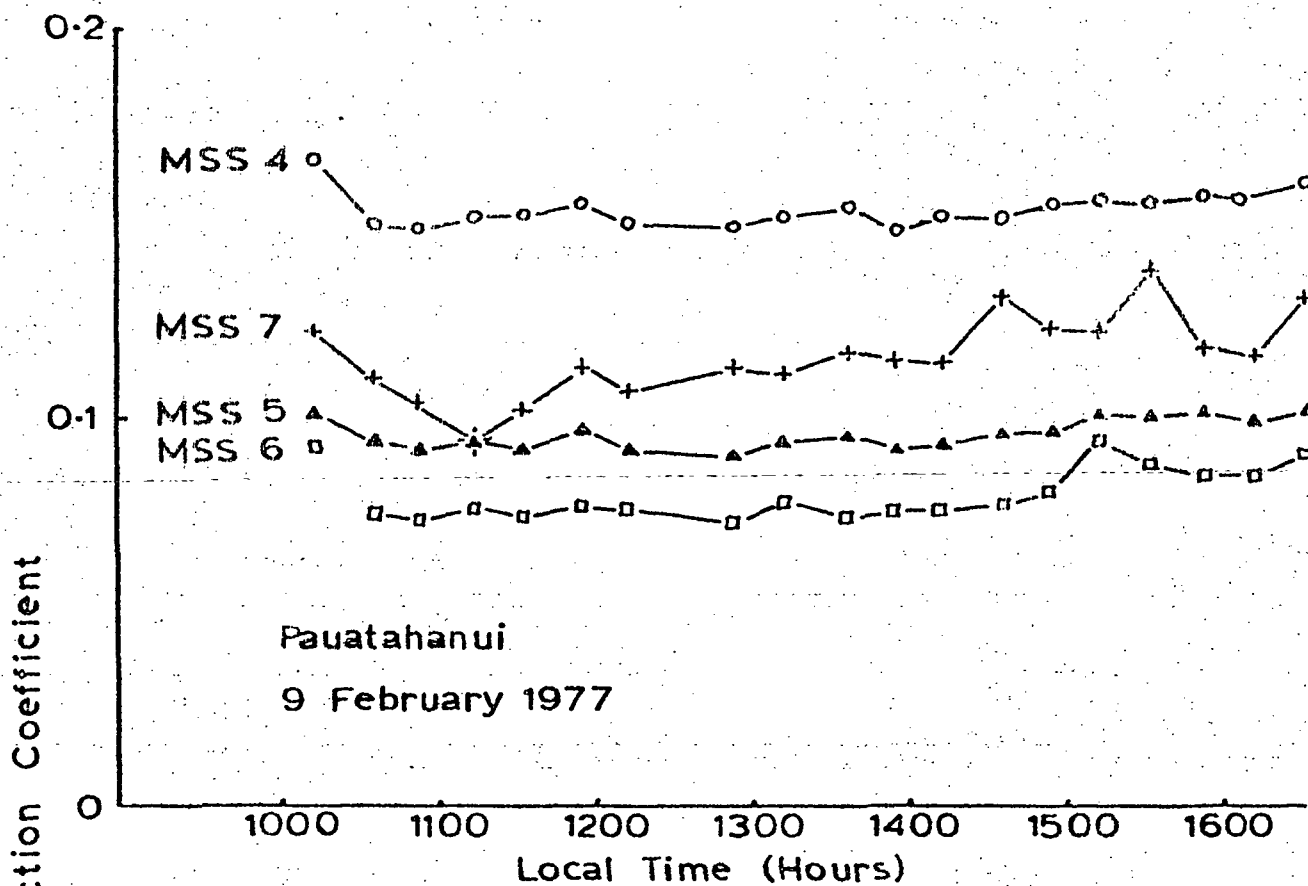
Fig 2·3·4 Variation of Atmospheric Extinction Coefficient

Figure 2·3·5   Variation of Atmospheric Extinction
Coefficient

2.4 IBM CCT Processing

2.4.1 CCT Reformatting

During this reporting period considerable attention has
been directed at optimising the Job Control Language and file
management routines used in taking the four strip EROS tape and
producing a five file reformatted product (one calibration data
file and four single band whole scene files). Further work has
also improved the PL/1 reformatting procedures. Present tests
indicate that a four fold reduction in IBM 370/168 CPU time has
resulted from this optimisation and restructuring exercise.
Once difficulties in sharing storage space, for the 31 M byte
whole scene on non-dedicated disk packs, with other users have
been overcome production runs will commence.

2.4.2 CCT Data on a Nationwide Computer Network

Using the New Zealand Government Ministry of Works and
Development IBM 370/168, being available to users on a time
shared terminal system throughout New Zealand, some basic
programs have been made available to investigators during the
reporting period. All CCT data files are stored under the
"alias" system in Wellington and, currently, may be accessed
in the batch mode through TSO. Programs that will furnish Bit
or EBCDIC dumps, complete CCT decode and 47 level coded picture
print outs are available. These programs are all written totally
in machine independent language - here PL/1. Card decks for
these programs are available through the P.E.L. Remote Sensing
Section as is a report describing the program packages.

2.5 CCT Processing on the HP 2100

The main achievement during this reporting period has been the development of a computer program package to perform a full geometric rectification of a LANDSAT subimage. The procedures adopted in these programs are explained in section 2.5.1. A number of corrected images have been prepared, using a 10 yard sampling interval and these are to be sent to Optronics to be written out on their colorwrite machine. These images should be ready for our final report in June. The development of the geometric correction program has allowed time sequential imagery to be produced by subtracting spatially registered but time separated LANDSAT scenes. A time sequential image of the Eyrewell forest area is also being sent to Optronics. Production of such images will be much simpler when we have our own photowrite machine.

Multispectral aircraft negatives of our Darfield test area have been scanned at Massey University on their Optronics Photoscan machine. Unfortunately we were not able to accurately register the different image bands as they were scanned. Consequently the negatives have been geometrically corrected in the computer so that they are now in register with each other, with the standard New Zealand UTM inch to the mile map series, and with corrected LANDSAT subimages of the same area. This should prove a considerable advantage in analysing the aircraft negatives.

2.5.1 Rectification of LANDSAT Subimages

The image rectification system developed for use on our HP 2100 computer is based on the system developed by Van Wie and Stein et al (1975, 1976) but differs from it in certain key respects. These differences will be made clear as the rectification system is discussed step by step.

The reason for developing our own rectification system is mainly financial. The Goddard system would involve us in too much expenditure for computer time on a large computer. However, we have available an HP 2100 minicomputer for which we are not charged. The Goddard system will rectify whole LANDSAT scenes in the UTM projection. Our system will rectify a LANDSAT subimage on the HP 2100 in any desired mapping projection. The size of the input subimage depends on the extent of the rotation required. This is due to the limited core storage available. For example a small input image (e.g. 128 x 128 pixels) can be fully rotated, whereas a large input image can only be rotated by a small amount.

There are many sources of geometric errors in LANDSAT imagery. Many of the errors need to be treated differently. The error sources will be discussed briefly here. For a more detailed discussion refer to Van Wie et al (1975, 1976). Band to band misregistration has already been corrected in the CCT's. The pixels inserted by NASA to compensate for line length variations cause an error on average of 28.5 m. These can be removed when the CCT's are reformatted. The effect of the sensor delay during sampling, and the earth's rotation cause each row to be offset from the preceding one. This is compensated for by adding a correction term to each column when an

image co-ordinate (row, column) is calculated. Variations in the mirror velocity profile cause an error in the column co-ordinate along each row which is approximately described by a sine error function. The sine error function is zero at the end of each row and goes through one cycle along each row. The amplitude of the sine error function is known to be about 7 pixels.

The Goddard approach is to explicitly correct the input LANDSAT image for the effects of sensor delay, the earth's rotation and the mirror velocity profile to give a corrected input image. The next step is to deduce a suitable mapping function from the UTM map projection to the corrected input image. Let the co-ordinates for the input image, the corrected input image and the map be (R,C), (U,V) and (X,Y) respectively. The Goddard system has available an affine transformation or a polynomial mapping function. For the polynomial mapping function, which is the more accurate, coefficients C_i and D_i are required for the general mapping described by

$$U = C_0 + C_1 X + C_2 Y + C_3 X^2 + C_4 XY + C_5 Y^2 + C_6 X^3 +$$
$$C_7 X^2 Y + C_8 XY^2 + C_9 Y^3 + \ldots$$

$$V = D_0 + D_1 X + D_2 Y + D_3 X^2 + D_4 XY + D_5 Y^2 + D_6 X^3 +$$
$$D_7 X^2 Y + D_8 XY^2 + D_9 Y^3 + \ldots$$

The desired order of polynomial is chosen according to the mapping accuracy required. Next the C_i and D_i are computed by means of a least squares fit to a number of known ground control points (GCP's) The polynomial mapping function is intended to correct for all errors which have not been explicitly compensated for. These are caused by satellite height and altitude variations, the earth's curvature and the tangential nature of the UTM projection itself. This last error is part of what Van Wie et al call perspective distortion. It is correctable if all the points in the original LANDSAT image are at the same height (e.g. sea level). However, points at different heights will be offset along rows because LANDSAT has a central perspective instead of the orthogonal perspective of a UTM map projection. This error is not correctable, although it is possible to correct the image for a single chosen height (e.g. sea level). This correction can be achieved by adjusting each GCP by an amount which depends on its altitude and distance from the satellite track through the centre of the image. This correction appears to have been neglected by Van Wie et al. If a GCP is taken on top of a mountain it could cause an error of several pixels.

Our approach is somewhat different. We have noted that the effect of the earth's curvature and the perspective distortion (for a given height) along rows both have the form of a sine error functi Thus, these errors can be included in the correction for the mirror velocity profile by adjusting the sine amplitude to an optimum value. This optimum value can be simply found by plotting the mean absolute GCP error against sine amplitude, and choosing the amplitud

which gives the minimum error. For the example image discussed
in section 3.1 this optimum amplitude is 5.65 pixels. The optimum
amplitude will vary with the map projection used and it will also
vary slowly with time. Correcting for the earth's curvature and
perspective distortion at the same time as the mirror velocity
profile gives a new corrected input image and reduces the need
to use a high order polynomial mapping function. We accept the
minor constraint that our output image should be a rectangle with
sides parallel to the map co-ordinate axes. In this case the
function for mapping a rectangle on the map into a quadrangle in
the corrected input image has the form

$$U = C_o + C_1 X + C_2 Y + C_3 XY$$

$$V = D_o + D_1 X + D_2 Y + D_3 XY$$

This particular mapping function has some special properties.
Firstly, straight lines on the map parallel to the co-ordinate
axes, map into straight lines on the corrected input image.
However, other straight lines on the map, map into curved lines
(see for example the diagonals in Figure 2.5.1). This is caused
by the XY term in the polynomial. Secondly, and most importantly,
the sampling grid in the corrected input image, corresponding to
the rectangular desired output image on the map, is formed by the
intersection of a grid of straight lines. For each output image
row, the endpoint co-ordinates of the corresponding corrected input
image sample line are obtained by adding a constant amount to the
previously used sample line endpoint co-ordinates. Similarly the
sample co-ordinates along each corrected input image line
(corresponding to an output image row) are simply obtained by
incrementing the previously used sample co-ordinate by a constant
amount.

This leads to a considerable saving in computation time. Each
sample co-ordinate needed in the corrected input image (corresponding
to an output image sample) does not have to be calculated separately
by means of the polynomial function above. Van Wie et al overcome
the problem of the time required to calculate the polynomial mapping
function for each output image sample by superimposing a coarse grid
system upon the output image, mapping this grid onto the corrected
input image and then performing bilinear interpolation between grid
lines. Our system is considerably simpler, but cannot obtain the
accuracy possible with the highest order (e.g. 4) polynomial mapping
functions.

Another advantage of the quadrangular mapping function is that,
being of low order, it is stable at the edges of the image. Also,
although the GCP's should be well spread out, our mapping function
is not over sensitive to their location.

For each required geometrically corrected output image sample,
its corresponding co-ordinate is calculated first in the corrected
input image and then (straight forwardly) in the input image itself.
The final radiance value is then obtained by nearest neighbour,
bilinear or cubic interpolation as is done by Van Wie et al. Results
for an example LANDSAT image are discussed in section 3.1.

REFEPENCES

Van Wie, P. and Stein, M. (1976). "A LANDSAT digital image rectification system". Report X-931-76-101, Goddard Space Flight Centre, Greenbelt, Maryland.

Van Wie, P., Stein, M., Puccinelli, E. and Fields, B. (1975). "LANDSAT digital image rectification system - preliminary documentation", Information Extraction Division, Goddard Space Flight Centre.
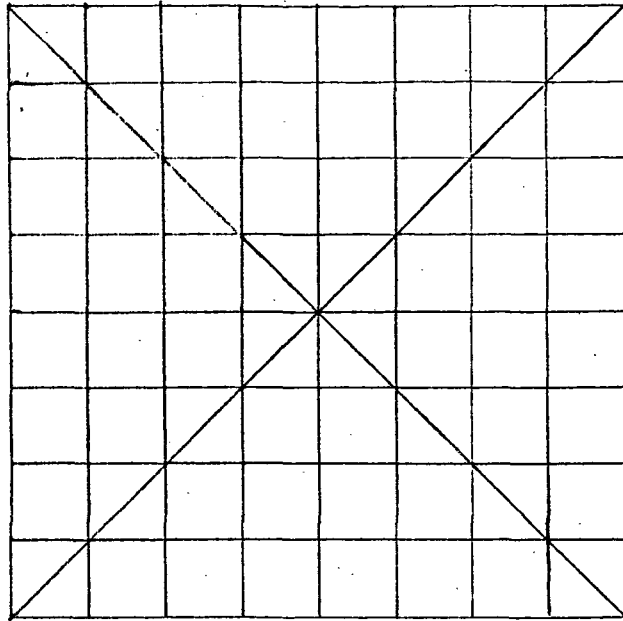
(a)
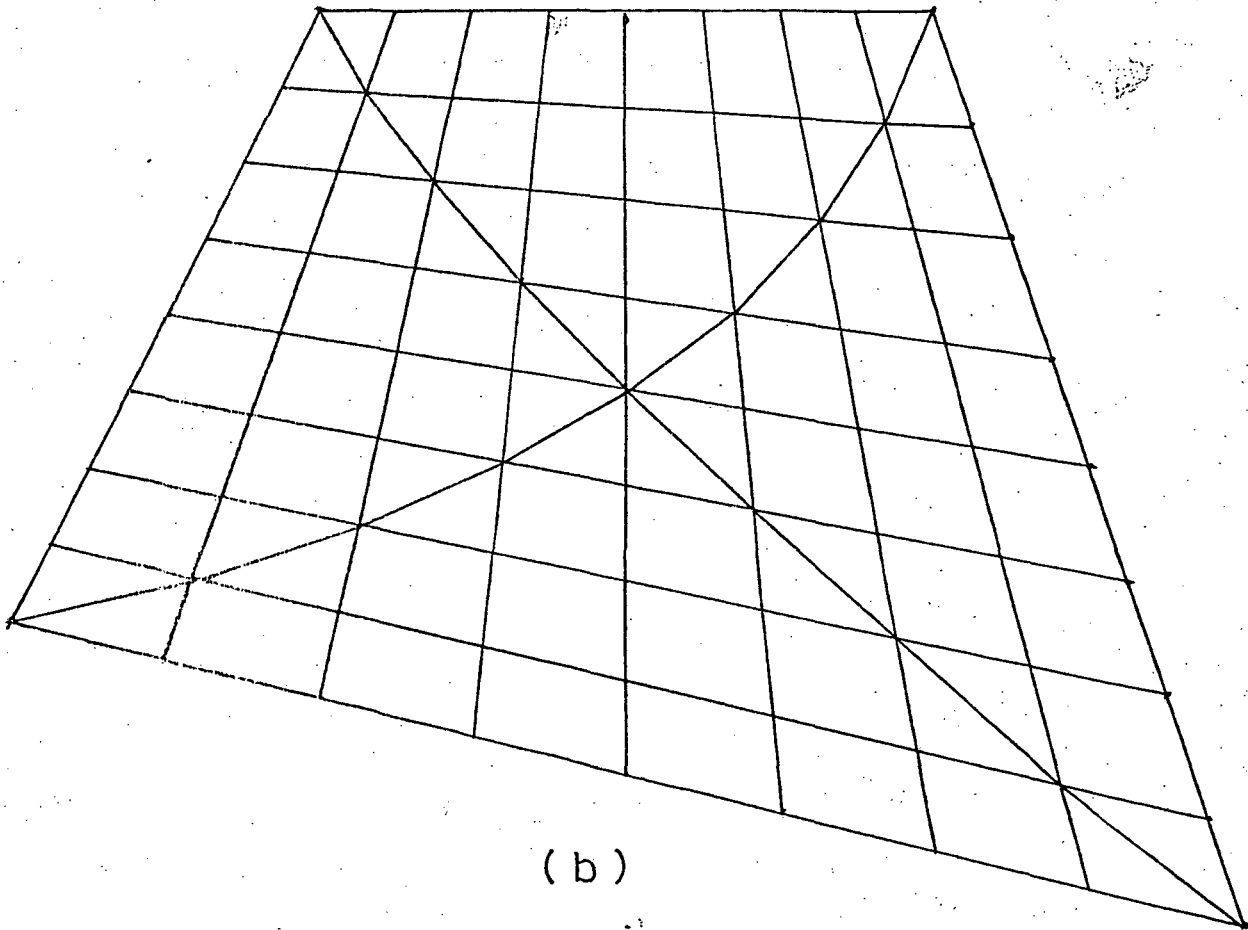
(b)

Figure 2.5.1   Example mapping of a rectangle on a
map (a) into a quadrangle in the
corrected input image (b).

2.6   Cartographic Reflector

The 4 ft diameter diverging reflector continues to be set up at the P.E.L. Auroral Station (45.04°S, 169.69°E) for every predicted LANDSAT 2 overpass for which cloud cover conditions are favourable. To date, due to the lack of sustained clear weather periods and satellite scheduling priorities, no imagery has been apparently recorded.

It is planned to design, build and install a plane reflector system at the above station during the next reporting period. The increase in orbital cross track drift control, combined with our orbital prediction programme shortly coming into use, will enable this system improvement to be made. An increase in reflected power density and uniformity will result from this upgrading.

2.7   "PEACESAT"

The link has not been used over the last reporting period due principally to Peter Ellis making a visit to GSFC and other agencies in the U.S. With the commencement of the Southern Hemisphere's academic year we look forward to further exchanges with our South Pacific colleagues.

2.8   Laboratory Upgrading

With the increasing interest being shown in remote sensing by outside agencies it has become necessary to provide more space and better facilities for users to work alongside the P.E.L. group. The analysis and darkroom areas are being redesigned to allow users to operate interpretative equipment independent of darkroom operations. These areas are scheduled to progress towards "clean room" status.

3. ACCOMPLISHMENTS, IMMEDIATE OBJECTIVES AND SIGNIFICANT RESULTS

3.1 Image Rectification Results

The package of computer programs for geometrically correcting LANDSAT subimages, which was described in section 2.5, has been tested on LANDSAT II scene 2334-21123. Preliminary results are presented in this section.

Nineteen points suitable for use as ground control points (GCP's) were chosen by inspection of the LANDSAT scene. These points were the centres of small lakes and forest road intersections, and mainly sharp water-land interfaces. A number of shaded computer lineprinter outputs were then obtained which included each GCP. New Zealand standard inch to the mile (1:63360) UTM maps were then obtained which also included each GCP. The co-ordinates of each GCP in the LANDSAT image and the map were then determined by examining, for each GCP, the appropriate shaded printout and map together. To obtain reasonable accuracy (i.e. $\pm$ 0.5 pixel in the image row and column co-ordinates and $\pm$ 20 yards in the map co-ordinates) it is most important that the printout and map should be examined together. Our experience is that the best type of GCP is a land-water interface with the land forming an acute angled peninsula.

In Table 3.1.1 the image co-ordinates and the map co-ordinates are given for the nineteen GCP's. It should be noted that the image columns given have not been corrected for the pixels inserted by NASA to correct for line length variations. Also shown in Table 3.1.1 in meters for each GCP is the distance between the result of mapping the GCP in map co-ordinates to the image, and the GCP measured in image co-ordinates. The distribution of the GCP's and the direction and size of the errors is shown in Figure 3.1.1. All possible corrections were included in the mapping function. The corrections for the altitude variation of the GCP's and the pixels inserted to correct for line length variations seemed to have little effect. This was perhaps because their effects were small compared to the mean absolute error of 49 m.

Many suitable GCP's were available in this image, as there are for most New Zealand scenes so long as there is not too much cloud cover. More images need to be processed, and the processed images need to be compared to maps before the mapping accuracy of this method can be fully evaluated. However, initial tests indicate the accuracy is sufficient for our purposes.

GCP Number	Image (pixels)		Map (yards)		Error (meters)
	Row	Column	Northing	Easting	
1	2001.2	180.2	377180	311220	34
2	1917.0	2155.5	357610	435460	102
3	1412.5	208.0	426220	326610	81
4	1003.0	2188.5	433830	458860	41
5	1166.3	1266.2	432600	397700	72
6	385.0	546.0	508040	371460	94
7	313.8	1402.5	502370	426290	40
8	240.5	2945.5	487700	523490	29
9	1359.3	3205.5	390300	513020	62
10	2024.2	169.6	375350	310050	18
11	1441.2	286.3	422800	330810	14
12	1009.7	2169.1	433550	457590	2
13	413.0	584.0	505050	373250	82
14	253.4	693.4	517110	383770	84
15	255.5	741.5	516220	386610	33
16	300.0	799.2	511750	389170	16
17	347.7	812.0	507580	388840	23
18	385.0	781.8	504890	386060	49
19	393.0	790.8	504100	386450	55
Mean absolute error					49

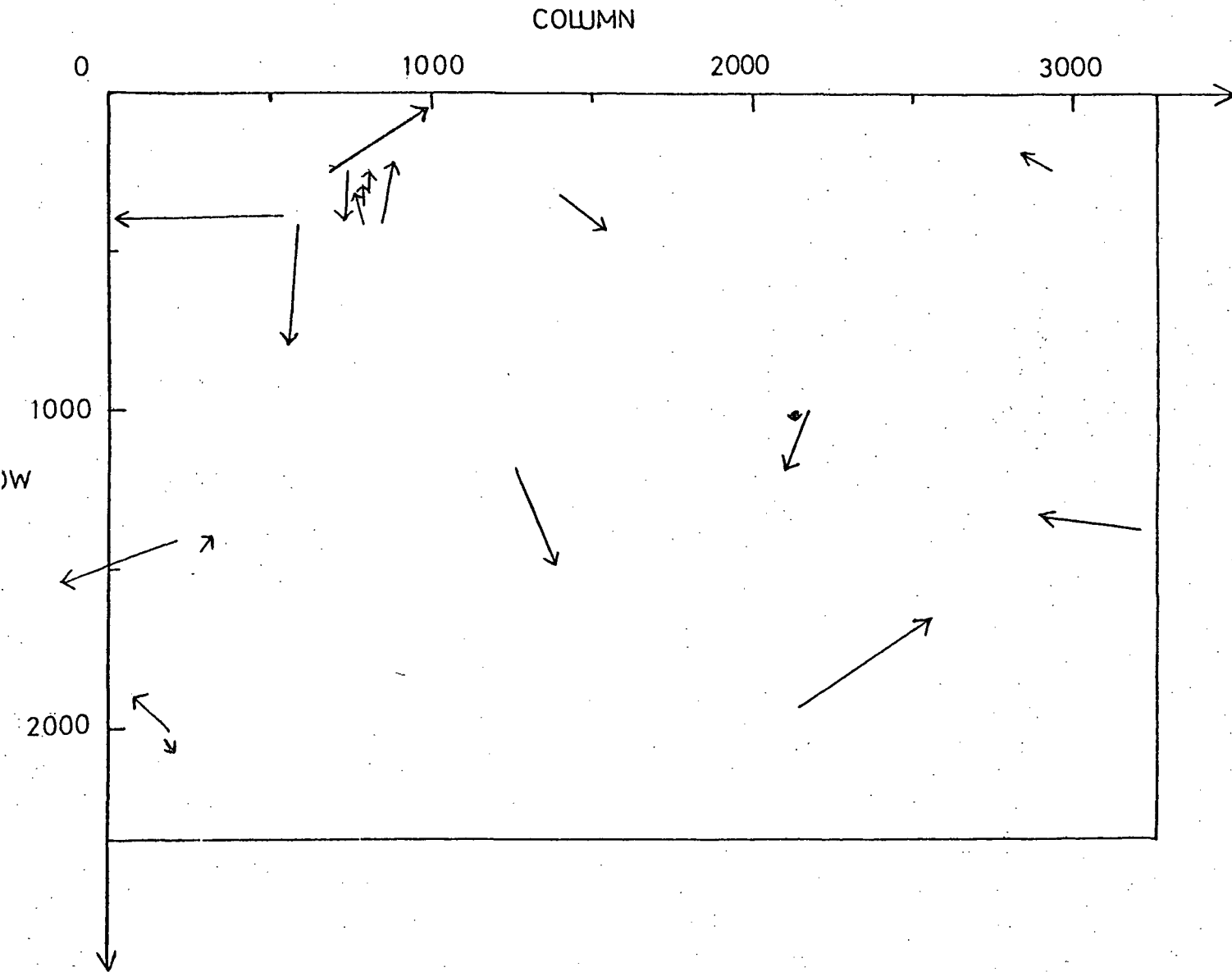Table 3.1.1   Image and map co-ordinates, and mapping errors for 19 GCP's.

Figure 3.1.1   The positions of the 19 GCP's used in
the geometric correction of LANDSAT
scene 2334-21123 are shown by the start
of the arrows. The length and direction
of the arrows depict the mapping errors
for each GCP.

3.2   Ship Detection from LANDSAT

Although the usefulness of LANDSAT data for mapping and monitoring earth resources has been demonstrated repeatedly, one potential application of the data which seems to have been overlooked is ship detection.   Recent inspection and analysis of pixels (picture elements) obtained from LANDSAT computer compatible tapes (CCT's) of New Zealand revealed that not only can ships and their wakes be detected but that information on the size, state of motion (stationary or moving), and direction of movement can be inferred by calculating the total number of pixels occupied by the vessel and wake, the orientation of these pixels, and the sum of their radiance values above the background level.   In this paper the procedures used for detecting ships are presented, and the problems and limitations of the technique as related to ship parameters, sea state and turbidity, pixel overlap and the relative geometric fidelity between pixels are discussed.

New Zealand is an isolated South Pacific country consisting of two main islands and a number of smaller ones.   Inter-island and international shipping activities are very important to the country's economy.   It is possible that future satellites such as SEASAT-A will provide a means of monitoring ship movement on a real-time basis.   In view of this it was of interest to test the feasibility of using LANDSAT II visible and near-infrared recorded radiometric data for ship detection.   SEASAT, with its active imaging microwave sensor, should prove more applicable to ship detection because of its improved resolution and its near all-weather and day/night imaging capabilities.   However, no satellite data of this type is yet available for evaluation.

Regular scheduling of inter-island ferries between the North and South Islands of New Zealand made it likely that the location of ships would be known at the time of a LANDSAT II overpass. Also, the generally low turbidity of the water in Wellington Harbour and Cook Strait simplifies ship detection.   For these reasons the Cook Strait area of New Zealand was a logical test site for this investigation.

A set of procedures was established in the early stages of the study to remove much of the subjectivity involved and to help make automatic ship detection through computer processing of LANDSAT data possible in the future.   Ship detection was accomplished using coded computer lineprinter outputs which displayed the radiance levels for each LANDSAT MSS band in a 128 pixel wide strip. Experience has shown that band 7, and to a lesser extent band 6, because of the very low radiance values from water (usually zero for band 7), is the best band for a "quick look" detection of possible ships.   The low background radiance values from water in bands 6 and 7 result in a high signal to noise ratio (S/N) even though the absolute value of the signal above the background (S-N) is considerably higher in bands 4 and 5.

The procedure used for establishing the pixels occupied by the target is as follows:

    I   Locate possible ship on MSS band 7 printout of
        radiance values.   Three levels above the modal

background (i.e., the most commonly occurring
radiance level for the sea in the printout) is
used as the threshold for establishing a possible
target.

II   Analyse the other three MSS bands to confirm
     that the target is present on all bands. An
     anomalously high value at the same pixel
     location as in I is sufficient test.

III Using the pixel with the highest value in band 7
     as the ship's center, and the center of a sampling
     array, five rows and nine columns are sampled in
     each band.

IV   A maximum background threshold is established
     for each band and row sampled in III by finding
     the maximum of 10 pixel values within the row but
     outside the sampled area. Where possible five
     pixel values are taken on each side of the sampled
     area. This sampling is done separately for each
     row to eliminate the six-line-striping characteristic
     of LANDSAT data. The sampling is done away from the
     suspected ship to prevent target contamination of
     the background noise level.

V   In each band and for each row the maximum background
     threshold value is then used to eliminate the pixels
     from III whose radiance values were not affected by
     the target. Pixel values less than or equal to the
     threshold are set to zero as are pixels above the
     threshold but not in a row or column adjacent to a
     target pixel. The center pixel in III is taken as
     the first target pixel.

VI   For each band, the average background value for
     each row is calculated from the ten sampled pixels
     in IV, and this is subtracted from the radiance
     value of each pixel not set to zero in V.

VII The result is a 9 x 5 matrix of pixel radiance for
     each MSS band that defines the number, location and
     radiance values of pixels occupied by the ship and
     its wake.

    Two LANDSAT II scenes of Wellington Harbour (2334-21132 taken
on GMT 22 December 1975 and 2335-21190 taken on GMT 23 December 1975)
were used in this study. Details on five ships known to be in one
or both of these images are given in Table 3.2.1. All of the vessels
except the HMNZS Rotoiti were successfully located. Table 3.2.2 gives
the CCT radiance levels, before and after the authors' processing,
from the four LANDSAT MSS bands for the Aratika, an inter-island
ferry, and a given surrounding area. Our experience is that the
location and size of a vessel is better indicated by the radiance
values above the average background for the near-infrared bands than
the visible bands. This appears to be due to the greater reflectivity

of the ship's wake[1]. The direction of ship movement can then be inferred from the position of the wake with respect to the ship (see Table 3.2.2).

At the time of satellite overpass, the Arahanga (GMT 22 December 1975) and the Aramoana (GMT 23 December 1975) are known to have been slow moving or stationary. This explains the low radiance levels for these two ships in Figure 3.2.1 and indicates that most of the reflected energy recorded in MSS bands 4, 5 and 6 is due to the ship's wake. Because band 7 is least influenced by the wake, as indicated by Figure 3.2.1 and Table 3.2.2, it is the best band to use as an indication of the ship's size and position.

Measurements of the total reflected energy (Figure 3.2.1) and the maximum value above threshold (Figure 3.2.2) are both subject to considerable error. Errors in the radiance levels as in Figure 3.2.1 are introduced by NASA quantisation techniques, the 22 m pixel overlap per 57 m sample spacing, and the authors' processing. Although pixel overlap does not contribute to the maximum radiance errors in Figure 3.2.2, it does introduce a larger variation resulting from the positioning of the pixels with respect to the vessel. For example, a ship, the length of a pixel, may be sampled completely within one pixel or straddle up to six pixels.

The best indication of ship size is given by the total radiance values in MSS band 7 (Figure 3.2.1). This is because the total radiance values for a given size are more consistent than maximum radiance levels (Figure 3.2.2) and also because of the low near-infrared reflectance of the ship's wake in MSS band 7. The smallest ship positively identified was 112 m long (see Table 3.2.1) In theory it should be possible to detect vessels 30 m long under favourable imaging conditions. For example, based on the average signal per unit ship area produced by the moving ships, the HMNZS Rotoiti would be expected to produce a total radiance value (after processing) of 3.1, 3.3, 3.4 and 1.0 in bands 4, 5, 6 and 7 respectively. This implies that a small boat may best be found by lowering the threshold level in band 7 to one level above the modal background and then confirm or reject the suspected target by examining the other bands as in step II of the procedure described previously.

Figure 3.2.3, a plot of signal to noise (S/N) ratio against band number for the five positively identified ships[2], indicates that MSS band 7 is the best band for initially locating ships because of the high S/N ratio.

---

1. The ship's wake is defined by the pixels which, after processing, are zero in band 7 but non-zero in band 4.

2. A number of other possible ships were also found, but ground truth for them was not available.

A number of problems were encountered in trying to detect ships. For example, the contribution of turbidity to radiance variations in the sea needs to be of low spatial frequency. Also the 22 m pixel overlap along rows needs to be taken into account in determining the most likely position for the vessel, as do the extra pixels NASA have inserted to compensate for variations in scan line length.

Anomalies were found in the data which we were unable to adequately explain. For example one pixel in the Tasman Sea in band 7 had a radiance value of 63. This is the maximum possible value in band 7 and is at least fifteen times greater than the maximum band 7 radiance for any ship studied. The pixel was surrounded by pixels of value 0. No anomalous radiance value was found nearby in either band 4 or 5 but a high value was found in band 6 which was, however, offset by two pixels along a row. The only plausible, but unlikely, explanation suggested was that the high values were caused by reflections from another satellite passing beneath LANDSAT II with the offset between bands being caused by the slightly different sampling times for bands 6 and 7.

Figure 3.2.4 is a coded computer printout of MSS band 7 showing the Aratika approaching the entrance to Tory Channel in the Marlborough Sounds.

Table 3.2.1

Description of Ships Present in LANDSAT II Scenes Studied

Ship's Name	Type	Length (m)	Breadth (m)	Tonnage	GMT date	Symbol i Figures
Osco Sailor	Oil Tanker	171.8	26.6	21,275	23 Dec 75	O
Aratika	Inter-island ferry	127.7	18.8	3,879	23 Dec 75	.
Arahanga	Inter-island ferry	127.5	18.8	3,894	23 Dec 75	+
Arahanga	Inter-island ferry	127.5	18.8	3,894	22 Dec 75	−
Aramoana	Inter-island ferry	112.2	18.6	4,160	22 Dec 75	▢
HMNZS Rotoiti	Fisheries protection vessel	32.1	6.1	134	23 Dec 75	

Table 3.2.2

LANDSAT Radiance Data for the Aratika

(Source: LANDSAT II scene 2335-21190)

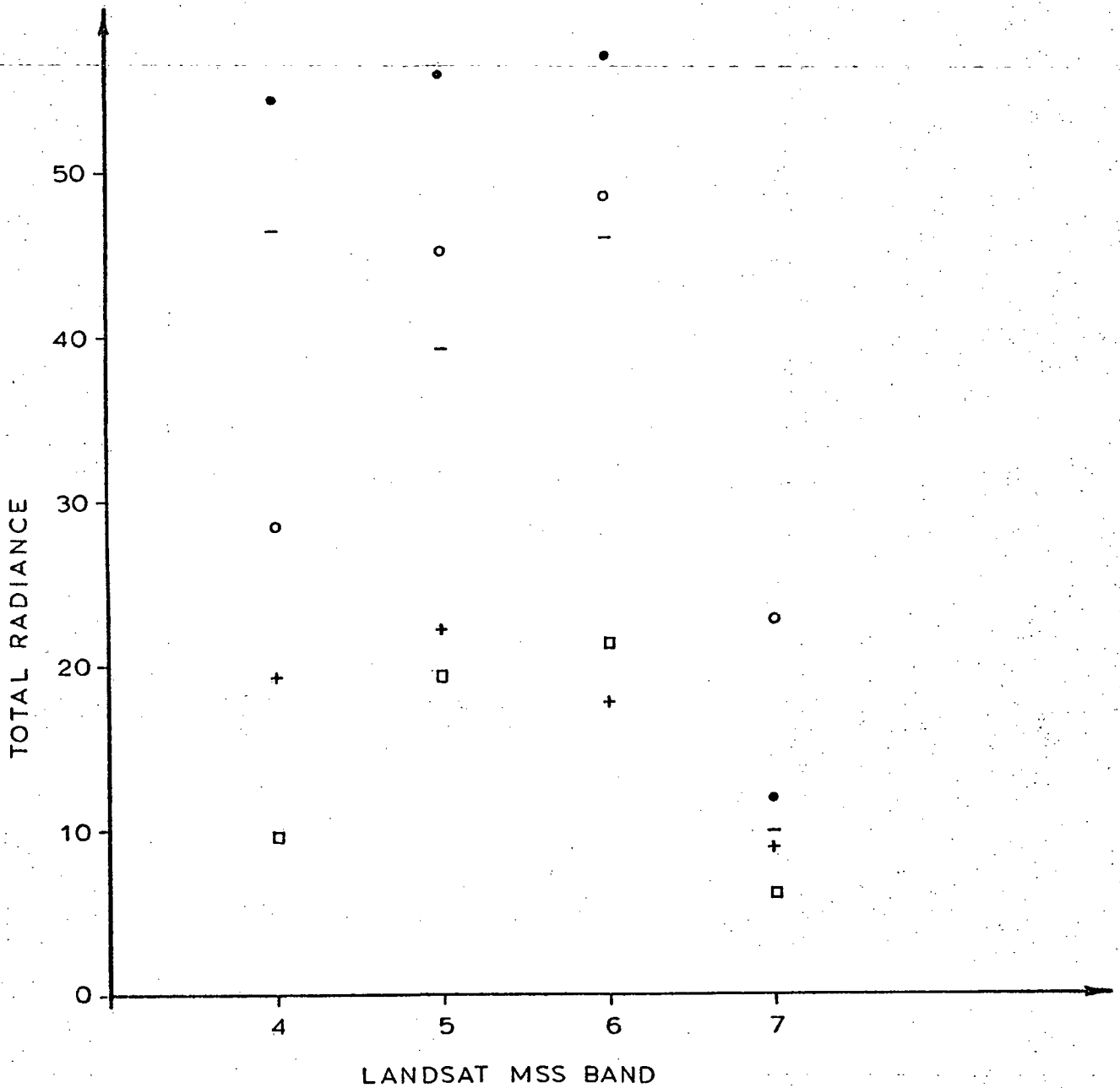|		Before Processing						After Processing					
		Column						Column					
		1462	1463	1464	1465	1466	1467	1462	1463	1464	1465	1466	1467
MSS Band 4													
	Row 739	16	16	15	14	14	14	2.2	2.2	1.2			
	740	12	16	22	24	19	13		3.0	9.0	11.0	6.0	
	741	12	12	13	17	24	19				3.7	10.7	5.7
	742	14	14	14	14	14	14						
MSS Band 5													
	Row 739	10	11	9	8	8	9	2.0	3.0				
	740	8	10	15	19	13	8		2.2	7.2	11.2	5.2	
	741	8	8	8	13	20	14				5.0	12.0	6.0
	742	8	9	8	9	9	8				1.4	1.4	
MSS Band 6													
	Row 739	4	4	4	4	2	2	2.6	2.6	2.6	2.6		
	740	2	6	10	12	8	2		3.4	7.4	9.4	5.4	
	741	5	4	5	10	16	10				5.3	11.3	5.3
	742	5	5	4	5	4	5						
MSS Band 7													
	Row 739												
	740			2	2						2	2	
	741				2	4	2				2	4	2
	742												

Figure 3.2.1   Total reflected energy (in LANDSAT quantised
                units) versus MSS band number for each of the
                five positively identified ships given in
                Table 3.2.1.

                O   Osco Sailor   +   Arahanga (GMT 23 Dec 75)
                .   Aratika   -   Arahanga (GMT 22 Dec 75)
                ⊡   Aramoana
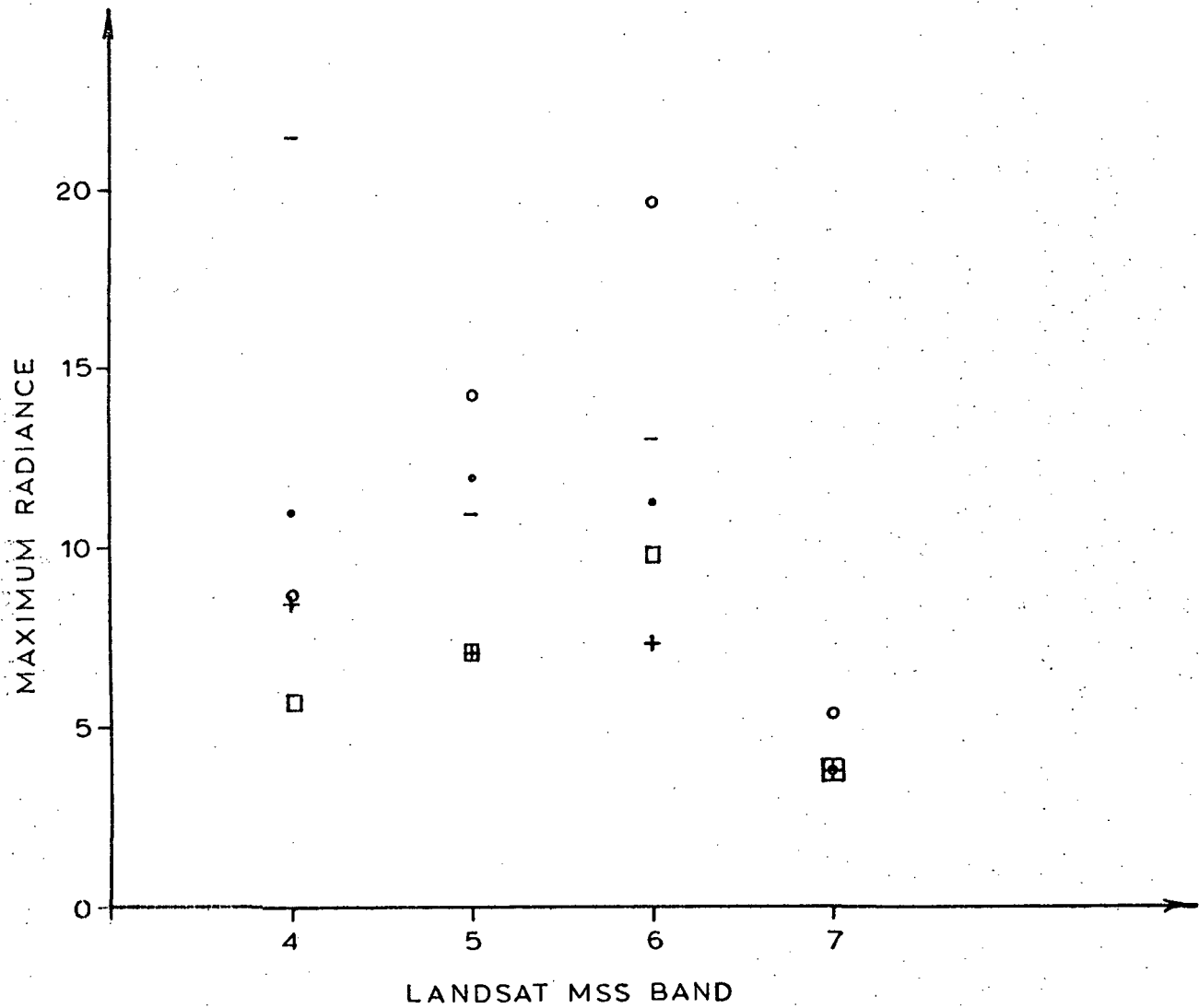
Figure 3.2.2   Maximum pixel value above threshold versus MSS
                band number for each of the five positively
                identified ships given in Table 3.2.1.

                O   Osco Sailor   +   Arahanga (GMT 23 Dec 75)
                .   Aratika   -   Arahanga (GMT 22 Dec 75)
                ☐   Aramoana
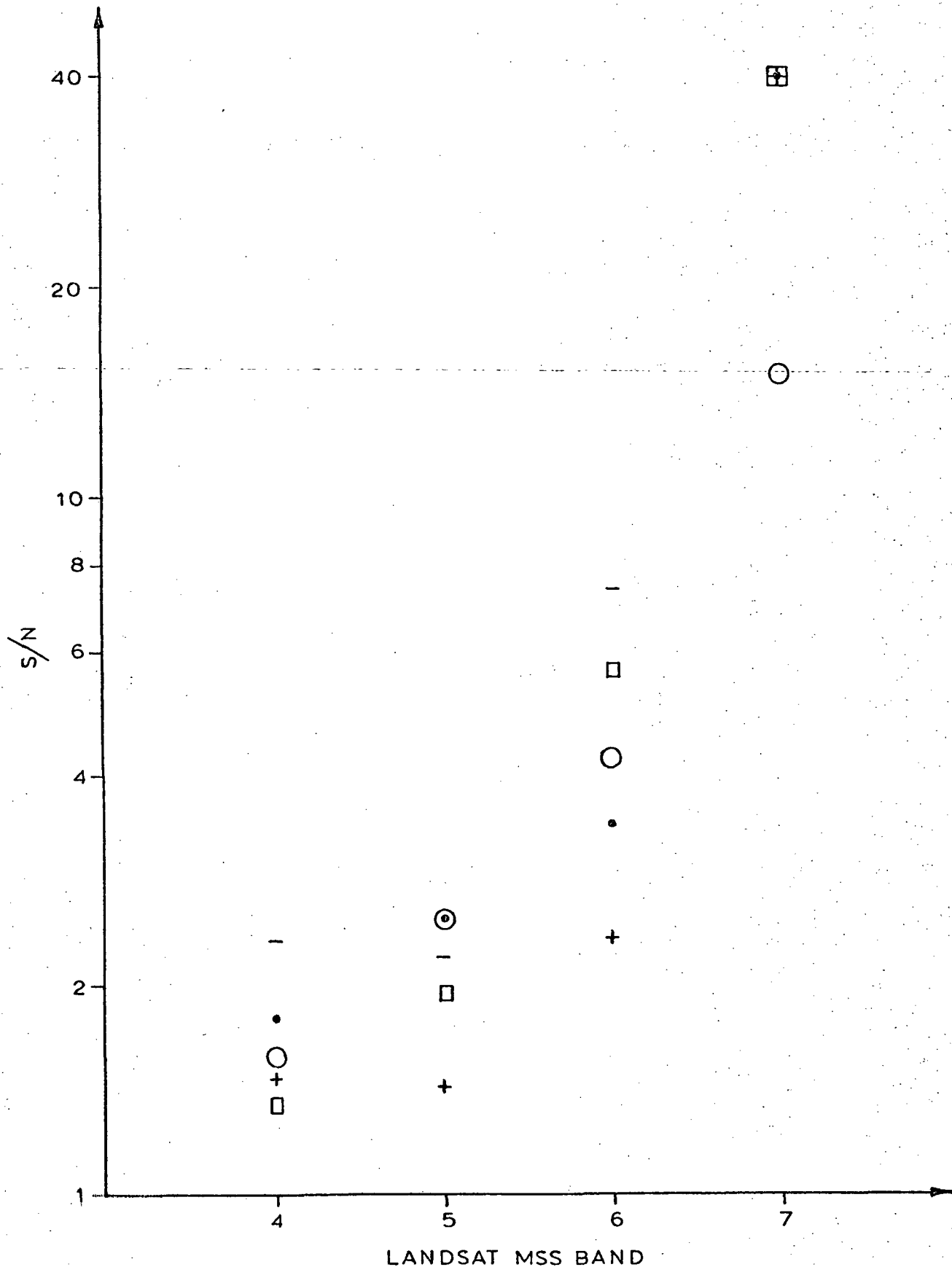
Figure 3.2.3   Signal to noise ratio (S/N) versus MSS band
                number for each of the five positively
                identified ships given in Table 3.2.1.

                O   Osco Sailor   +   Arahanga (GMT 23 Dec 75)
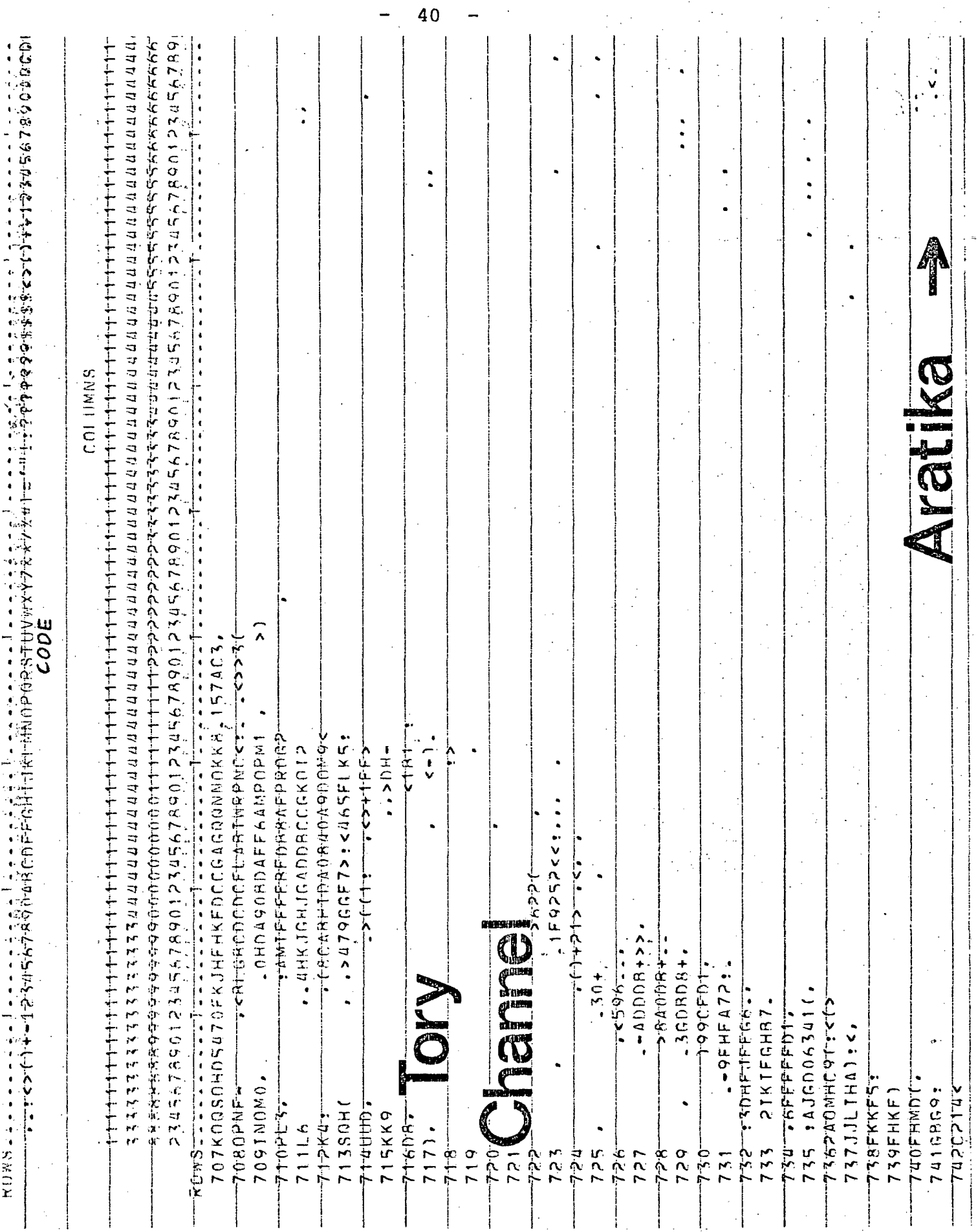   .   Aratika   -   Arahanga (GMT 22 Dec 75)
                □   Aramoana

Figure 3.2.4   Coded computer printout of MSS band 7 showing the Aratika approaching the entrance to Tory Channel (GMT 23 Dec 75) LANDSAT scene 2335-21190.

3.3 Kaingaroa State Forest Interpretation

Figure 2 in Part I of our Third Quarterly Report is a computer
enhanced image showing the Waimihia State Forest and much of the
Kaingaroa State Forest on 22 December 1975. This image has been
compared with the New Zealand Forest Service species distribution
map of the area which was correct at 31 March 1975. The purpose
of the comparison was to determine what forest categories would be
distinguished using LANDSAT imagery.

Forest species on the map were divided into ten categories
which are shown in Table 3.3.1. For each category, the colour or
range of colours associated with it in the LANDSAT image is also
given in Table 3.3.1. Areas of forest which had been logged showed
up clearly as light blue. It was easy to see areas of forest which
had been cleared since the map had been compiled. It was not
possible to divide the LANDSAT image into ten distinct colours
corresponding to the somewhat arbitrary Forest Service categories.
However, P. radiata, Ps. menziesii and P. ponderosa did form
distinct colour groups. P. nigra looked like P. ponderosa or pre
1941 P. radiata (unthinned). Within a single species (e.g. P. radiata
the main colour differences were due to variations in the age of the
trees (as the age increased the colour darkened). Variations due to
treatment (e.g. thinning) were much less obvious and were only
noticed for P. radiata. Forest plot 629 was dark green instead of
orange-red, apparently indicating a mistake on the forest map. It
is possible that the areas which appear black in the LANDSAT image
would have occupied a wider colour range if the image had been
enhanced solely for forest areas.

In conclusion, most major forest categories can be distinguished
on LANDSAT imagery. However, the LANDSAT imagery seems to be most
useful for updating and checking existing forest maps, rather than
making new maps with many forest categories.

Table 3.3.1   Forest categories used in Forest Service
31 March 1975 map of Kaingaroa State
Forest, and their corresponding colours
or colour ranges in Figure 2 of Part I
of our Third Quarterly Report.

Forest Category	Description	Colour
1	P. radiata pre 1941 - not thinned	Black
2	P. radiata 1941 to 1974 - treated to thinning after high pruning	Dark brown with a slight green tinge
3	P. radiata 1941 to 1974 - not treated to thinning after high pruning	Dull red-brown to light green-brown
4	P. radiata pre 1941 - thinned	Very dark brown
5	Ps. menziesii pre 1941 - thinned	Bright red
6	Ps. menziesii pre 1941 - not thinned	Bright red
7	Ps. menziesii 1941 to 1974	Orange-red
8	P. ponderosa	Green to dark green
9	P. nigra	Dark green to black
10	Other species	Variety of above colours

3.4 Use of LANDSAT MSS Data in Snowfield Assessment

Introduction

In order to adequately assess New Zealand's snow resources time sequential LANDSAT imagery is essential. This is currently not available and this study is directed at exploring the technique of utilising such imagery based on one LANDSAT scene. LANDSAT 1, 2 areal resolution is generally adequate for most such studies. P.E.L. was approached by the New Zealand Forest Service acting on behalf of the National Parks Authority to jointly assess the relative merits of two snowfield areas for possible skifield development. (This joint study was first reported on in the Forest Service section of the Third Quarterly Report and is added to here.)

Common to all snow field assessment studies are the questions of snow area, type and depth. The peculiar questions of access, slope and general terrain are left, in this study, to the skiing fraternity.

The two areas considered in this study are Mt. Robert (41.85°S 172.80°E) and Six Mile Creek Basin (41.88°S, 172.85°E).

Methods

The study has been divided into three stages: transect selection, aereal planimetry, and analysis and interpretation of CCT data for snow depth/typing. All stages use the one cloud-free LANDSAT scene available of the study area. (Scene ID no. 2282-2125 recorded on 31 October 1975 (GMT).)

Transect Selection

The first stage was the selection of a suitable transect line for a continuing programme of ground measurements on snow depth/typ On the basis of the colour-coded isodensitometric analysis of the MSS 4 positive transparency using a Datacolor 703, reported on in the Third Quarterly Report for this investigation, a transect was located as indicated in Figure 4c of Part V of this report.

New Zealand Forest Service field inspection of snow conditions commenced in early November 1976. A transect was established from 5,200 ft to 5,900 ft elevation above sea level. Six permanent stations were positioned so that snow depth and surface conditions could be recorded. These stations consisted of a centre pole and measurements were taken at 10 locations each 10 metres apart to the right and left of the six centre poles. Similar data will be collected at regular intervals corresponding to future satellite overpasses during the snow season. Occasional aerial surveys are to accompany the ground surveys and ground photographs are to be taken during the field survey.

Planimetry and Snow Area Measurements

The second stage of the study, again executed by the New Zealand Forest Service, used the colour-coded isodensitometric analysis of the MSS 4 positive transparency to derive using a planimeter the area covered by each of the four highest intensity levels recorded on the photographic product.

This was done by first projecting the 35 mm colour slide, taken off the Datacolor 703 screen, onto a base map. This map/ projector system was suitably oriented to counteract most distortions and scale differences. Following transferral of the four highest regions standard planimetric techniques led to the deduced percentage areas presented in Table 3.4.1.

Table 3.4.1

Percent of Area by Intensity Categories: Six Mile Creek and Mt. Robert.

Intensity Category	Percent of total area studied	
	Mt. Robert	Six Mile Creek
I. Highest level (purple)[1]	26%	43%
II. Second (orange)[1]	36%	30%
III. Third (yellow)[1]	35%	19%
IV. Lowest level[2] (black)[1]	2%	7%
Total Area	193.9 ha	498.4 ha

Source: MSS band 4 positive, Scene # 2282-21252

1. Colours refer to Figure 6, Part V of the Third Quarterly Report.

2. Interpreted as open ground - no snow cover.

Analysis of CCT Data

The third stage, conducted by P.E.L., was directed at relating the CCT derived radiance profiles along transects to the likely snow conditions at the time of the overpass.

In further assessing the two snow field areas, Mt. Robert and Six Mile Creek, 47 level coded character printouts of each MSS band of the CCT data for the 31 October 1975 scene (no. 2282-21252) were prepared on the IBM 370/168.

CCT Transect Lines

Four transect lines were selected for study: one approximately along the existent Mt. Robert Ski Field tow line and three in the Six Mile Creek Basin (Figures 4a and 4b of Part V of this report). Transect (D-A) was placed along the New Zealand Forest Service snow sampling line. Transect (D-C) was established to approximate the sun illumination angle on the Mt. Robert transect (E-F) and transect (D-B) was set up on the predominantly sunward slope approximately opposite the D-A transect.

Aided by black and white enlargements of the area for each MSS band and topographic maps, ground control points were transferred to the coded computer printouts.

The computer user has no control over the column or row spacing or over the character size used in the line printer output. Consequently mapping distortions are present in the line printer products, particularly when sampling is oblique to the LANDSAT scan lines. To partially overcome this distortion the control points were always established by measuring direction and distance either parallel or perpendicular to scan lines, from a known location. As a consequence a positional accuracy of + 2 pixels may be ascribed to the relationship between the ground feature and the CCT derived radiance.

Determination of the Radiance Levels from the CCT Data

The CCT level data was converted to radiance data in (milliwatt per steradian per square centimetre per bandwidth), for the followi reasons:

1. Small variations in spectral radiance could signify different melt/freeze histories or density regimes in the snow (O'Brien and Munis, 1975).

2. The low gain mode in three of the four MSS channels has approximately the same full scale radiance response but such is not the case for MSS 7.

3. The CCT data for MSS 4, 5, 6 is decompressed
   (range 0-127) whereas, the MSS 7 data is in the
   linear mode (range 0-63).

The bandwidths of MSS 4, 5, 6 are all nominally the same
at 100 nm but that for MSS 7 is nominally 300 nm. This latter
MSS band spans a number of water vapour absorption bands in the
atmosphere, whose contribution is largely uncertain. Consequently
the radiance is expressed in "bandwidth" terms rather than in
"nanometer" terms.

The pixel radiance values were plotted together with the
topographic elevation profile and presented in Figures 3.4.1, 2,
3 and 4. (The uncertainties in the four MSS band radiances are
$\pm$ 0.03 (mw ster^{-1} cm^{-2} bandwidth^{-1}) for MSS 4, $\pm$ 0.02 for MSS 5,
$\pm$ 0.02 for MSS 6 and $\pm$ 0.09 for MSS 7.)

Criteria for Boundary Selection

The next step was the determination of the snow region
boundaries along each transect. Obviously in regions where the
snow cover is sparse the uncovered terrain will contribute to the
final recorded radiance levels for each pixel.

Realising that snow will always increase the recorded radiance
over that of the basic ground terrain leads to the two major
criteria for selecting a boundary between terrain and snow and
then between types of snow.

The first criterion involves plotting the frequency of
occurrence, in selected radiance intervals for each MSS band, and
noting natural groupings of radiance "blocks" at the greater
radiance end of the scale. For this study data from all four
transects were used in these plots so that this "radiance block"
classification criterion would be uniform between the Mt. Robert
and Six Mile Creek Basin. The plots are presented in Figure 3.4.5.

The second criterion relies on all bands responding to
changing terrain/snow or snow/snow boundaries by all recording
increased or decreased radiances together. This "radiance gradient"
classification criterion was used to check the suggestions advanced
by the "radiance block" selection process. (This selection order
was used to avoid any possible analyst bias in boundary selection.)

As a final check the selected boundaries were marked on the
Figures 3.4.1, 2, 3 and 4, and the topographic elevation noted. In
the "control" basin, which spanned a range of sun illumination
angles but had essentially the same climatic regime, a similar
altitude would be expected for each boundary.

Boundary Selection

Upon inspection then of Figure 3.4.5 the "radiance block"
selections were performed for each band and then checked using the
"radiance gradient" criterion for each of the transects. The

selected boundaries were then marked by vertical bars on the transect plots (Figures 3.4.1, 2, 3 and 4).

It rapidly became evident that the "radiance gradient" criterion was a far more sensitive aid to boundary selection than "radiance blocking". For this reason extra boundaries to those indicated solely by "radiance blocking" were marked on Figure 3.4.1, 2 and 3. (Another could have been appropriate on transect E-F but the increased radiance values were not maintained and the ground topography changed character at the suggested boundary (around 5,000 ft elevation).) It was also apparent that MSS 7 "radiance block" values often did not reinforce the boundary positions indicated by the other bands. Its role in "radiance gradient" determination was equal to that of other bands.

The topographic elevations, and the applicable variations, were now read from the plots (Figures 3.4.1, 2, 3 and 4) and the results are presented in table 3.4.2.

Table 3.4.2

Topographic elevation (in feet), and variation of various ground cover/snow and snow/snow boundaries[1] extracted from the radiance transect plots of Figures 3.4.1,2,3 and 4.

Transect	D-A	D-B	D-C	E-F
Ground/snow	4850 $\pm$ 50 A	4700 $^{+\ 100}_{-\ 200}$ A	4600 $\pm$ 50 A	4650 $\pm$ 50 A
Snow/snow	5300 $\pm$ 50 A	5200 $^{+\ 100}_{-\ 200}$ A	4900 $\pm$ 150 A	(4900 $\pm$ 50 A possible only as history against it)
Snow/snow	5500 $\pm$ 50 B	5650 $^{+\ 100}_{-\ 50}$ A Overload obscures extra regions	5300 $\pm$ 50 A Overload obscures extra region	

1. These snow/snow boundaries labelled A would seem to indicate less dense/drier history snow at higher elevations. Those labelled B could mark denser/wetter history snow at higher elevations.

Field Data Collection

Several light aircraft overpasses were made with hand held oblique colour photographs being taken during September and October 1976. The photographs taken on 29 October 1976 (Figure 3.4.6) have been used to aid the analysis of LANDSAT CCT (31 October 1975) data. The time-lag of approximately one year is partially reconciled by inspection of New Zealand Meteorological Service climatic data for September and October of 1975 and 1976. Monthly summaries of temperature and precipitation for the Lake Rotoiti station (located between the two basins) indicate that there was little difference between the two years. Monthly mean temperature differences were less than 1°C and monthly precipitation differences were less than 4 mm. Snowfall for Lake Rotoiti station also indicates similar conditions prevailed at the time of the overpass to that shown in Figure 3.4.6. One week prior to each overpass fresh snow fell to the same elevation (2,500 ft). Sun elevation and azimuth angles differ between the overpass and the overflight due to the different times. The sun elevation and azimuth was 44° and 65° respectively for the LANDSAT overpass and 60° and 21° for the aircraft flight.

Field data and hand-held photographs were also acquired by one of the authors (AJL) during November 1976.

Interpretations and Conclusions

The primary objective of this study, to compare snow conditions in the two basins, has been accomplished using LANDSAT data. There is little question that the two basins exhibited great differences in the percentage of snow covered area (see Table 3.4.1) and the lower elevation of 100% snow cover when transects of MSS radiance values from the Six Mile Creek (Figure 3.4.3) and Mt. Robert (Figure 3.4.4) are compared. Upon inspection of these figures, it is noted that the Six Mile Creek Basin transect (D-C) has similar radiance values below 4,600 ft; slightly higher values between 4,600 and 5,000 ft; and much higher radiance values above 5,000 ft than the Mt. Robert Basin transect (E-F). It is therefore concluded that the differences in radiance levels indicate a greater areal snow cover in Six Mile Creek Basin, with the effect of lower radiance values from vegetation/snow regions contributing to the sample within the pixels in the Mt. Robert area. A comparison of the two visible bands (MSS 4 and 5) for the two basins demonstrates this difference. Over 50% of the transect in Six Mile Creek Basin has radiance values higher than the maximum radiance values in the Mt. Robert Basin. Confirmation of this conclusion is substantiated by the colour oblique photography (Figure 3.4.6) taken of the two basins at different times but, as mentioned previously, with similar snow conditions.

The LANDSAT data can be divided into different radiance/topographic categories that show similarity between transects (Table 3.4.2). Although a correlation of these numerical categories with natural conditions of snow is deemed possible, confirmation requires simultaneous field and satellite cover.

- 49 -

Several general observations have been made from the data that should help future interpretation of MSS radiance values from snow covered areas. The most important of these is the effect of local slope angles and orientation, on the radiance from the snow. The effect of orientation with respect to the sun is evident in a comparison of transects D-A (Figure 3.4.1), a south-facing slope directed away from the sun, and D-B (Figure 3.4.2), a north-facing slope directed towards the sun. Higher radiance values and even overloading in three bands was recorded for the sun facing slope. From aircraft photographs taken in September 1976 of the Six Mile Creek Basin, local hot spots from solar reflection appear at several locations along transect D-C. Overloading of the MSS 5 sensor well below the crest suggests that a similar phenomenon has occurred on the satellite overpass, i.e. strong solar reflection from a local slope facet resulting in a hot spot.

The areal extent of a snow field together with the snow/vegetation boundary is easily gleaned from the LANDSAT MSS data and requires little data manipulation. However, further information may be deduced from the natural breaks that occur in the MSS data. Although not confirmed, in this case, by corroborative ground data the breaks suggest variations in snow type, depth, history or some combination of the three did exist at the satellite overpass time.

The general increase in radiance values in the three Six Mile Creek Basin transects strongly suggests that the snow is fresher and drier as the elevation increases. This relationship of snow radiance and the condition and/or moisture content of snow was reported by O'Brien and Munis (1975). Along with the natural breaks in the data, this has been used with apparent success to categorise and classify these snow transects into four regions (Table 3.4.1). The two higher levels are interpreted to be potentially skiable snow and the two lower levels are probably non-skiable with the lowest radiance region being below the snow line.

Reference

O'Brien H.W. and Munis R.H. "Operational applications of satellite snowcover observations" published by NASA Report SP-391, p 345, (1975).
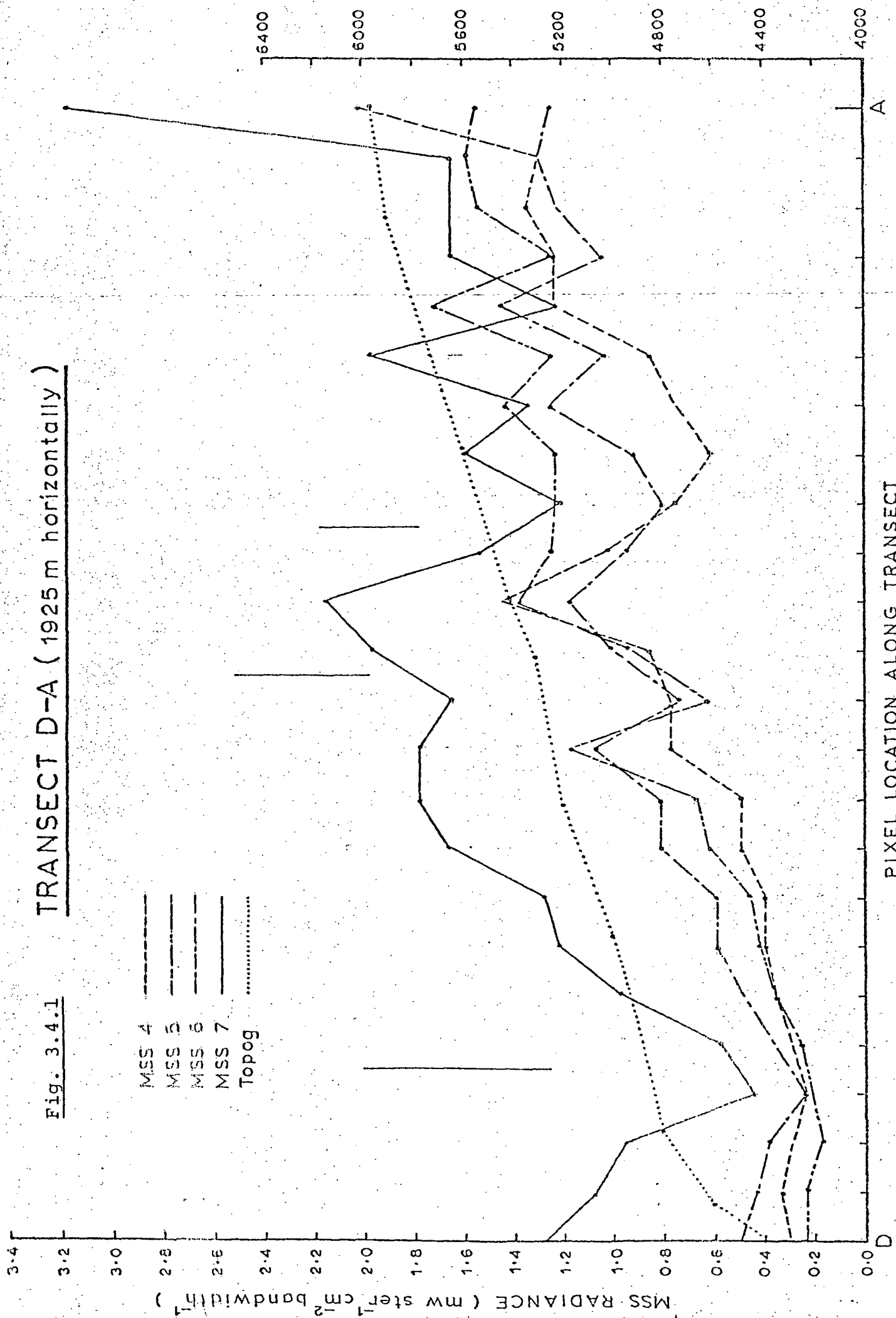
FIGURE CAPTIONS

Figure 3.4.1   The variation in MSS radiance along the D-A
                transect together with the ground topography
                profile. Suggested snow region boundaries
                marked by vertical bars.

Figure 3.4.2   As for Figure 3.4.1 for transect D-B.
                Overload regions shown as O-O-O-O.

Figure 3.4.3   As for Figure 3.4.2 for transect D-C.

Figure 3.4.4   As for Figure 3.4.1 for transect E-F.

Figure 3.4.5   The differential and cumulative frequency of
                radiance occurrence for each of the MSS bands.
                (This plot includes the data from all four
                transects D-A, D-B, D-C, E-F.)

Figure 3.4.6   Oblique aerial photographs taken on
                29 October 1976. Mt. Robert in the top
                photograph and Six Mile Creek in the bottom
                photograph.

Fig. 3.4.1

TRANSECT D-A (1925 m horizontally)

TOPOGRAPHIC ELEVATION (ft.)

MSS RADIANCE (mw ster^{-1} cm^{-2} bandwidth^{-1})

PIXEL LOCATION ALONG TRANSECT

MSS 4
MSS 5
MSS 6
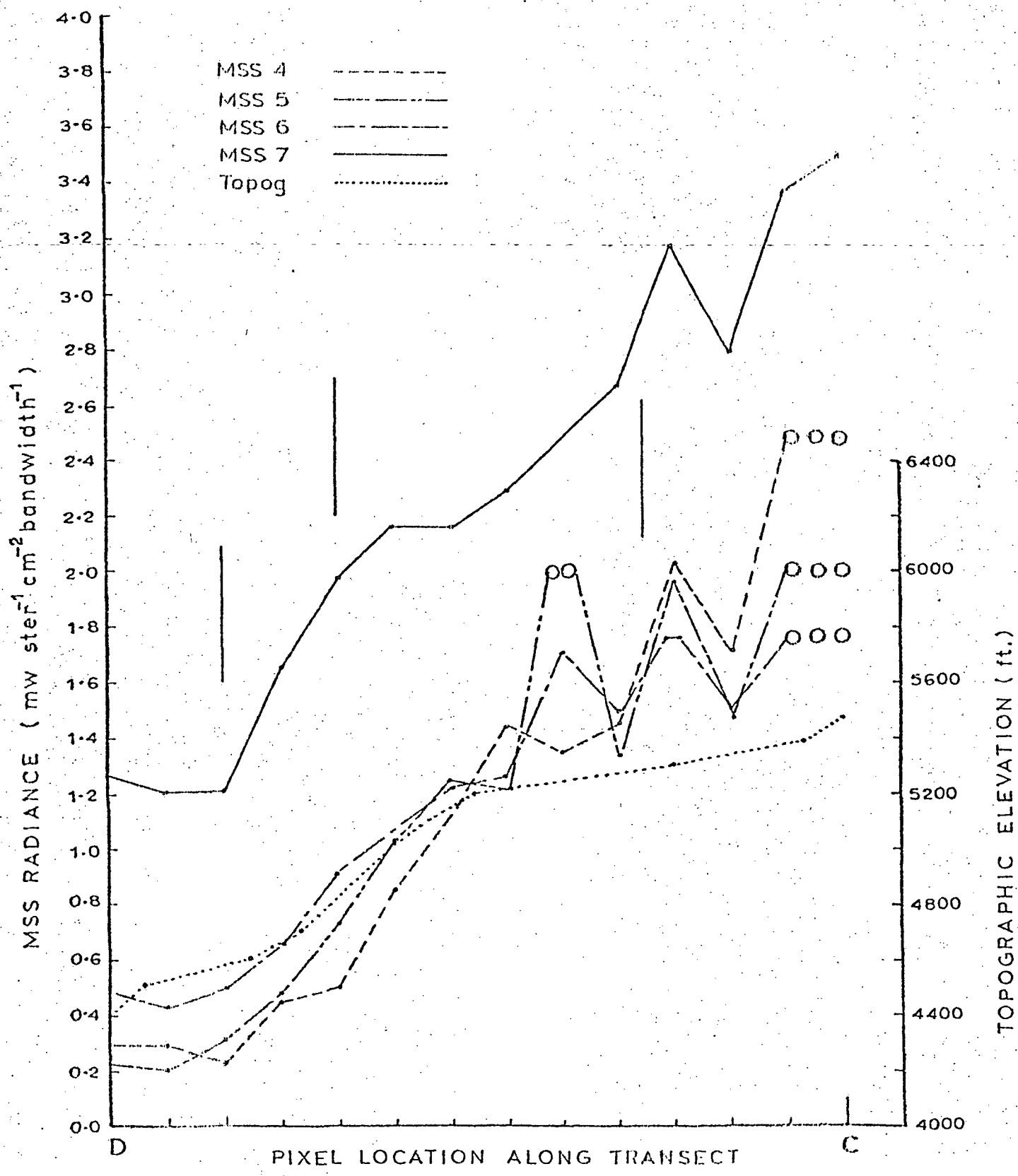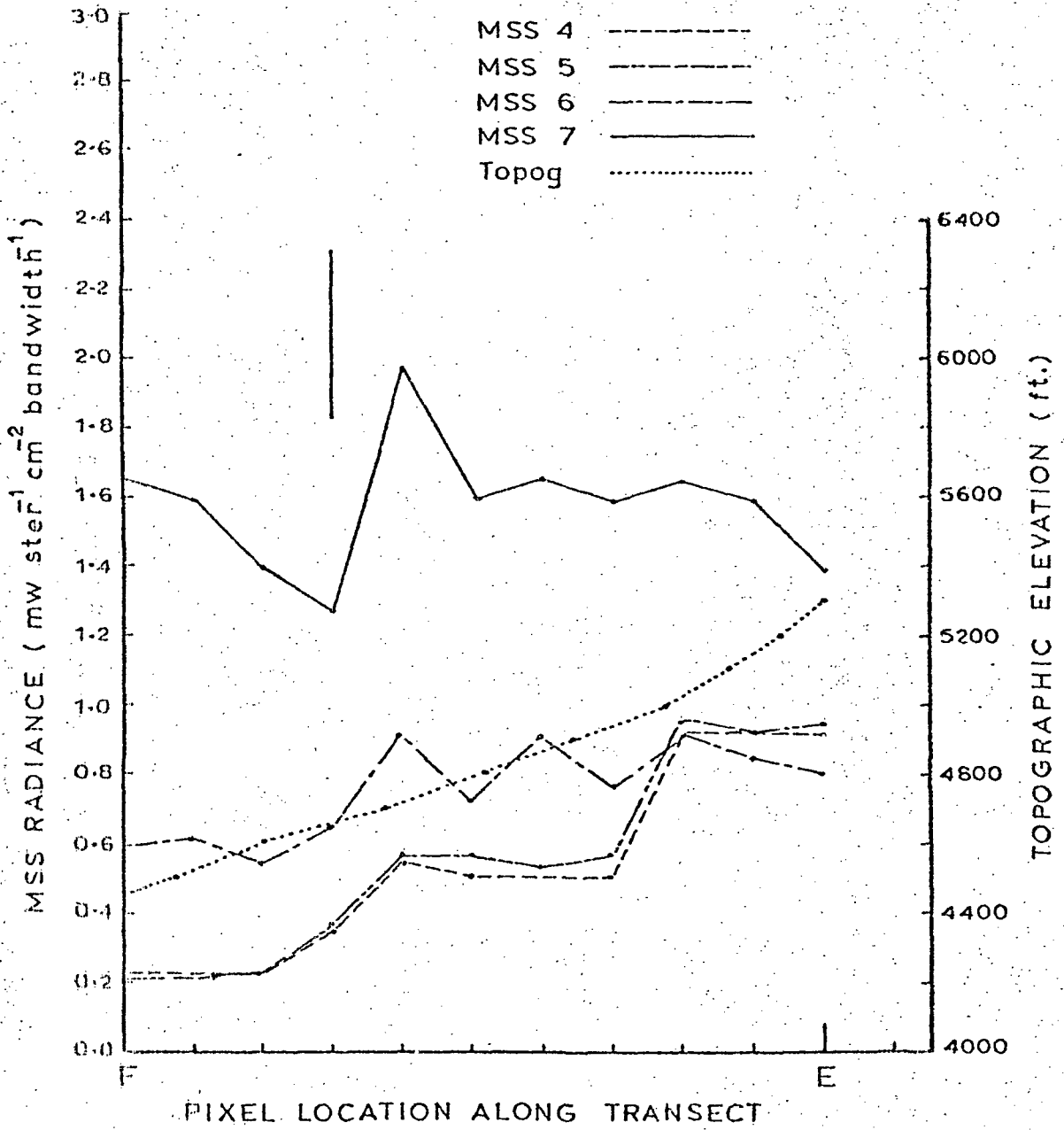MSS 7
Topog

- 51 -
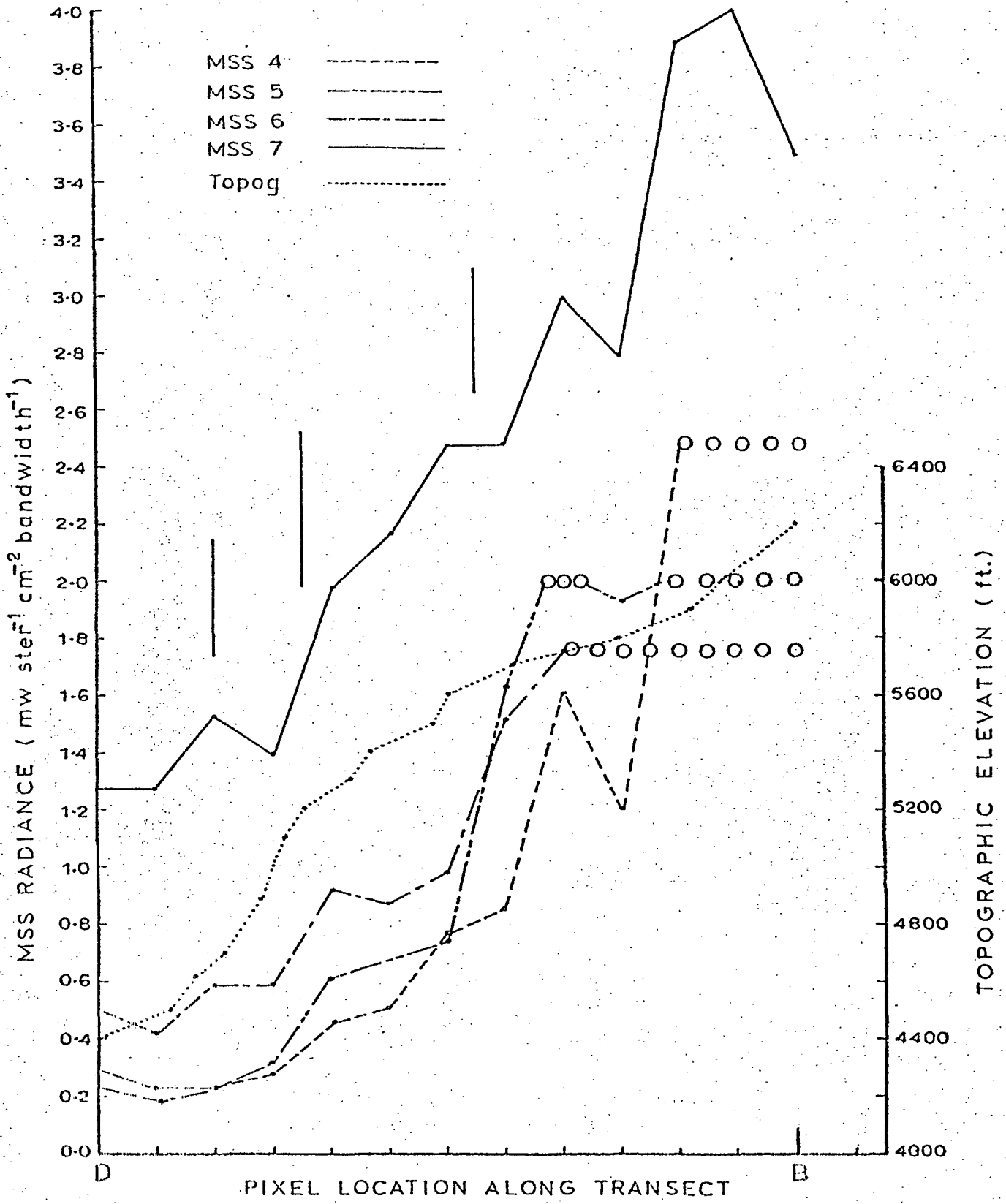
TRANSECT D–B (1400m horizontally)

Fig. 3.4.2

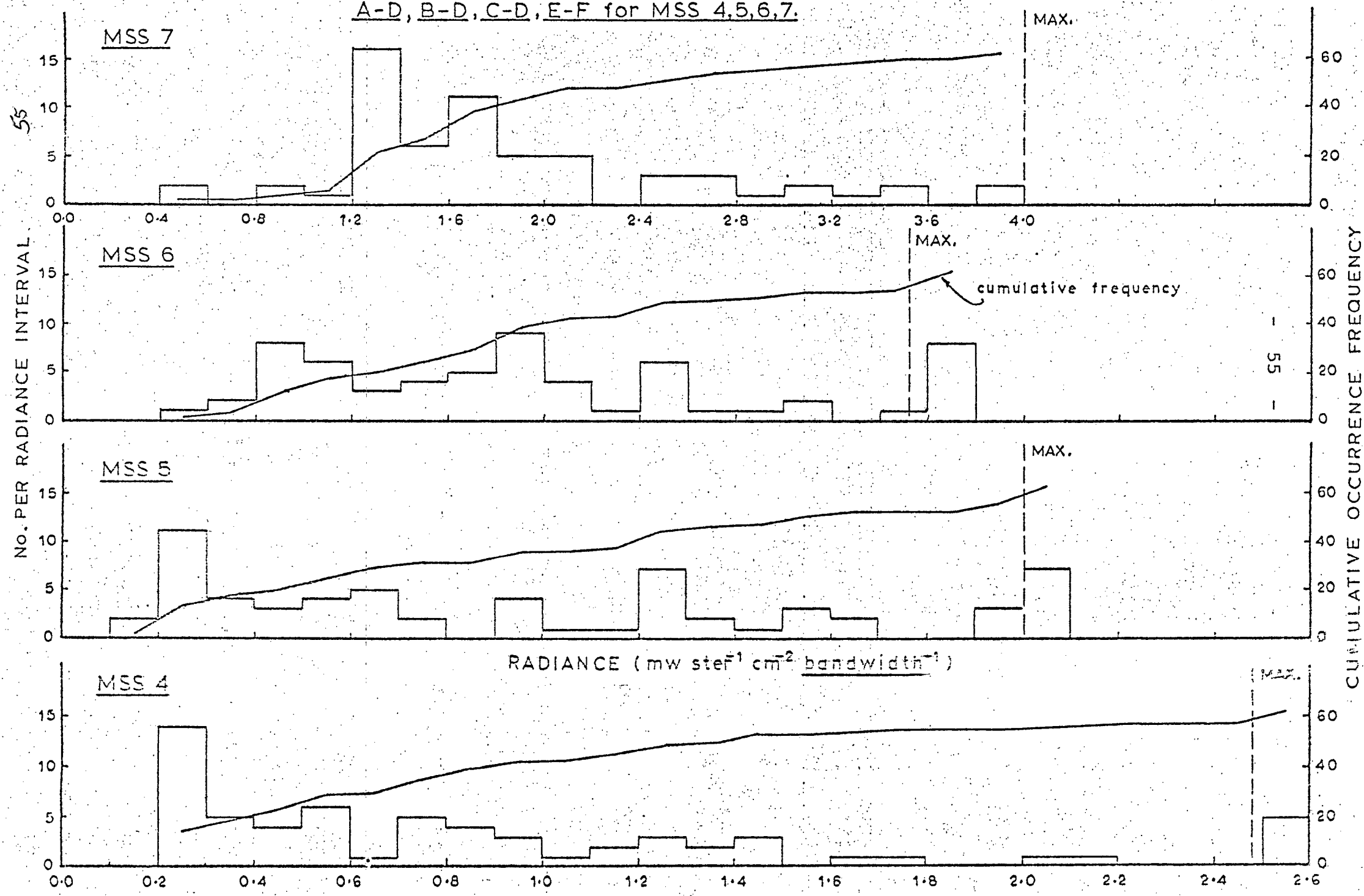TRANSECT D-C (1475 m horizontally)

Fig. 3.4.3

- 54 -

TRANSECT F-E (875 m horizontally)

Fig. 3.4.4

Fig. 3.4.5 Frequency of radiance occurrence transects A-D, B-D, C-D, E-F for MSS 4,5,6,7.
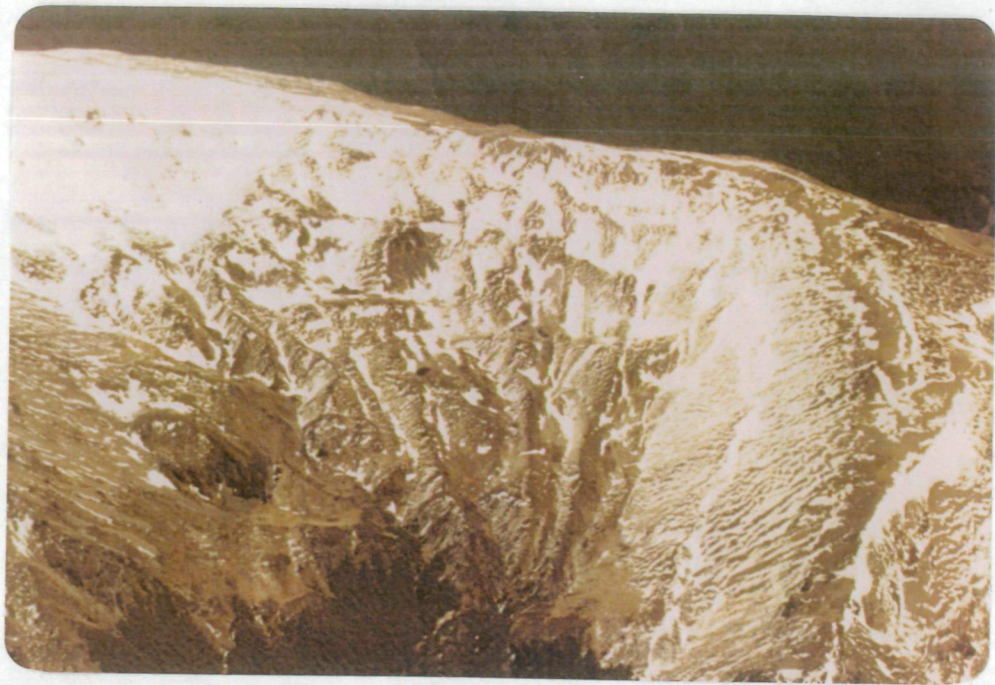
Figure 3.4.6   Oblique aerial photographs taken on 29 October
1976. Mt. Robert in the top photograph and
Six Mile Creek in the bottom photograph.

3.5 How Critical are Soil Type/Crop Stress etc. Influences in Differentiating Wheat Types Using MSS Sensing?

As a preliminary to the single crop (wheat) inventory planned for the Canterbury Plains it was decided to gauge the magnitude of local influences on the resultant classification. These local influences include soil type, variations in soil structure due to subsurface strata, crop stress, ploughing/spraying/seeding patterns etc. Was it possible that such local influences could obscure perhaps the classification between different types of wheat and indeed is such a finer crop classification possible?

In endeavouring to assess the likely answers to these questions it was decided to examine in some detail the effect of such influences on the spectral radiances recorded from two paddocks containing two different varieties of wheat.

These two paddocks, indicated as A and B in Figure 3.5.1, contain the Kapara and Karamu varieties of wheat respectively. Both have been planted in "associated dry subhygrous yellow-brown shallow and stony soil" on the property of Sir T. Mulholland and Sons in the south of our Darfield test area. As far as we know both wheats were planted within a week of one another and were subjected to similar past agricultural history - spraying etc. At the time of aircraft underflight 14 November 1975, and LANDSAT 2 overpass the Kapara wheat was around 12 inches in height with the Karamu between 10 and 12 inches. To the ground observer both crops appeared almost identical in hue and stance.

As seen in Figure 3.5.1, being a colour composite prepared from the MSS compatible PEL Hasselblad camera system, the two stands of wheat are quite distinct one from the other. This is the "standard" colour balance of MSS 4 negative being printed through a blue filter, MSS 5 negative through green, and MSS 7 negative printed through red.

The LANDSAT 2 scene 2282-21254 also recorded these two paddocks and an "Image 100" colour composite output is portrayed in Figure 3.5.2. This was prepared by Peter Ellis as part of the studies undertaken during his visit to the EROS Data Centre in October 1976.

The colour composite derived from the "Image 100" has proved to be significantly better than could be obtained from colour composites of 70 mm products. (Compare Figure 3.5.2 with Figure 6 in 2nd Quarterly Report.) A more detailed analysis of the Canterbury test site using "enhanced" Image 100 products will be presented in the final report.

Once again it is evident that the two varieties of wheat are visually distinguishable on the standard LANDSAT 2 colour composite.

The radiant intensity values for these two paddocks were row printed out from the CCT product using a 47 level coded character line printer output. Averaging the CCT values for each band over each paddock, and plotting their variation within each band led to the plot given as Figure 3.5.3. (The decompressed (MSS 4, 5, 6) and

linear (MSS 7) CCT data were related to the calibrated maximum
radiances for the MSS system ("LANDSAT" Users Handbook) in order
to derive the plotted "radiances per channel bandwidth".) This
latter variation, apparently evident in the aircraft scene, would
seem to have resulted from underlying structure in the alluvial
stratas of the soil together with farming, ploughing and seeding
practices. Some evidence too of crop stress would seem to be
evident, from both CCT and aircraft products, near the northern
and southern paddock boundaries. The variation in the CCT radiance
over each paddock is indicated by the relevant "error bars" in
Figure 3.5.3.

From this figure it is noted that the Kapara wheat exhibits
a marginally higher spectral radiance in MSS 4 and 5 than the
Karamu wheat with the roles being markedly reversed in MSS 6 and 7.
It is further noted that local influences could have greater effect
in crop variety classification in MSS 4 and 5 than in MSS 6 and 7.

Three conclusions, then, emerge from this study:

1. It is apparently possible to classify between some
    varieties of the wheat crop provided adequate ground
    truth information is applied to the recorded spectral
    radiance set.

2. Adequate ground truth for a test area pilot study
    should include: crop type and variety, date of
    planting, fertiliser/spraying history, soil type
    and moisture stress patterns together with grazing
    history.

3. The role of MSS 6 and 7 in the complete visual and
    computerised classification procedure for wheat
    should be further investigated.

FIGURE CAPTIONS

Figure 3.5.1   A colour composite of part of the Darfield
                      test area showing the Kapara wheat paddock
                      as A and the Karamu wheat paddock as B.

                      MSS 4 -ve   printed through blue
                      MSS 5 -ve   printed through green
                      MSS 7 -ve   printed through red

Figure 3.5.2   An Image 100 colour composite of the part
                      of scene 2282-21254 showing the Kapara/Karamu
                      plots.

Figure 3.5.3   A comparison of target radiance (in terms of
                      mw cm^{-2} ster^{-1} per MSS channel bandwidth) as
                      a function of MSS band for Kapara and Karamu
                      wheat. The data for the two wheats are
                      plotted horizontally offset one from the
                      other. (From scene 2282-21254.)

Figure 3.5.1   A colour composite of part of the Darfield test
area showing the Kapara wheat paddock as A and
the Karamu wheat paddock as B.

MSS 4   -ve   printed through blue
MSS 5   -ve   printed through green
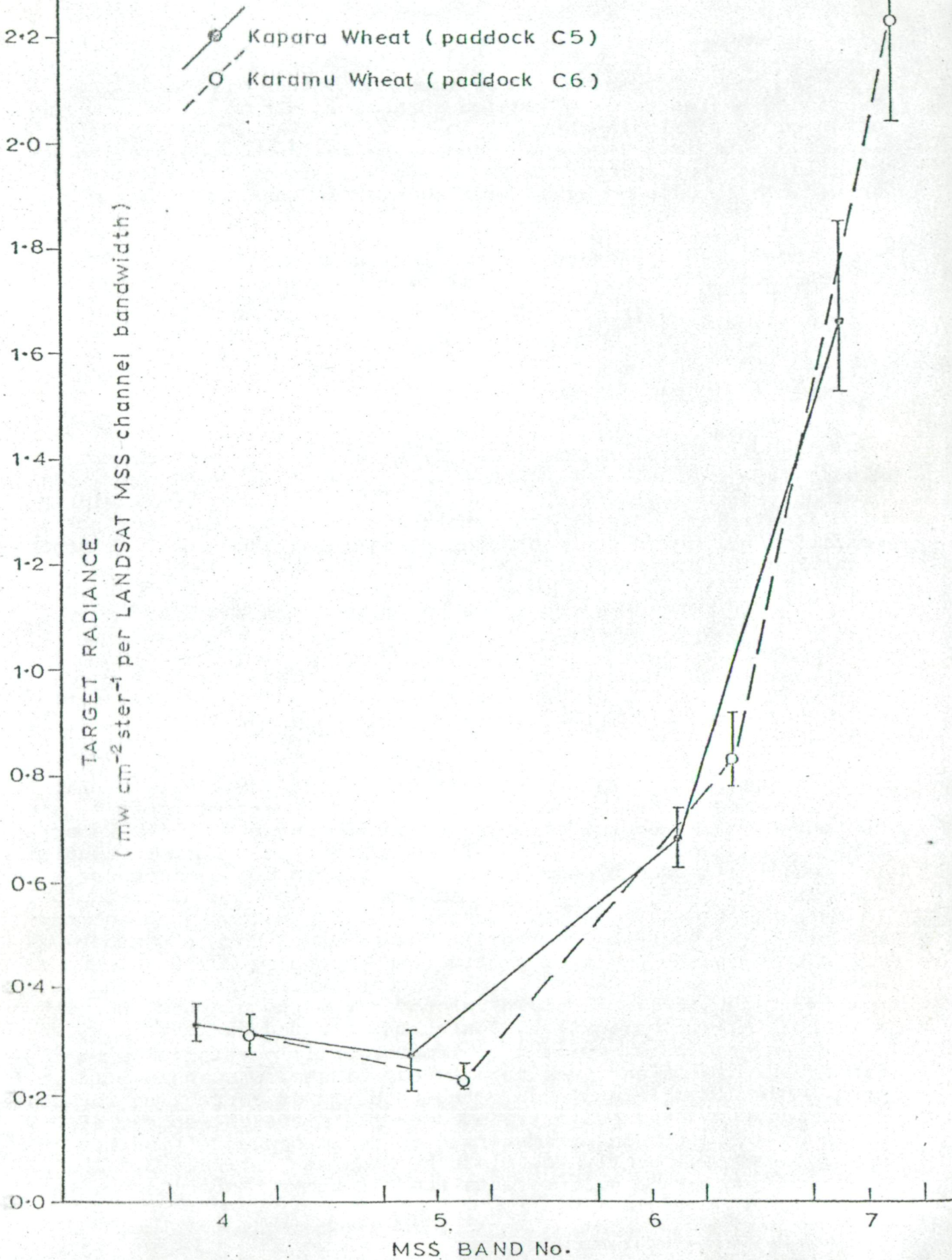MSS 7   -ve   printed through red

61

Figure 3.5.2 An Image 100 colour composite of the part of
scene 2282-21254 showing the Kapara/Karamu
plots.

Fig. 3.5.3

Scene ID#:2282−21254

Date: 31 Oct.,1975

Kapara Wheat (paddock C5)

Karamu Wheat (paddock C6)

TARGET RADIANCE

(mw cm^{-2} ster^{-1} per LANDSAT MSS channel bandwidth)

MSS BAND No.

3.6 Monitoring Suspended Sediment and Siltation Changes in a Tidal Basin Using LANDSAT MSS CCT Data

Introduction

The spatial resolution required to monitor motions of suspended sediments or siltation changes within tidal basins is often compatible with that attainable using LANDSAT 2 MSS data. Repeated satellite coverage reduces the reliance upon previously charted bathymetric control and diminishes some of the uncertainties introduced by unknown tidal modification influences within the basin.

CCT data was used to monitor the motions and approximate structure of sediment patterns along a transect line for two stages in a tidal cycle within Pauatahanui Inlet, New Zealand (41° 06'S, 174° 54'E).

The Analysis

The scenes selected and the factors applicable to them are given in Table 3.6.1. The tidal data was derived from material kindly made available by Heath (1977). The tidal influence will obviously be modified within the basin but similar tidal heights with dissimilar tidal states were chosen to aid in monitoring possible sediment pattern changes - realising that some two months separated the available scenes.

Coded picture printouts were prepared from the CCT data on an IBM 370/168 using the programs discussed by Thomas (1977).

These line printer outputs, coded such that for each band the radiance level is represented by one of a 47 character set, were then studied and the band 7 (lowest water penetration) boundary outlined.

As CCT products are not normally corrected for altitude/attitude variations between overpasses the extracted transect profile data must be tied to recognisable ground control points. With water/land boundary monitoring this is easily accomplished. Better identification is usually achieved by using a sharp land protrusion into the water than a water incursion into the land mass. (This is due principally to changing creek patterns as estuarine outflow patterns change from the time of topographic survey.) The transect for this study was taken between the two land protrusions Moorehouse Point and the shoreline below the Ration Point Trigonometrical Site. The surveyed bathymetry chart (Irwin, 1976) provided the topographic and bathymetric data for this investigation. Using the charted distance between the two transect control points, the topographic location of a particular picture element's data was readily established. Such identified ground control points overcome the problems of correcting for scale and orientation changes introduced by the different spacecraft altitude and attitude parameters - influences present in the raw CCT data. Consequently the plots of Figures 3.6.1 and 3.6.2 were prepared. Figure 3.6.3 presents the bathymetric profile for the transect (from Irwin (1976)).

Table 3.6.1

The LANDSAT scenes used in this study and factors
pertinent to the conditions for each scene.

Scene No.	2281-21194	2334-21132
GMT Date	30 Oct 1975	22 Dec 1975
GMT Time	2120 GMT	2113 GMT
Predicted tidal parameters at inlet entrance		
Height	0.6 m	0.6 m
Previous tide to overpass time	High	Low
Time of previous tide	1730 GMT	1900 GMT
Time difference overpass/ tide turn	3 h 50 m	2 h 13 m
Tidal state	Ebbing	Flooding
Tidal range	1.1 m	1.1 m
Rainfall recorded at Porirua - adjacent to Pauatahanui		
During preceding 4 days	0.0 mm	0.0 mm
Over previous 4 days	43.4 mm	22.0 mm

The positional accuracy of a particular element depends upon the identification accuracy of the ground control points. In this study it is believed to be ± 1 picture element for both the desired plots - Figures 3.6.1, 3.6.2.

Results and Discussion

Suspended sediment motions may be differentiated from siltation changes by study of the changing radiant intensity patterns with differing positions in the tidal cycle.

On the ebbing tide (Figure 3.6.1) an increased radiant intensity block is evident in band 6 near the surface between 500 and 1200 m - upstream of the permanent shallowing between 300 and 500 m. This block exhibits shallow structure between 600 and 1000 m (band 6) and extends to greater depth from 1200 to 1600 m (deduced from bands 4 and 5).

Figure 3.6.2 shows that with the flooding tide suspended sediment is present at moderate depth in the upper reaches of the inlet between 1500 and 1900 m. This region samples the outlet from the Horokiwi Stream but, as no rainfall had fallen in the predominantly grazing catchment during the previous four days, it would seem that the detected sediment has been placed between 1500 and 1900 m by the flooding tide.

As consistent features other than that between 300 and 500 m are absent from both figures 3.6.1 and 3.6.2, the conclusion that no major siltation shallowing has occurred between overpasses may be drawn. However, repeated overpasses would be necessary to identify any slow silt accretion or depletion.

REFERENCES

Heath R. (1977) Private Communication. DSIR Oceanographic
    Institute, New Zealand.

Irwin J. (1976) "Pauatahanui Inlet Bathymetry 1:5,000"
    DSIR Oceanographic Institute Chart No. 47, New
    Zealand.

Thomas I.L. (1977) "Basic programs for accessing and
    utilising LANDSAT MSS CCT data using the PL/1 language
    on an IBM 370/168 computer". DSIR Physics and
    Engineering Laboratory Report No. 566.

FIGURE CAPTIONS

Figure 3.6.1   Radiant intensity variations along the transect line for scene 2281-21194.

Figure 3.6.2   Radiant intensity variations along the transect line for scene 2334-21132.

Figure 3.6.3   Bathymetry profile along the transect line from Irwin (1976).

———

Fig. 3.6.1

PAUATAHANUI INLET TRANSECT
Scene No 2281-21194   30 Oct.'75

MOORHOUSE Pt.

RATION Pt.TRIG SHORE LINE

UNCERTAINTY BARS

BAND 4 ——————
BAND 5 ---------
BAND 6 —·—·—·—
BAND 7 —··—··—

MSS CCT RADIANT INTENSITY LEVELS

DISTANCE (x 100 m)
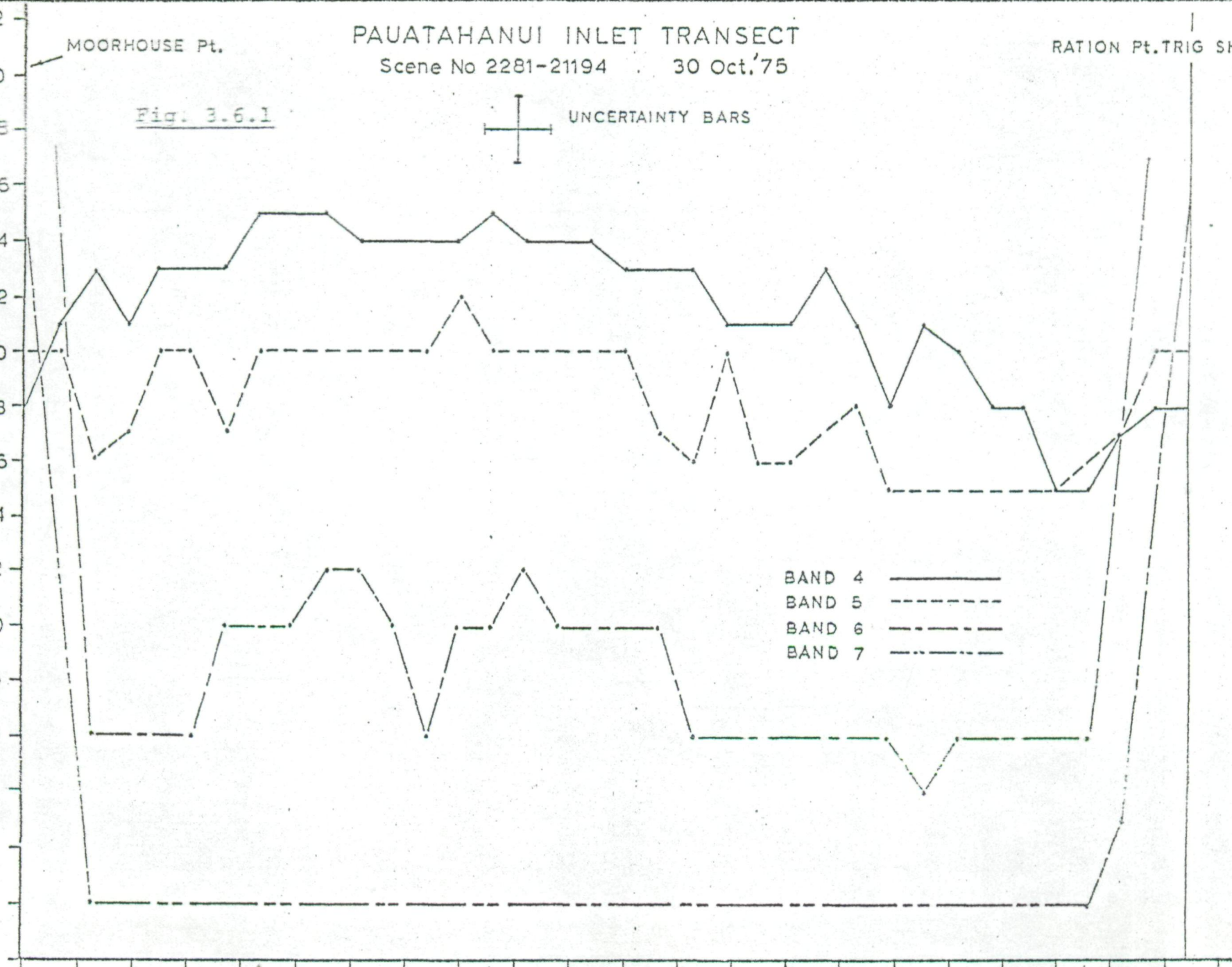
PAUATAHANUI INLET TRANSECT
Scene No. 2334-21132   22 Dec.'75

Fig. 3.6.2

MOORHOUSE Pt.

RATION Pt. TRIG SHORE LINE

UNCERTAINTY BARS

BAND 4 ————
BAND 5 --------
BAND 6 —·—·—·
BAND 7 —··—··—
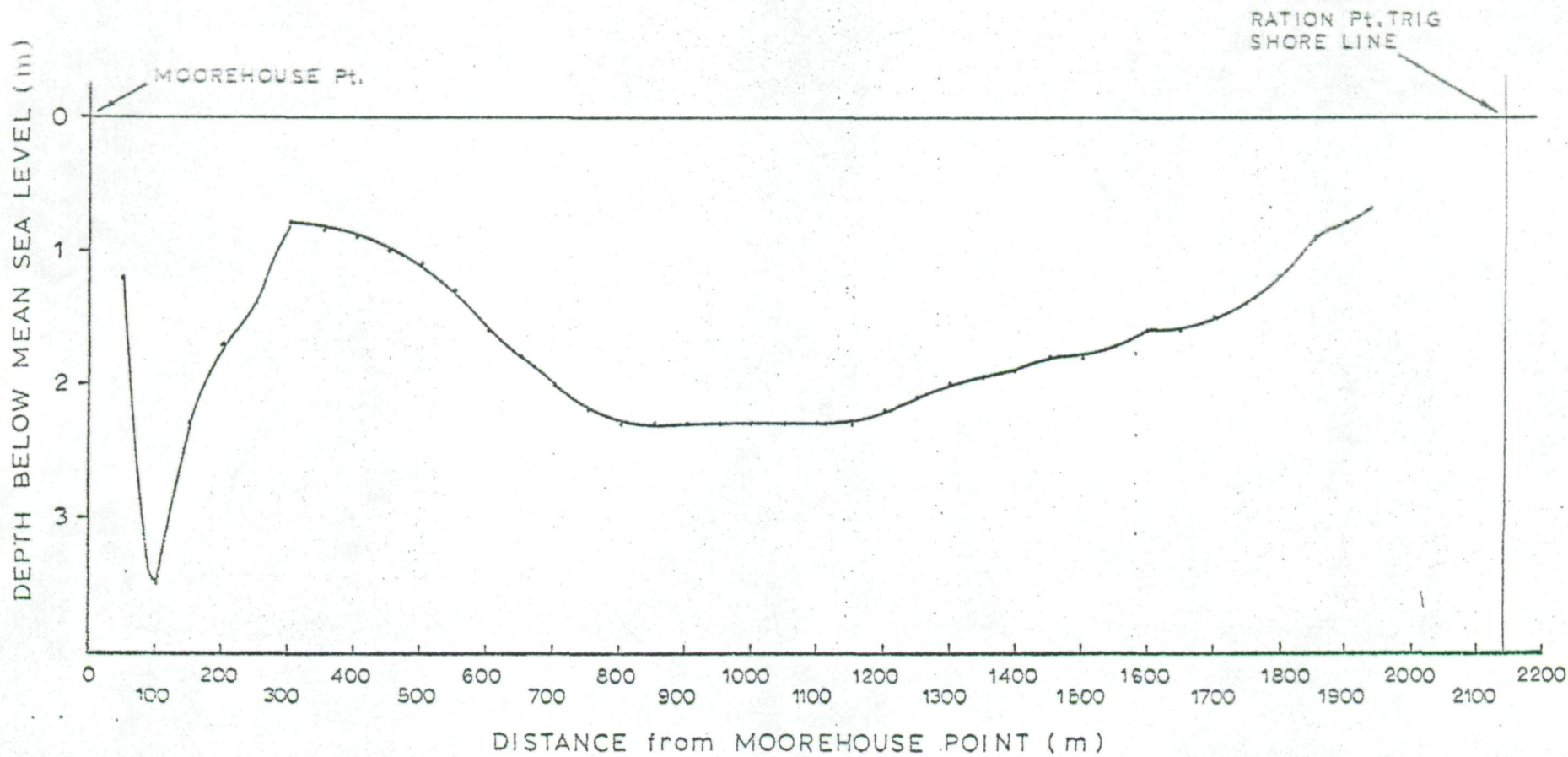
MSS CCT RADIANT INTENSITY LEVELS

— 69 —
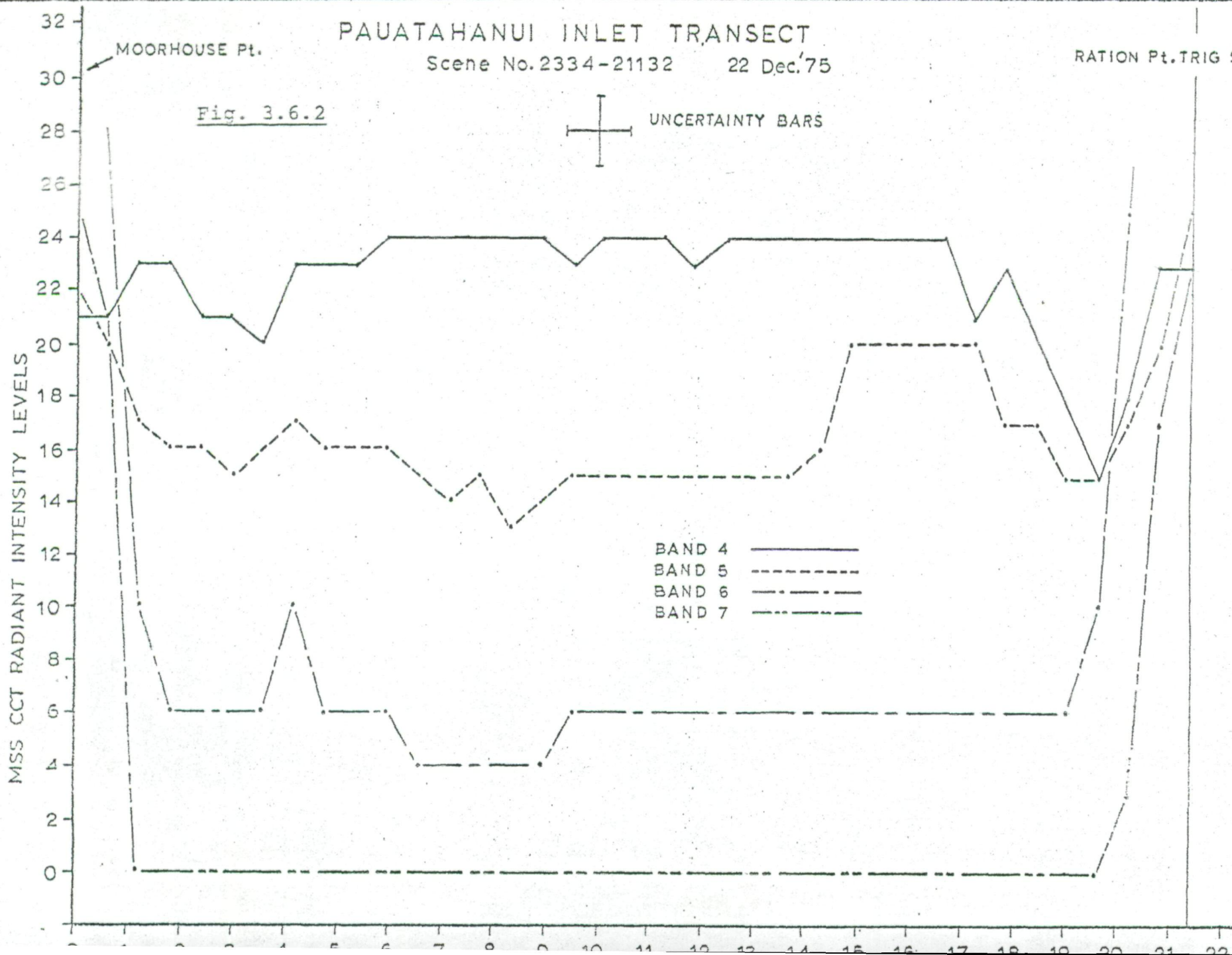
Fig. 3.6.3

PAUATAHANUI INLET TRANSECT

Bathymetry Profile
(from Oceangraphic Inst. chart 47; 1976)

4. PUBLICATIONS

4.1 P.E.L. Reports

P.J. Ellis   "Overseas Visit to NASA and the EROS Data Center, U.S.A., October/November 1976". P.E.L. Overseas Visit Report No. 72, November 1976.

M.J. McDonnell   "Computer programs for processing LANDSAT imagery on an HP 2100 computer: Part III". P.E.L. Report No. 567, March 1977.

I.L. Thomas   "Basic programs for accessing and utilising LANDSAT MSS CCT data using the PL/1 language on an IBM 370/168 computer". P.E.L. Report No. 566, March 1977.

4.2 Newsletter

One copy of the "Remote Sensing Newsletter" was circulated in late 1976. Its main purpose was to furnish the predicted LANDSAT 2 overpass dates in time for planning co-ordinated field programmes over the coming year through New Zealand.

5.   PROBLEMS

5.1 LANDSAT 2 Coverage of New Zealand

    To our knowledge no scenes have been recorded over New Zealand
since 31 May 1976 despite the best efforts of NASA staff to take
advantage of cloud cover/priority slots to support our investigations.
Of the 39 scenes so far recorded by LANDSAT 2 seventeen were
recorded in response to a special request for coverage between
14 and 17 February 1976 - whether cloud was present or not.

    The fact that tape recorder limitations and higher priority
coverage requirements in other areas has reduced that coverage
obtainable over New Zealand would seem to be less of a constraint
than this country's high incidence of cloud cover.

    As New Zealand is a relatively small country with markedly
diverse agricultural/forestry geologic etc. patterns occurring
well within the scope of one LANDSAT image, we should like to
suggest a reappraisal of our initial scheduling request of cloud
cover tolerance of 30%. Scenes with greater than 30% cloud cover
have been used to extract data useful to New Zealand investigations
(e.g. West Coast lineament study contained in Third Quarterly
Report).

    It is rare for New Zealand to be wholly cloud covered and
consequently we speculate as to the possibility of some coverage
being scheduled for New Zealand between the bounds of the predicted
cloud fronts rather than the complete orbital track being essentially
cloud free, as would be required by our earlier request of a 30%
cloud tolerance.

    An inspection of cloud cover imagery received by the New
Zealand Meteorological Service from the NOAA spacecraft would
indicate that this would be a more fruitful approach than that
initially employed.

    We would welcome NASA comment on this problem area.

5.2 Data Products

    No photographic products were received during the reporting
period. CCT products have been received from both LANDSAT 2 as
part of investigation no. 2823, and from LANDSAT 1 being purchased
in support of such studies. Currently, at 28 February 1977, we
hold 12 LANDSAT 2 CCT sets, of the agreed 22 sets, with a further
10 LANDSAT 2 CCT sets on order.

5.3 CCT Line Length Variations

    It is perhaps worth pointing out that in the CCT's we have
received the first two registration fill characters at the end of
each scan line are not $(X^1 FF^1)$ but some random number. Also the
last two to four pixels for each band in each scan line are zero.
The number of non-zero pixels in a given scan line thus varies with
the band number, even though according to the end of line calibration
data, the scan line length is the same for each band. This seems to
be in contradiction to the 1976 LANDSAT Data Users Handbook and needs
clarification.

6. ACKNOWLEDGEMENTS

Part II

Seismotectonic, Structural, Volcanologic and Geomorphic Study of New Zealand

Investigation No.:   2823 A

Co-Investigator: Dr Richard P. Suggate

Agency: N.Z. Geological Survey

Address: Department of Scientific and
                              Industrial Research
                          P.O. Box 30-368
                          Lower Hutt
                          New Zealand

Telephone No.:   Wellington 699-059

Author: Mr P. Oliver

———

LANDSAT II PROGRESS REPORT

LANDSAT imagery of selected areas has been examined for geological features. A covering of vegetation masks the lithology but lineaments related to faulting, and large scale lithologic structures, were observed. In all cases linear features were found to be clearly visible on black and white positive transparencies of MSS bands 6 and 7.

1. NORTH CANTERBURY-SOUTH MARLBOROUGH AREA

Cloud-free images (E-2192-21265) of this area were examined. Figure 1 shows the lineaments on these images. Many of the major lineaments correspond to known faults which are predominantly orientated in a north-east to south-west direction. A secondary set of lineaments is orientated in an approximately north to south direction.

Along the eastern margin of the Southern Alps there is a high density of parallel minor linear features. These are predominantly sub-parallel to the major faults, but are also locally parallel to the known strike of the Torlesse sandstone and siltstone beds mapped by Gregg (1964). In the area west of Hawarden the lineaments curve around to strike north. This is consistent with the strike of the beds in this area, which have been mapped in detail by Bradshaw (1972), and indicates that these parallel sets of minor lineaments are related to bedding structures rather than faults.

The area covered by the parallel sets of minor lineaments also corresponds to a low relief topography giving this area a geo-morphologically distinct erosion pattern easily distinguished from that to the west that forms the Southern Alps. On the basis of their textural appearance on the LANDSAT images, the rocks of the Cavendish Hills and Okuku Range appear to be similar to the Jurassic rocks of the Lowry Peaks Range.

Minor lithologic lineaments were not observed in the Southern Alps as these had a covering of winter snow. The west part of this area is also covered by summer-time LANDSAT II image (E-2409-21293) in which minor lineaments were observed (Third Quarterly Report, No. 553, Sept. 1976). The summer images of the Southern Alps were not only predominantly snow free but, because of a higher sun angle, also showed major lithologic units as dark and light bands. In the winter images (E-2192-21265) the low sun angle did not favour visual recognition of lithologic units. The low sun angle also resulted in long shadows that obscured many of the features observed, in the larger valleys, in the summer images. This shadowing effect was, however, of direct benefit in the recognition of the sets of parallel minor lineaments observed on images E-2192-21265. Thus where there was low relief topography the long shadows caused by a low sun angle accentuated the erosional features that were predominantly controlled by lithology.

2. MID TO SOUTH CANTERBURY, AND NORTH OTAGO AREA

LANDSAT images (E-2192-21272) covering this area were examined. The hill country areas are tussock-covered, and lithologic units and boundaries were not visible. Linear features generally formed parallel sets.

North of the Rangitata River the lineaments correspond to known faults. No bedding structures are visible in the images. Between the Rangitata and Pareora Rivers there are two sets of parallel lineaments; one with a north-south orientation, and one with an approximately east-west orientation. The cause of these linear features has not been determined. The area between the Waitaki and Pareora Rivers contains major lineaments. The most prominent of these is on the north-east flank of the Hunters Range and is parallel to the Hunters Fault along the foot of the Range. A set of minor parallel lineaments west of the Hunters Range cuts the predominant strike of the bedding and schistosity at right angles and is therefore probably a fault controlled set. South of the Waitaki River is a set of parallel lineaments that strike north-west. These lineaments are parallel to the Kauru Fault (Gage, 1957) which itself is not a conspicuous lineament.

3. WESTERN CENTRAL NORTH ISLAND AREA

LANDSAT images (E-2389-21172) of this area gave cloud free coverage from Kawhia to Mt Ruapehu. As with most areas of New Zealand, lithologic features are masked by vegetation. Lineaments were observed in some areas, the most prominent being the north-south trending lineaments near Kawhia Harbour. A major lineament striking north-east, and situated west of Te Kuiti, has a parallel set of minor lineaments in the Triassic and Jurassic rocks of the Herangi Range. East of these lineaments are a set which strike north. Most of the lineaments would seem to be fault controlled.

The Ohura Fault is visible for part of its known length. West of Taumarunui is a large curved feature adjacent to which are a set of minor parallel lineaments that are parallel to the strike of bedding in this area.

4. LOW LEVEL AIR-PHOTOGRAPH INTERPRETATION OF A STRONG LINEAMENT IN MARLBOROUGH

In the second quarterly report prepared by N.Z. Geological Survey for the Second Quarterly Report of the LANDSAT II investigation No. 28230 (PEL Report No. 531) it was noted that a strong lineament in the headwaters of the Branch and Saxton Rivers was aligned roughly parallel to the major Wairau and Awatere Faults.

Lensen (1962) did not map the feature and hence considerable interest was generated regarding the possibility of a hitherto unknown major fault in Marlborough. Recent work has included a detailed perusal of available air photographs.

In detail the lineament is observed as a series of co-linear segments that take on the appearance of a single near linear feature on the much larger scale LANDSAT images. Each segment is characterised by a linear stretch of riverbed and frequently by continuation along a small stream flowing into the river. Between watersheds the topography rises steeply to ridges and peaks over 1500 m. No evidence of Quaternary fault movement was observed from the available air photographs. Although much of the course of the lineament is along active riverbeds or scree-covered slopes it is felt that if a Quaternary active fault were present then some evidence would be observed.

Lensen (1962) shows that the strike of beds in the area are subparallel to the strike of the lineament. Without fieldwork it is thought probable that the lineament has strong bedding control.

Fieldwork, which is proposed, may reveal mineralised crush zones, springs or changes in lithology that will indicate Pre-Quaternary fault control for the lineament.

References:

Bradshaw, J.D. 1972: Stratigraphy and structure of the Torlesse Supergroup (Triassic-Jurassic) in the Foothills of the Southern Alps near Hawarden (S60-61), Canterbury. New Zealand Journal of Geology & Geophysics, Vol. 15 No. 1, pp. 71-87.

Gage, M. 1957: The Geology of Waitaki Subdivision. New Zealand Geological Survey Bulletin n.s. 55.

Gregg, D.R. 1964: Sheet 18 Hurunui (1st ed.) "Geological Map of New Zealand 1:250,000" DSIR, Wellington, New Zealand.

Lensen, G.J. 1962: Sheet 16 Kaikoura (1st ed.) "Geological Map of New Zealand 1:250,000". Department of Scientific and Industrial Research, Wellington, N.Z.

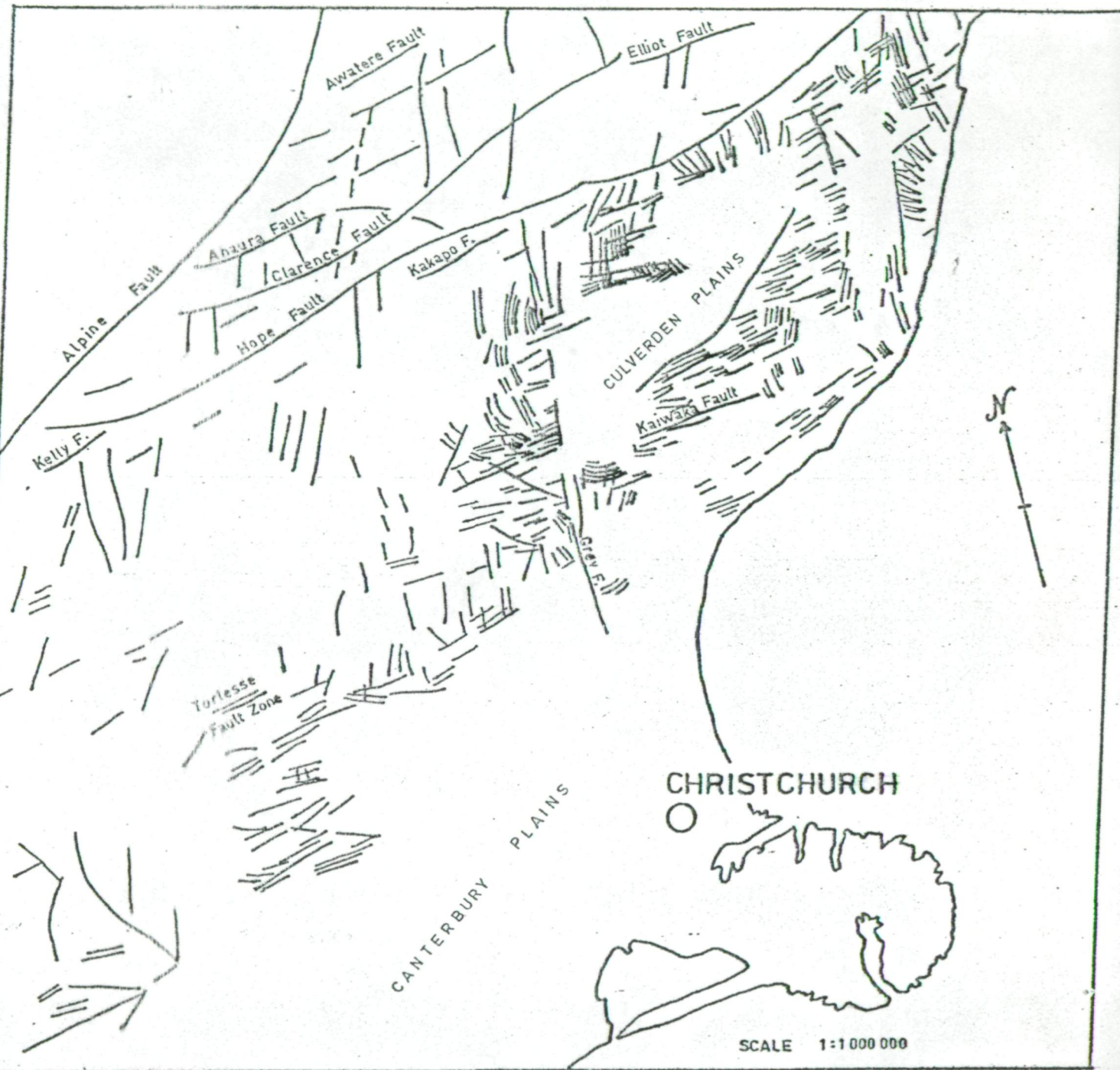Figure 1. Linear features observed on positive transparencies of MSS bands 6 and 7 (E-2192-21265).

Figure 1 (A)   MSS BAND 7 (E-2192-21265)

Figure 2. Linear features observed on positive transparencies
of MSS bands 6 and 7 (E-2192-21272).

7

E171-00I   E171-30I   E172-00I   E172-30I
02AUG75 C S44-30/E171-57 N S44-31/E171-54 MSS   7   R SUN EL14 AZ046 I92-2679-N-I-N-D-IL NASA ERTS E-2192-21272-7 01
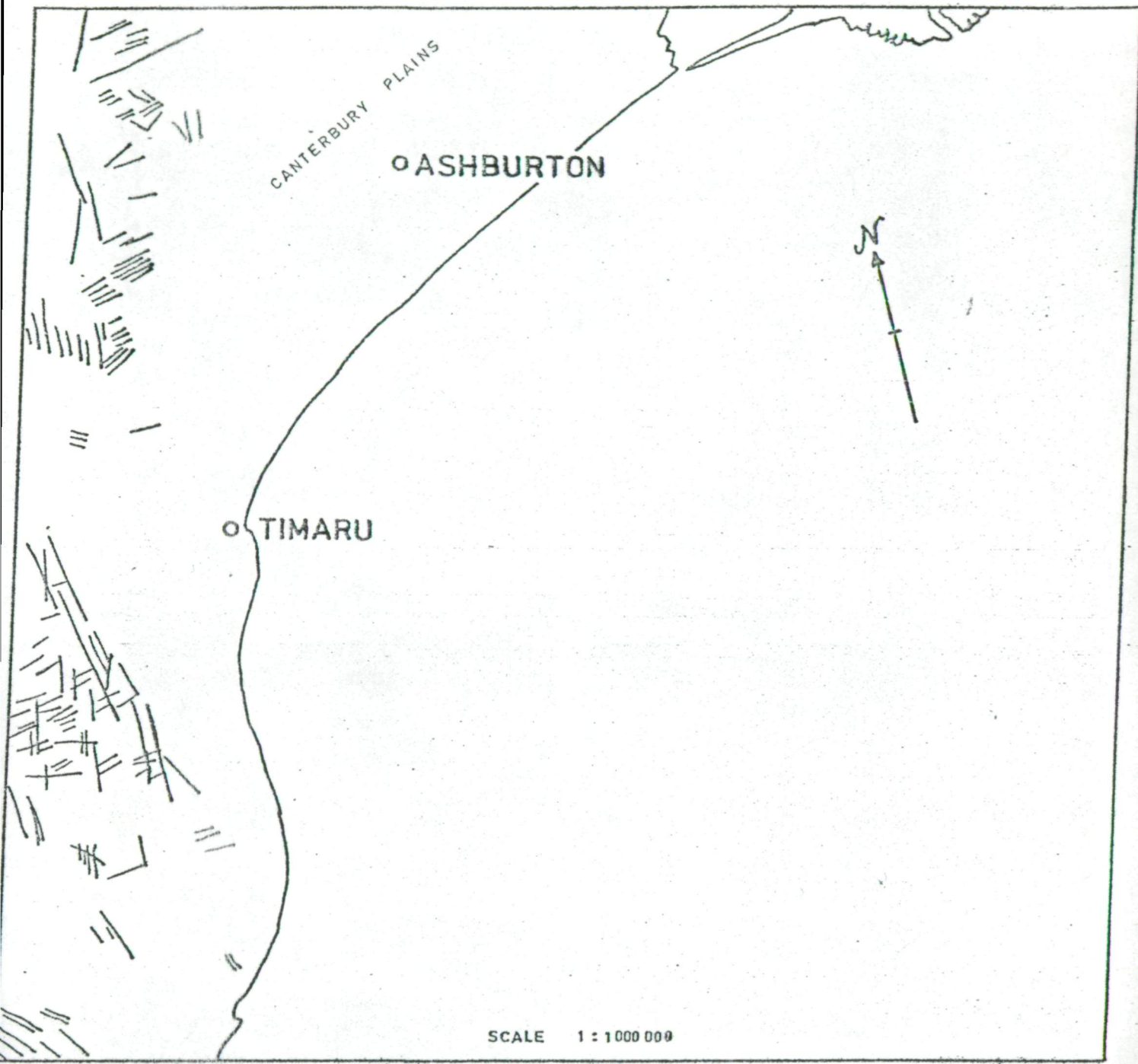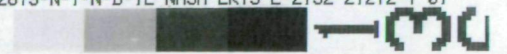
Figure 2   (A)   MSS BAND 7 (E-2192-21272)
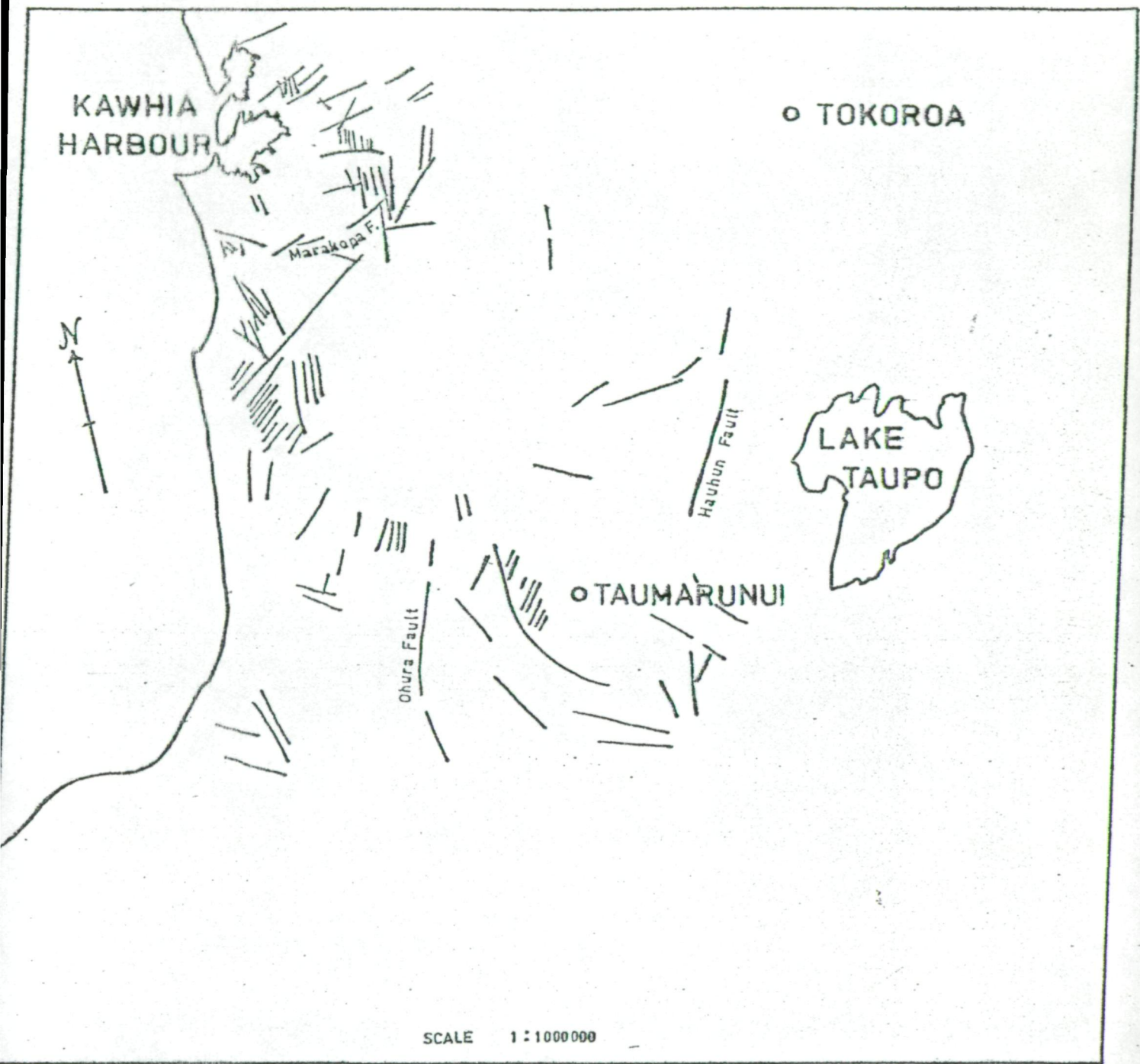
Figure 3. Linear features observed on positive transparencies of MSS bands 6 and 7 (E-2389-21172).

Figure 3   (A)   MSS BAND 7 (E-2389-21172)

10

Part III

Indigenous Forest Assessment

Investigation No.:   2823 B

Co-Investigator: Mr Michael G. McGreevy

Agency: Forest Research Institute

Address: Private Bag
Rotorua
New Zealand

Telephone No.:   Rotorua 82-179

Author: Mr Michael G. McGreevy

INDIGENOUS   FOREST   ASSESSMENT

To achieve the original objective of assessing New Zealand's indigenous forest resource using multi-stage sampling in conjunction with LANDSAT cover of New Zealand's forest resource, it wa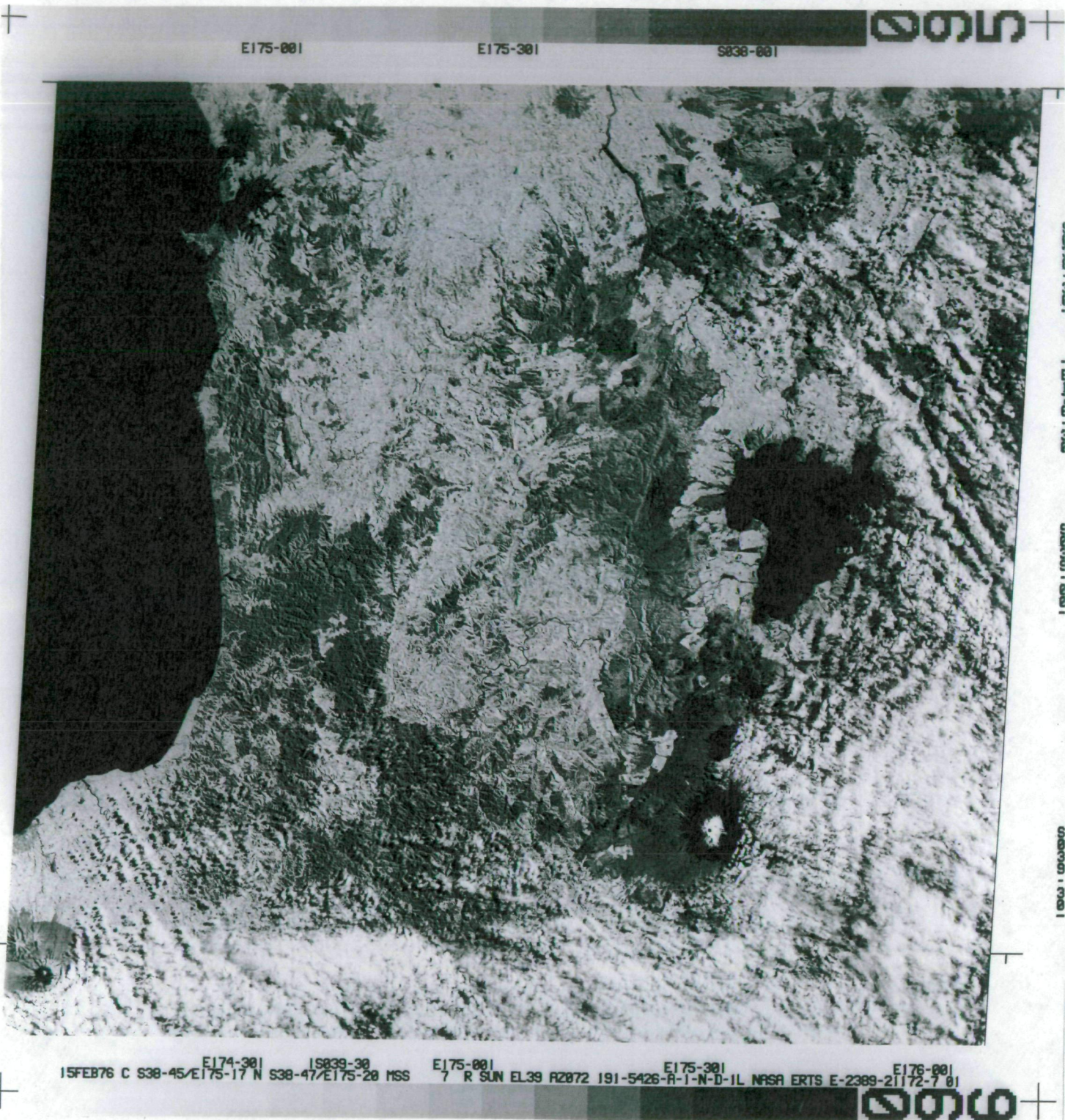s hoped that seasonal variation in the spectral signatures of major forest types would help to define them on the imagery. Insufficient imagery has been received to allow a seasonal comparison. Any variation which is due to the date of the imagery must be included as part of the variation within the individual type's spectral signature.

A second problem, varying solar elevation among images, has made visual comparisons of signatures on more than one image nearly impossible. Possible solutions to this problem would be to use raw digital tapes in defining signatures, using digital tapes which are corrected for differences in solar elevation, or to treat each image as a separate entity and define a signature only in terms of that image. Due to delays in obtaining and processing digital imagery, we adopted the latter approach in initial interpretation. Using visual interpretation of colour composites we have been able to distinguish the following classes: beech and beech complexes, hardwoods, and scrub. These of course can be distinguished from agricultural and urban areas.

It is desirable to define as many forest types as possible in the initial stage of sampling. To determine if other types can be defined on digital imagery, we have photographed 11 areas of indigenous forest on flat (less than 5 degrees) topography in colour and panchromatic negative films. The areas are indicated on image ERTS E-2334-21123-4 and the type definition which they represent are given in Table 1. If no positive results are found in this test the inventory will proceed using the types identified previously in conjunction with available LANDSAT imagery.

ASSESSMENT OF DOTHISTROMA PINI IN PINUS RADIATA

Initial investigations showed no positive correlation between radiance measurements from LANDSAT and disease levels in various stands. To ensure that this lack of correlation is not due to varying topography, stand age, and silvicultural treatment in these stands, stands which are of the same age, have had the same silvicultural treatments, and are on slopes of less than 10 degrees have been identified on LANDSAT imagery. Digital information from image ERTS E-2281-21185 is being compared with visual assessment made approximately 1 month prior to the image. The mean and variance of the radiance levels on these stands are presently being derived. The correlation analysis between these levels and the disease level should be completed during the next reporting period.

TABLE 1

TYPE SEPARATION OF NATIVE BUSH ON
### LANDSAT IMAGE NO. 2334-21123

Ground Areas

1. Poutu Intake (Tongariro). Forest Class: Rimu - Beeches

2. Tiraka Stream (Kaimanawa Forest Park). Forest Class: Beeches

3. Clements Mill Camp (Kaimanawa Forest Park). Forest Class: Beeches

4. Lake Ruapani (Urewera National Park). Forest Class: Beeches Forest Type: K6 red beech - silver beech

5. Aniwaniwa Stream (Urewera National Park). Forest Class: Rimu - General Hardwoods - Beeches. Forest Type: I2 rimu-miro-red beech - silver beech/Kamahi-tawari

6. Mixed beech-podocarp

7. Kahikatea Range (Urewera National Park). Forest Class: Beeches Forest Type: K10 mountain beech - red beech - silver beech

8. North Tarawera. Forest Class: Lowland Steepland and Highland Softwoods - Hardwoods. Forest Type: G1 Hall's totara/kamahi - broadleaf.

9. North Okataina. Forest Class: (a) Rimu - Matai - Hardwoods
                                   (b) Tawa
                    Forest Type: (a) D3 rimu-rata/tawa-pukatea
                                   (b) N7 rata/tawa-rewarewa-
                                       mangeao-kamahi

10. Horohoro Cliffs. Forest Class: Rimu-matai-hardwoods

11. Mamaku. Forest Class: (a) Rimu-tawa
                          (b) Tawa
            Forest Type: (a) D1 Rimu-rata/tawa-kamahi
                          (b) N2 Rata/tawa-kamahi
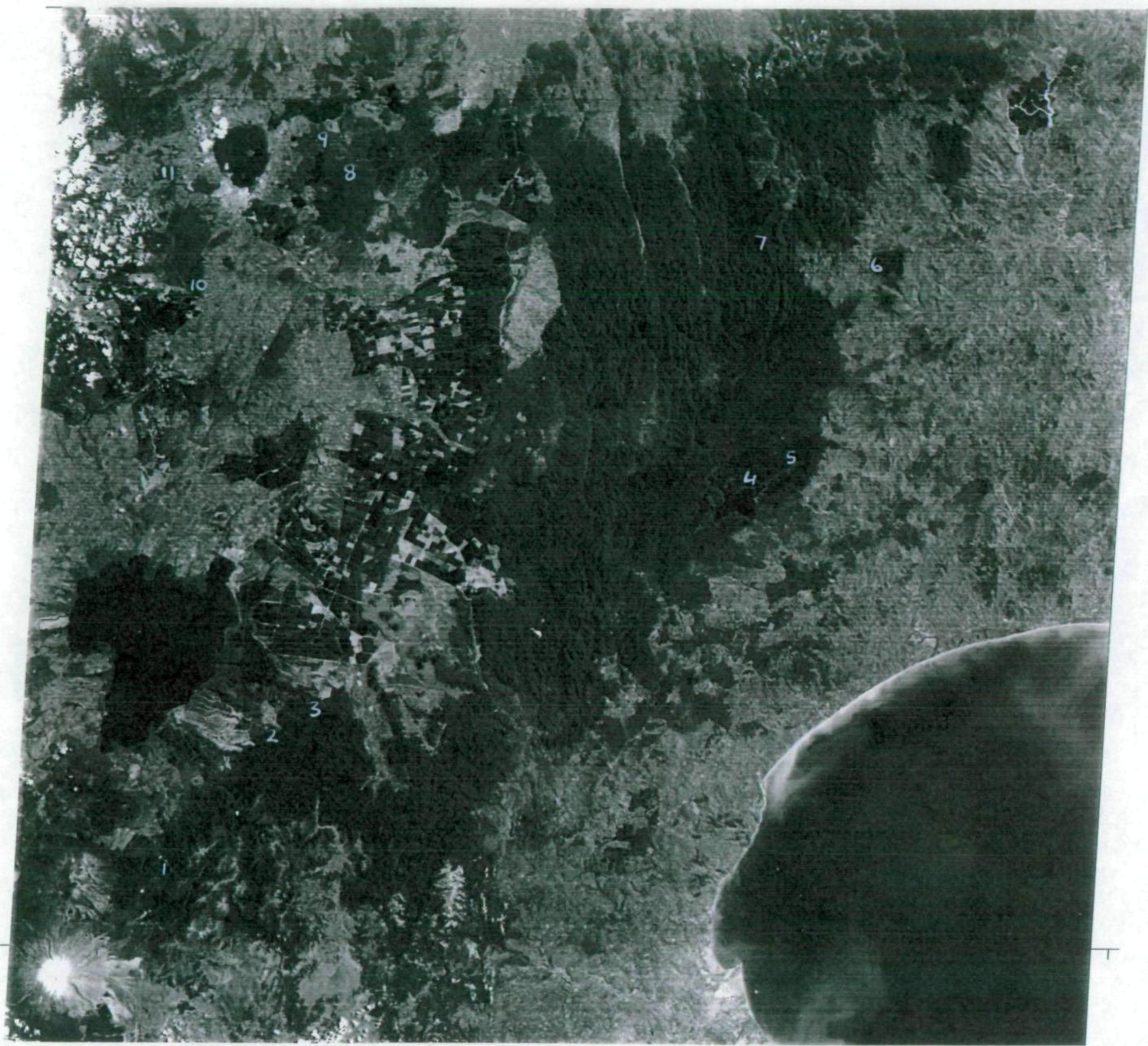
Figure 1   MSS BAND 4   (E-2334-21123)

4

PART IV

MAPPING LAND USE AND ENVIRONMENTAL

STUDIES IN NEW ZEALAND

Investigation No.:   2823C

Co-Investigator: Mr Ian F. Stirling

Agency: Department of Lands and Survey

Address: Private Bag
                            Wellington
                            New Zealand

Telephone No.:   Wellington 735-022

                            Extension 286

Author: Mr R.C. Child

———————

5

CONTENTS

6

LIST   OF   ILLUSTRATIONS

1. INTRODUCTION

1.1 Over the period since the third quarterly report our Department's activity has undergone changes. The most significant and disruptive at this time has been the return to Scotland of the author of the previous reports, Mr Douglas McK. Scott. His valuable co-ordination and knowledge will be missed by the New Zealand remote sensing team, especially by the present author. Consequently sometime has been taken up with consolidating and reassessing our activity.

1.2 Previous interest and minor involvement with LANDSAT imagery as a possible source of information in the resource mapping field by this author as Divisional Cartographer, Planning and Inventory Division of Cartographic Branch, has led to his appointment as a replacement to Doug Scott.

1.3 The Department of Lands and Survey has continued its investigation and use of LANDSAT imagery in the environment and land use study field. The eventual aim being to reduce the expensive and long acquisition times usually involved in studies of this nature with the subsequent increase in output.

1.4 There is a slow but growing awareness and interest to use the potentials of multi spectral imagery in the land planning field which is itself becoming a more active discipline.

1.5 As has been mentioned in previous reports, the opportunities for applying some of the benefits of LANDSAT imagery has coincided with several major changes in our national mapping programme.

1.5.1 Recently we have given a critical reappraisal of our resource mapping programme. We have initiated changes aimed at meeting basic requirements of planners, that resource data is collected and presented visually in as short a time as possible. Previously our maps were based on productive/unproductive, developed/undeveloped interpretive information. It was found that this form became out of date and of limited use for planning purposes but there was a need for a Land Use map that showed an 'as is' situation. A pilot study has been initiated in Northland (north of Auckland) at a scale of 1:100,000 with topics that include Geology, Soils, Land Use, Land Tenure, Vegetation and Wildlife. The general specifications have also been adopted for a combined Departments study of the King Country area in the North Island. It is from the 'ground truth' information compiled for the Land Use map of this study that investigation into the potential use of LANDSAT imagery for this purpose has been conducted. Areas of future resource study are the McKenzie Basin, Stewart Island, an extension of the King Country study and Northland.

1.5.2 The recent change to metrics involved the calculation of a new map projection and grid and the remapping of the basic map series of New Zealand at 1:50,000. This mapping incorporates information from new source material. Also involved is the production of a new 1:250,000 based on the 1:50,000 sheetlines. It is in the production of this 1:250,000 series that LANDSAT imagery is proving to be increasingly useful.

Page Intentionally Left Blank

is now compared for hydrographic selection and generalisation, topographic shape, vegetation cover etc. The use of a variation in the composition of the colour in the composites and experimentation with colour isodensitometer images is being investigated. Evaluation will be made with the eventual aim being to produce, if possible, primary source material from LANDSAT.

The use of imagery for relief shading purposes continues as indicated in previous reports. The 'overview' presentation offered by these images has no alternative equivalent. For small scale map hill shading reductions of large scale material became expensive and numerous.

A serious limiting factor experienced in the use of LANDSAT images for this scale of mapping is the discontinuous coverage of New Zealand.

2.2.2 1:500,000 scale mapping

The 1:500,000 scale ICAO maps covering New Zealand in 4 overlapping sheets that utilised LANDSAT imagery for comparative purposes has now been printed.

2.2.3 1:1,000,000 scale mapping

The production of a new edition of this map is now in progress. Source material will be checked against available LANDSAT images to assess the contribution possibilities of this more recent data. A suggested mosaiced image of New Zealand is hampered by the non-availability of total cover but methods of producing such an image are being investigated for eventual publication.

2.2.4 Offshore Islands

As indicated in our initial proposal we hoped that LANDSAT imagery would facilitate our mapping of numerous offshore islands especially their orientation and position in relation to the main islands. Cuvier Island has been mapped from aerial photography but orientation is hampered by the fact that there is only one co-ordinated triangulation point on the island. Orientation could be achieved from LANDSAT imagery especially if control points could be marked by reflectors.

2.2.5 Antarctic Mapping

Our Department has had recent discussions with R.H. Lyddon, Chief, Topographic Division, U.S. Geological Survey on the subject of mapping activity in Antarctica. It was agreed generally that co-ordinated mapping in the Ross Sea, Victoria Land area would be investigated and undertaken utilising LANDSAT imagery. This activity is outside our contractual agreement but is reported for interested parties.

2.3 Distribution of Imagery

Interest in our 'Quick look' prints produced for LANDSAT II imagery received in New Zealand has led to the requirement for users for a set of prints for LANDSAT I images. Although much of our

LANDSAT I imagery was not of a high quality 'Quick look' print sets as well as being distributed to contributors and investigators of the imagery are made available throughout New Zealand in twelve main centres for public viewing.

2.4 Reflector Programme

The coincidence of our reflector programme and the particularly cloudy summer in New Zealand has suggested to some that this reflector has great possibilities as a rain making machine! On each overpass until recently there has been too much cloud cover to expect satisfactory results. We are optimistic enough of good results to be considering modified reflectors in other parts of the country where mapping requirements suggest marked control.

2.5 Remote Sensing Workshop

As a follow up to last year's introductory workshop, a further informal gathering of Department personnel:

Mr W. Robertson	Director of Planning
Mr D. Francis	Director of Mapping
Mr P. Sadler	Chief Cartographer
Mr R. Child	Divisional Cartographer
	Remote Sensing

and guest Professor A. Lewis, Louisiana State University discussed future resource planning activity and the contribution remote sensi could give. Also discussed was a future workshop for planners to indicate the availability of remote sensing data and facilities and to promote the use of LANDSAT imagery.

2.6 Other Activities

Transparencies produced by P.E.L. have been investigated in comparison with prints for interpretation and plotting purposes and the transparency has been found to reveal more detail. We have found that the use of transparencies in photogrammetric instruments has produced promising results.

2.7 Conclusion

Our investigations have reached several stages. The initial aims have been pursued and in most cases are yielding better result than were considered possible at the early stages of research. Thi has led to more intensive effort being applied. The objective is to reach conclusions for these original objectives this year and to then view supplementary requirements that have been initiated. This has become and is still growing into a field of research that has yet to show its full potential.

My thanks to the P.E.L. team whose co-operation and liaison have made my taking over from Doug Scott much easier than it would otherwise have been and who manage to co-ordinate the varied and expanding spheres of interest in remote sensing in New Zealand.

NORTH TARANAKI BIGHT

174°

39°

Sugar Loaf Is

NEW PLYMOUTH

e Egmont

Oakura
Tataraimaka
Bell Block
Waitara
Tongaporutu
Omata
Motunui
Ahititi
Puniho
Okato
Taurutangi
Sentry Hill
Brixton
Pukearuhe
1005
Warea
Huiang
Tikorangi
Urenui
880
Pungarehu
2243
Lepperton
907
Uruti
Tumahu
Egmont Village
1080
Farihaka Pa
4591
1055
Rahotu
Okahu Stream
Kaimiro
1285
1433
Oaonui
Inglewood
1065
1316
Stony R
Mt EGMONT 8260
Kaimata
Tarata
1460
Opunake
Ngatoro Stm
Tariki
Waitara Riv
1065
Purangi
1501
Te Kiri
Waiaua River
1049
1491
Kohuratahi
Awatuna
Pembroke
Tuna
Huiroa
1184
Pihama
Mahoe
Cardiff
Midhirst
Kupe
1202
Whangamomona
Deo
Riverlea
Te Popo
Huiakama
1723
Auroa
Kaponga
Stratford
Wharehuia
Te Wera
1786
Otakeho
Kapuni
Lowgarth
Toko
Douglas
43
Kaupokonui
Mangatoki
Ngaere
Pukengahu
Huinga
1473
Makahu
1615
Kaupokonui
Okaiawa
Matapu
Eltham
Rawhitiroa
Mangamingi
Tututawa
1786
Manaia
Inaha
Te Roti
Puniwhakau
1465
Ohawe Beach
Tokaora
Normanby
MATEMATEAONGA
Te Mapou 2446
Hawera
1211
Ararata
1552
2339
1933
2402
2313
Wharepa
Ohangai
Meremere
1405
1780
1853
SOUTH TARANAKI BIGHT
Mokoia
1349
1670
1558
RANGE
1920
Manutahi
1522
1565

Figure 1   Sample of ICAO 1:500,000 map

Kakaramea
Alton
Hurleyville
1846

DEPARTMENT OF LANDS AND SURVEY

NEW MAPS

BACKGROUND

Accelerating environmental and social changes have accentuated the need for reliable topographic maps, providing an inventory of the country's physical features, and have increased the requirement for up-to-date cadastral maps, presenting a positive identification of all land parcels and their legal status.

Such maps used in conjunction form a basis for the planning and administration of housing, commercial and industrial development, provision of public and social services, protection of the environment, maintenance of law, defence, and the other administrations of government and local authorities in the modern society.

The existing basic topographical map series at one inch to one mile (NZMS 1) was commenced in 1936. Coverage of the North and South Islands was completed in 1976. This series has served the country well over the 40-year period and will continue to meet needs in some areas for several years. However, the specifications of this series no longer fully satisfy the requirements of many users. In addition, the intensification of land use and development and provision of services has created a demand for comprehensive map coverage on scales larger than those at present produced.

Nationwide coverage (except for south-west Fiordland) of the basic cadastral mapping series at one inch to one mile (NZMS 177) was accomplished in 1968. Deficiencies are contained in many sheets which were merely reproduced from much earlier maps, and this series no longer provides an adequate base for recording legal boundary changes or for printing reproduction. For convenience, the scale and sheet layout of this series must be changed to agree with changes made to the new basic topographical map layout. Also, as with topographical maps, the requirements of land administration and planning have created a demand for cadastral map coverage on scales larger than those at present produced.

On 1 January 1973 the Department inaugurated a one-colour survey plan system and introduced metric units for the execution and presentation of all surveys affecting land title. More recently, a single projection and a single grid that allow for the accurate presentation of the whole country on a uniform system were devised. A further development has been the introduction of new cadastral record sheets on transparent foil. This will facilitate the efficient and economic compilation of basic cadastral maps. Reproduction of urban cadastral maps will be by way of plan prints.

It is opportune with the implementation of these innovations to reconsider all aspects of map production with a view to improving scales, layouts, and specifications of basic mapping in order to meet the requirements of map users.

NEW PROJECTION AND GRID

The new projection is conformal but is otherwise unlike any other projection used for detailed mapping. Scale variation is within ± 0.024%, considerably less than that of any other projection previously used for New Zealand.

The new grid, to be known as the New Zealand Map Grid, provides the sheetlines for the new basic map series. The true origin (Lat 41°S: Long 173°E) is assigned arbitrary coordinates sufficiently large to render all coordinates positive, or east and north, of a "false origin". In a metre coordinate system sufficiently extensive to cover the whole country the northing must reach seven integral figures. In the scheme now adopted the coordinates have seven integral figures in all cases. To avoid confusion, the coordinates have been numbered so that eastings are always less than 5 000 000 metres and the northings always greater. The grid is oriented so that the north-south axis of coordinates is tangent to the 173°E meridian at the true origin.

The New Zealand Map Grid, and the layout of the new basic 1:50 000 topographical and cadastral map series are illustrated in Fig. 1.

THE NEW SERIES

To implement the programme of new mapping the Department is to produce the following new map series.

NZMS 260 NEW ZEALAND TOPOGRAPHICAL MAP 1:50 000

This new series of 324 sheets will supersede the present NZMS 1 series. It is to be based entirely on new photogrammetric mapping plotted at a scale of 1:25 000 from up-to-date aerial photography. (Refer to NZMS 270 Topoplot Map at 1:25 000.) Production will be by progressive expansion in selected areas of the country. Sheet format is to be 40 km x 30 km. Contours are to be shown at 20-metre vertical intervals and this substantial upgrading of relief presentation will greatly facilitate planning, utilisation, scientific, and development activities. Map detail is to be "bled" off the top and right edges of the sheets to facilitate continuity of information on to adjoining sheets. Many other improvements on the NZMS 1 series have also been introduced. Drawing has commenced on the first NZMS 260 sheets.

NZMS 261 NEW ZEALAND CADASTRAL MAP 1:50 000

This new series has the same basic sheet layout as NZMS 260 and will supersede the present NZMS 177 series. Production of the new maps is well advanced with many sheets already published and most others in some stage of preparation. The series should be complete at an early date. Production will economically utilise material from existing maps and from larger scale record maps. The new maps present a uniform and up-to-date record of boundaries.

NZMS 262 NEW ZEALAND TOPOGRAPHICAL MAP 1:250 000

This series will supersede the 26 sheet NZMS 18 1:250 000 series. Each of the 18 sheets will have a format of 200 km x 150 km with sheet lines based on the NZMG. As metric contours covering a wide area will not be available for some time, and because of difficulty in interpolation of metric contours from existing material, this series is to be published initially without contours. However, relief will still be adequately represented by spot heights and improved relief shading. These maps will meet an increasing demand by government, local authorities, and the public for up-to-date, comprehensive information at this scale.

The sheet layout for NZMS 262 is illustrated in Fig. 3

EXISTING SERIES AVAILABILITY

Until maps in an entire region are superseded by the new series previously described, all existing map series will be maintained by revision and reprint to ensure that up-to-date information remains readily available.

NZMS 269 NEW ZEALAND TOPOGRAPHICAL MAP 1:10 000

This will be an entirely new series, initiated to provide larger scale mapping of major built up areas and their environs, and in other areas if required. Sheet lines will be those of the 1:10 000 Cadastral Record Maps, each sheet covering an area 5 km x 7.5 km. Specifications are yet to be prepared but it is possible that this series will consist of orthophoto (true-to-scale photo) maps, overlaid with 5-metre vertical interval contours produced by photogrammetric methods.

NZMS 270 NEW ZEALAND TOPOPLOT MAP 1:25 000

These sheets are plotted at 1:25 000 by photogrammetric methods as a base for the preparation of the NZMS 260 1:50 000 series. Sheetlines are a subdivision of the 1:50 000 sheet lines and have a map coverage of 20 km x 15 km. The maps will not be published in colour but are available in plan print form, initially as unchecked plots, then, after field checking, as NZMS 270 maps. In final form contours will be available separately from other detail and vice versa, if required, for ease of interpretation. Photogrammetry is to be produced on a progressive basis and various areas of New Zealand will be covered systematically on a priority basis. See Fig. 2 for NZMS 270 sheetlines and numbering.

OTHER CADASTRAL MAPS

The preceding paragraphs provide a brief description of the main map series the Department is producing or proposes to develop. To acquaint users with the full system some further explanation is necessary with regard to cadastral mapping. Prior to metrication, cadastral information was produced as:

(a) NZMS 177 Cadastral Maps 1:63 360.

(b) Town Series Cadastral Maps, i.e., NZMS 16, NZMS 189, and miscellaneous tracings.

(c) The record map system.

As mentioned earlier, the NZMS 177 series is being replaced by the NZMS 261 Cadastral Map Series.

A new record map system has been introduced with the maps being drawn on transparent foils. This will be a black-and-white system and maps will be kept up to date by constant revision. Copies will be available at any time in print form. It will also be possible to produce transparencies or prints of the cadastral linework pattern only, for planning or other purposes. In special cases this can be produced at any scale.

SHEET NUMBERING SYSTEM

The advantages of adopting rational sheet layouts based on the N.Z. Map Grid have been recognised by numerous organisations outside the Department of Lands and Survey. It is clear that scales larger than those used by the Department for its records are required by other users, and after consultation with other organisations a standard numbering system that can be adopted by any organisation has been devised.
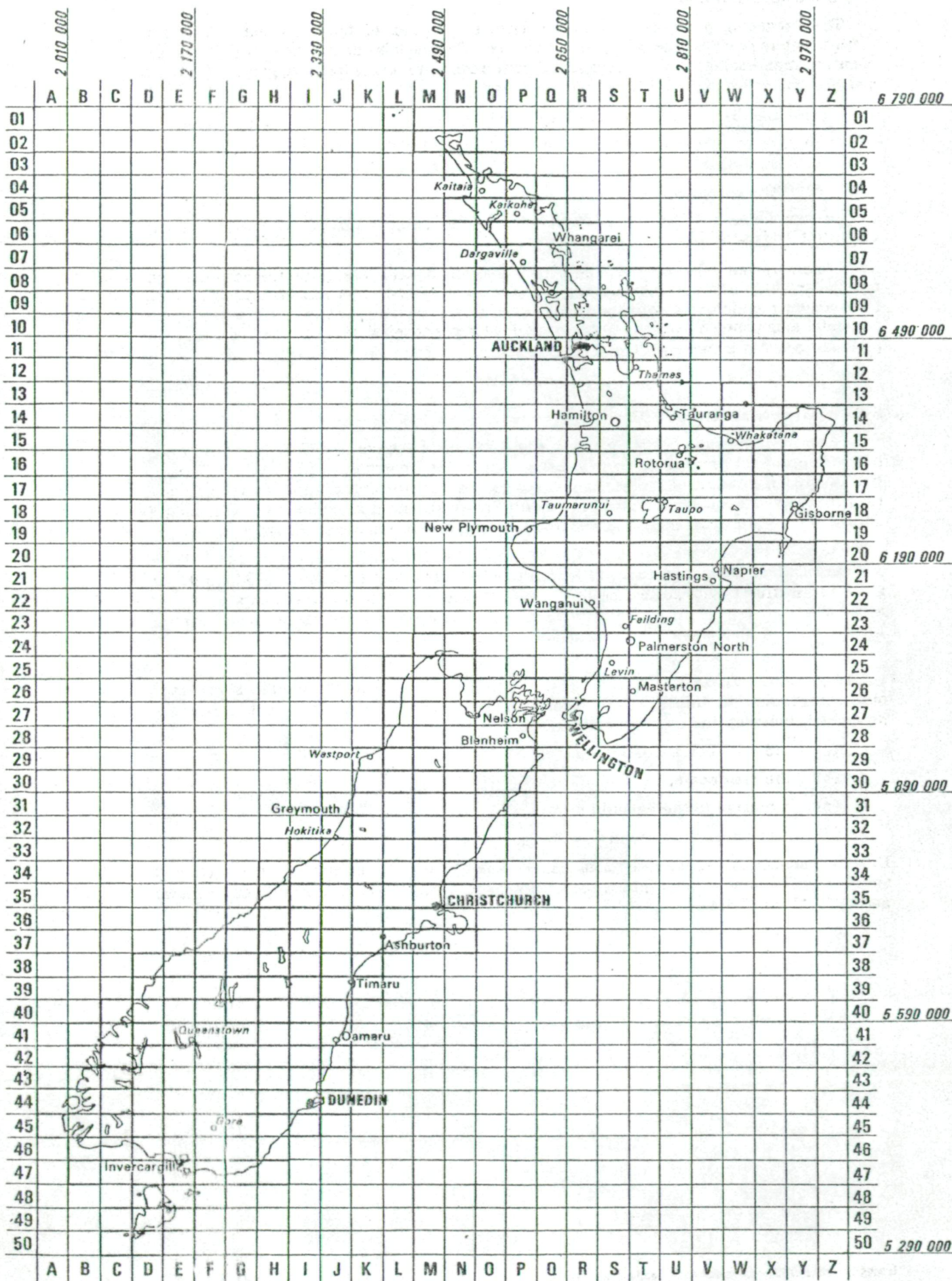
The 1:50 000 sheet layout provides the basis for the new numbering system. Each 1:50 000 sheet area, known as a "Prime Rectangle" has a map coverage of 40 km x 30 km and is identified by the alphanumeric system illustrated in Fig. 1, with sheets numbered and named. The 1:25 000 NZMS 270 Topoplot Maps and Cadastral Record Maps also have an alphanumeric system illustrated in Fig. 2

Larger scale cadastral record maps at 1:10 000, 1:2 000, and 1:1 000 are also based on a breakdown of the 1:50 000 sheets but the system differs from that previously described, being made up of four components:

(a) the 1:50 000 sheet number;

(b) the map scale;

(c) a number in the easterly row;

(d) a number in the southerly column.

Each component is separated by a standard symbol, i.e., (a) and (b) by a dash, (b) and (c) by a stroke and (c) and (d) by a stop. Hence the number of a 1:10 000 sheet is shown as R 27 - 10 000/8.4

q

2 010 000   2 170 000   2 330 000   2 490 000   2 650 000   2 810 000   2 970 000

A B C D E F G H I J K L M N O P Q R S T U V W X Y Z   6 790 000

01 ... 50

Kaitaia
Kaikohe
Whangarei
Dargaville
AUCKLAND
Thames
Hamilton Tauranga
Whakatane
Rotorua
Taumarunui Taupo
New Plymouth Gisborne
Hastings Napier
Wangahui
Feilding
Palmerston North
Levin
Masterton
Nelson
Blenheim WELLINGTON
Westport
Greymouth
Hokitika
CHRISTCHURCH
Ashburton
Timaru
Queenstown Oamaru
DUNEDIN
Gore
Invercargill

6 490 000
6 190 000
5 890 000
5 590 000
5 290 000

INDEX TO 1:50,000 MAP SERIES SHEETS
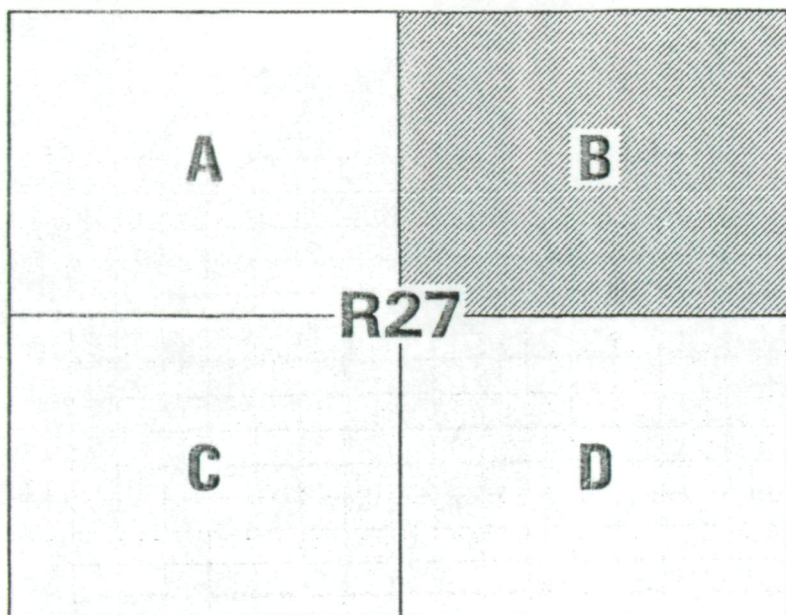
Reference by letter and numerals e.g. R 27

New Zealand Map Grid   (values in Metres in italic figures)   (Sheet size 40km×30km)

By Department of Lands and Survey – 1976

MAP NUMBERING SYSTEM

1:50 000

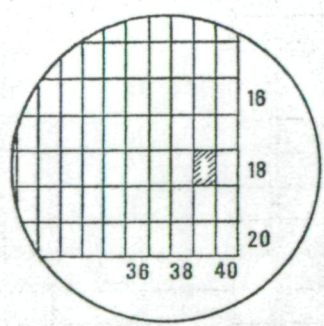This sheet is
NZMS 270 R27B
(1 : 25 000 scale)

Sheet size 20 X 15 km

	1	2	3	4	5	6	7	8
1	1.1	2.1	3.1	4.1	5.1	6.1	7.1	8.1
2	1.2	2.2	3.2	4.2	5.2	6.2	7.2	8.2
3	1.3	2.3	3.3	4.3	5.3	6.3	7.3	8.3
4	1.4	2.4	3.4	4.4	5.4	6.4	7.4	8.4

This sheet is
R27–10 000 / 8.2
(1 : 10 000 scale)

Sheet size 5 X 7.5 km

(8 X 4 sheets in each
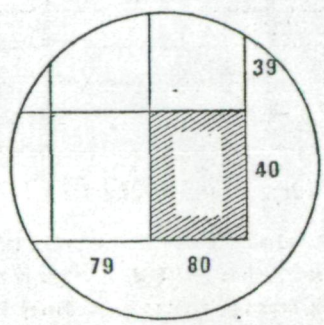1 : 50 000 prime rectangle)

1 : 2000 scale

(Size 1 X 1.5 km

40 X 20 sheets
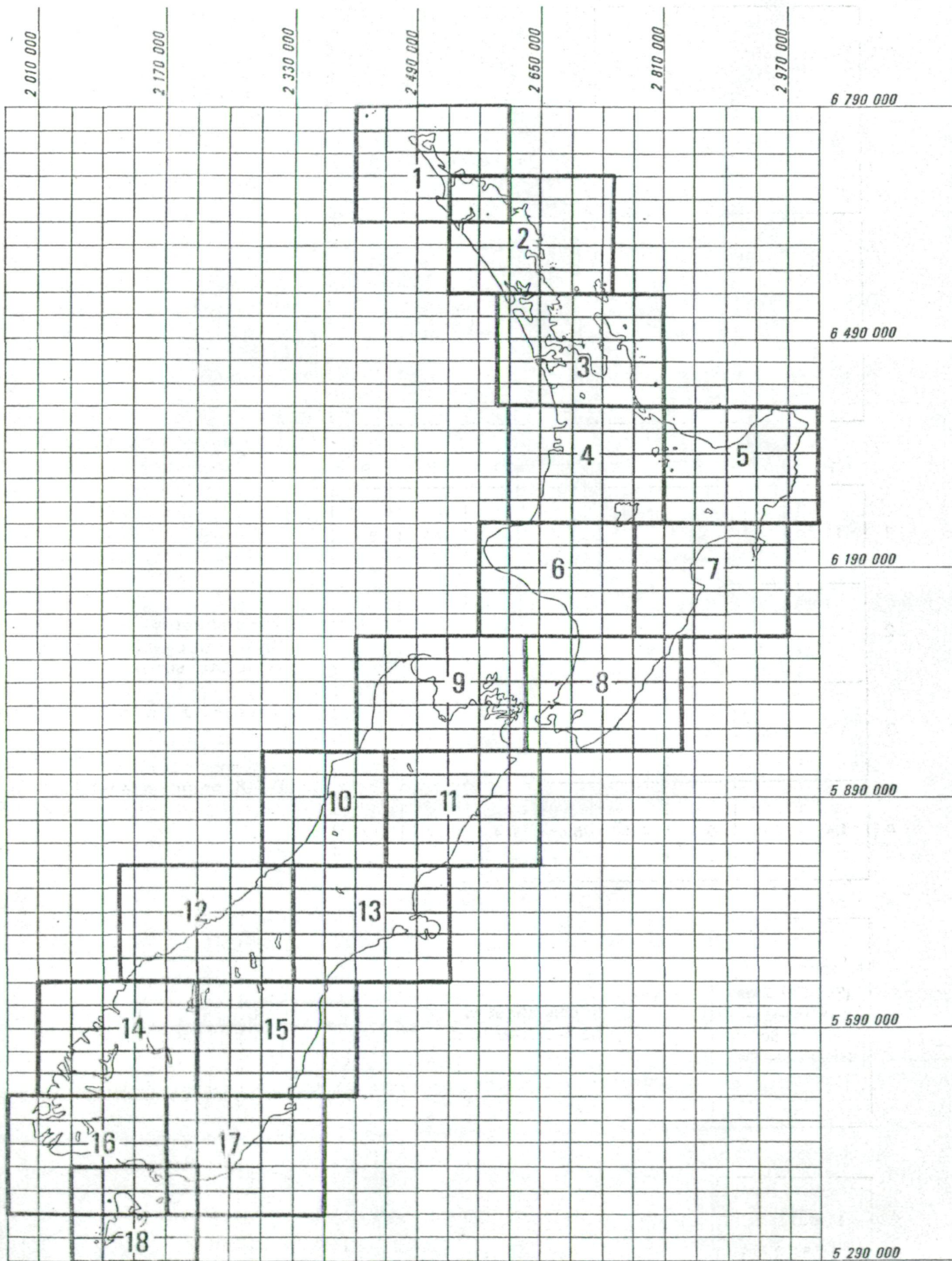in each 1 : 50 000
prime rectangle)

This sheet is
R27–2000/39.18

1 : 1000 scale

(Size 0.5 X 0.75 km

80 X 40 sheets
in each 1 : 50 000
prime rectangle)

This sheet is
R27–1000/80.40

11

INDEX TO NZMS 262 NEW ZEALAND TOPOGRAPHICAL MAP SERIES 1:250 000

Based on 1:50 000 SERIES SHEET LINES
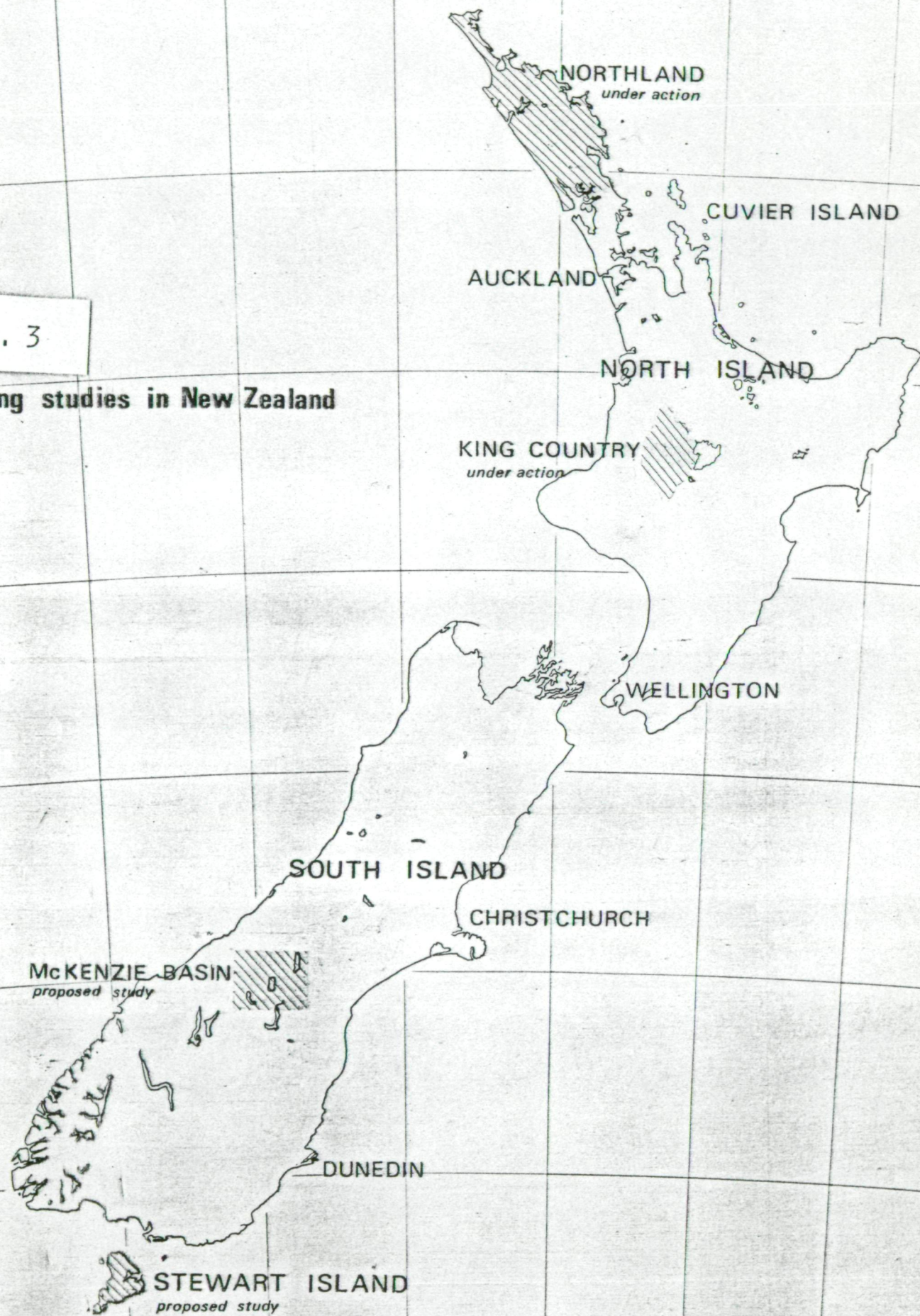
New Zealand Map Grid   (values in metres in italic figures)

By Department of Lands and Survey 1976

12

Fig. 3

planning studies in New Zealand
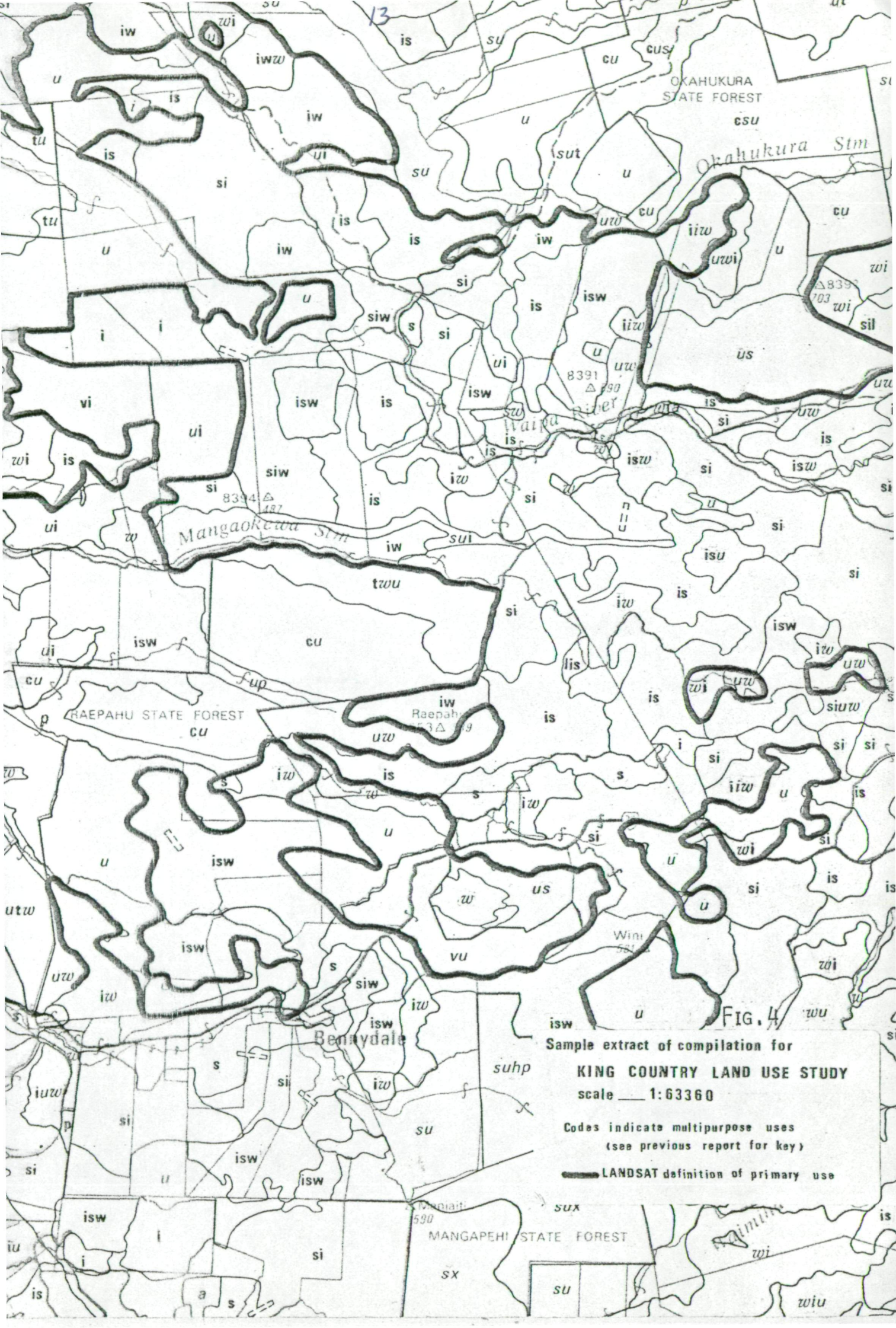
NORTHLAND
under action

CUVIER ISLAND

AUCKLAND

NORTH ISLAND

KING COUNTRY
under action

WELLINGTON

SOUTH ISLAND

CHRISTCHURCH

McKENZIE BASIN
proposed study

DUNEDIN

STEWART ISLAND
proposed study

FIG. 4

Sample extract of compilation for

KING COUNTRY LAND USE STUDY
scale ____ 1:63360

Codes indicate multipurpose uses
(see previous report for key)

⸺ LANDSAT definition of primary use

Part V

New Zealand Forest Service

LANDSAT Projects

Address: New Zealand Forest Service
                              Private Bag
                              Wellington

Telephone No.:   Wellington 721-569

NZFS Co-ordinator: Mr Neville Ching

Authors: Mr N. Ching   (NZFS, Wellington)
                              Mr B. Lean   (NZFS, Christchurch)
                              Mr R. Dale   (NZFS, Auckland)

- 1 -

CONTENTS

———

FIGURE CAPTIONS

Figure 1   Ground truth map of Eyrewell State Forest
            applicable to scene no. 2282-21254.

Figure 2   Relation between the colour coded LANDSAT composite
            of scene 2282-21254 and panchromatic aerial imagery
            of various regions in Eyrewell State Forest. (For
            interpretation Key see text.)

Figure 3   Eyrewell Forest windthrow interpretation obtained
            from LANDSAT scene no. 2282-21254.

Figure 4   Location of transect lines for the St. Arnaud
            Mt. Robert snow cover study

            (a) Transect line for CCT radiance comparisons
                on Mt. Robert

            (b) CCT radiance transect lines at the head of
                Six Mile Creek Basin on the St. Arnaud
                Range.

            (c) Ground sampling transect line.

1.   CANTERBURY WINDTHROW   - B.M. Lean   (NZFS, Christchurch)

LANDSAT Imagery of Eyrewell State Forest

From 31 October 1975 LANDSAT imagery (1) composite colour prints of bands 4, 5 and 7 were produced by STATOS and ANAC line printers at an approximate scale of 1:38,000 covering a portion of the Eyrewell pine plantation that contained windthrown trees.

Ground Truth: By comparing these prints with 1:10,000 panchromatic photography taken on 1 November 1975 (2) categories of plantation conditions were selected that proximate each other. The "ground truth" map, Fig. 1, was compiled on this basis from the 1:10,000 photography.

Interpretation Keys: Selective keys were used to aid the interpretation of the composite colour prints derived from the LANDSAT imagery. Several keys are illustrated in Fig. 2.

Note - The numbered photographs coincide with the numbered areas overlaid over the LANDSAT imagery. Aerial photographs were taken at a scale of 1:10,000 on 1 November 1975.

1. Windrowed site   6. 6 yr stand, $\pm$ 60% cover
2. Recent planting   7. Logged area
3. Mostly windthrown   8. 7 yr stand, $\pm$ 70% cover
4. Completely windthrown   9. 5 yr stand, $\pm$ 35% cover
5. Thinned stand, $\pm$ 40% cover   10. 6 yr old stand

Interpretation: A tentative interpretation based on the STATOS print was illustrated in the last report.

The ANAC print is easier to read although some variations, such as scattered windthrow areas, do not show up as prominently.

Standing Crop: Almost all of the healthy stands depicted are Pinus radiata planted in 1966 and later. A correlation between age, height, thinning and crown density cover is indicated in Table 1.

A comparison of the LANDSAT imagery on the colour composite prints with the ground truth map show that the pattern indicated in the above table is broadly reflected.

This aspect of the present study is suggestive that REGULAR SEQUENTIAL LANDSAT IMAGERY COULD BE USED AS A MONITORING AND SURVEY TOOL TO IDENTIFY AREAS OF SOME FOREST OPERATIONS, such as logging, thinning, and changes in forest canopy extent or condition. Once recognition techniques are developed the computer should be able to recognise areas of 1.6 hectares and greater and perhaps down to 0.4 hectare depending on how the particular area is distributed over the "pixels".

(1) Scene 2282-21254

(2) Aerial Survey No. 2872

(One stand of planting was recorded as being 6.2 ha in area and the LANDSAT imagery drew our attention to it and was subsequently revealed on checking to be a strip of planting half of the width indicated on our maps.)

TABLE 1

Years After Establishment	Approx. Height in metres	Approximate Crown Cover	Thinning Treatments	Approx. Crown Cover After 1st Thinning
1	0.5			
2	1.0	5%		
3	2.0	20%		
4	2.8	30%		
5	3.7	40%		
6	5.0	55%	1st	
7	6.0	70%	thinning	35%
8	8.0	75%		55%
9	9.0			70%
10	10.6		Planned	Windthrow 40%
11	12.0		2nd	Partial to
12	13.0		thinning	severe windthrow

Windthrown Trees: Of particular interest was the extent to which windthrown areas could be distinguished in a visual interpretation of the colour composite prints. From the ANAC and STATOS prints an interpretation is mapped in Fig. 3.

In Fig. 3 the locality of 503 hectares of windthrown plantation are shown. Almost all of the scattered windthrow areas on the east (right) side of the map shown in strips are of such a pattern that 67 hectares are to be retained as productive stands.

Of the remaining 436 hectares, 64% was clearly identified with windthrow, 13% was recognised as windthrow with uncertainty, 11% showed up as low crown density covered areas, and 12% was not picked up on the colour composite prints.

Contributing factors for some windthrow areas not to print up could be:

(a) the distribution of the area over the pixels

(b) the pattern that the scattered windthrown trees and upright trees make together over the pixels, especially where the two categories of trees tend to balance each other.

Generally, stands covered with windthrown material show up
distinctively on the colour composite prints, but where standing
trees and land surface areas become mixed with the windthrown
trees then it shows up on the prints with varying success.

Summary

The colour composite prints produced by the ANAC line printer
are easier to interpret. The expanding crown coverage of the young
tree crop was reflected and some forest operations showed up.
Significant areas of windthrown trees were recognised and mixed
areas of windthrown and standing trees were partially indicated.

Remarks

An improvement in the computer classification and subsequent
prints (colour or computer printout) is needed.

The windthrow classification of the pixels is affected by
three scene object variables:

1.   windthrown material

2.   standing trees

3.   visible land surfaces.

Familiarisation with the apparent radiances of the subject
matters in the various LANDSAT bands should help, and (if feasible)
perhaps "proportion estimation" of chosen signatures in selected
LANDSAT wavebands by the computer would refine classification.

If completely windthrown areas and areas of varying density of
windthrow could be emphasised on the colour composite prints or
computer printouts then this should help interpretation and checking.

2.   CLASSIFICATION OF FOREST TYPES IN THE KING COUNTRY -
     Mr R. Dale   (NZFS, Auckland)

     The LANDSAT photographic data (Fig. 4 - colour diapositives
off the isodensitometer and 1:63,360 enlargements of Fig. 3, which
both appeared in the Third Quarterly Report) have been of little
use for this land use study. The reason for this is the resolution
of the imagery for forest typing and forest descriptions must be
greater than that available. The only use made of the photographs
was in identification of clearfelling and conversion areas,
particularly for private forests in the absence of up to date
large scale aerial photography. The 1:63,360 enlargements, although
used, were of poor definition but the information was gained by the
help of two photos similar in scale to Fig. 3 of the Third Report.

     Unfortunately the tight deadlines imposed for the completion
of the land use study and the sheer volume of work involved has not
enabled a closer study of the applications of LANDSAT in forest
typing for this form of study.

3.   MAPPING OF SNOW AREAS ON THE ST. ARNAUD MOUNTAIN RANGE

     A transect has been set out on the ground and measurements
are being made to coincide with the satellite overpass - weather
permitting.

     The transect was located on a south facing slope. This site
was chosen as it appeared to be the most likely location for a
ski field.

     The transect's centre line was marked out with a series of
pegs - approximately 100 ft apart. Depth readings are made along
the centre line and at a distance 100 ft either side of the centre
line.

     This is indicated between locations on Fig. 4c which shows
the centre line and a line 100 ft either side where the outer readings
are made.

     Staff at P.E.L. are utilising coded computer print out data to
plot changes in four band MSS radiant intensity along the four
transect lines shown in Fig. 4 (A-D, C-D, B-D, E-F). The scene under
study here using CCT data is the same as that studied using
photographic techniques and shown in Figs. 5b and 6 of the Third
Quarterly Report - scene no. 2282-21252. A progress report on this
study is given in Part I of this quarterly report.

4.   HANMER FIRE DAMAGE MONITORING

     As outlined in the Third Quarterly Report it was planned to use
multispectral imagery to monitor any changes in vigour within the
foliage of the Hanmer State Forest damaged by fire on 22/23 March 19
Bad weather has acted against acquisition of all the desired satelli
aircraft coverage but one flight, on 4 February 1977, has been possi
The results are currently being studied.

Part EYREWELL STATE FOREST

GROUND TRUTH

PLANTATION COVER

☐ Over 65% crown cover	☐ Windthrow (sc'td.=scattered)	
☐ 65 – 35% „ „	☐ Logged	
☐ 35 – 20% „ „	☐ 1975 planting	
☐ Less than 20% „ „	☐ Site prepared partially	

Scale 1: 38 000
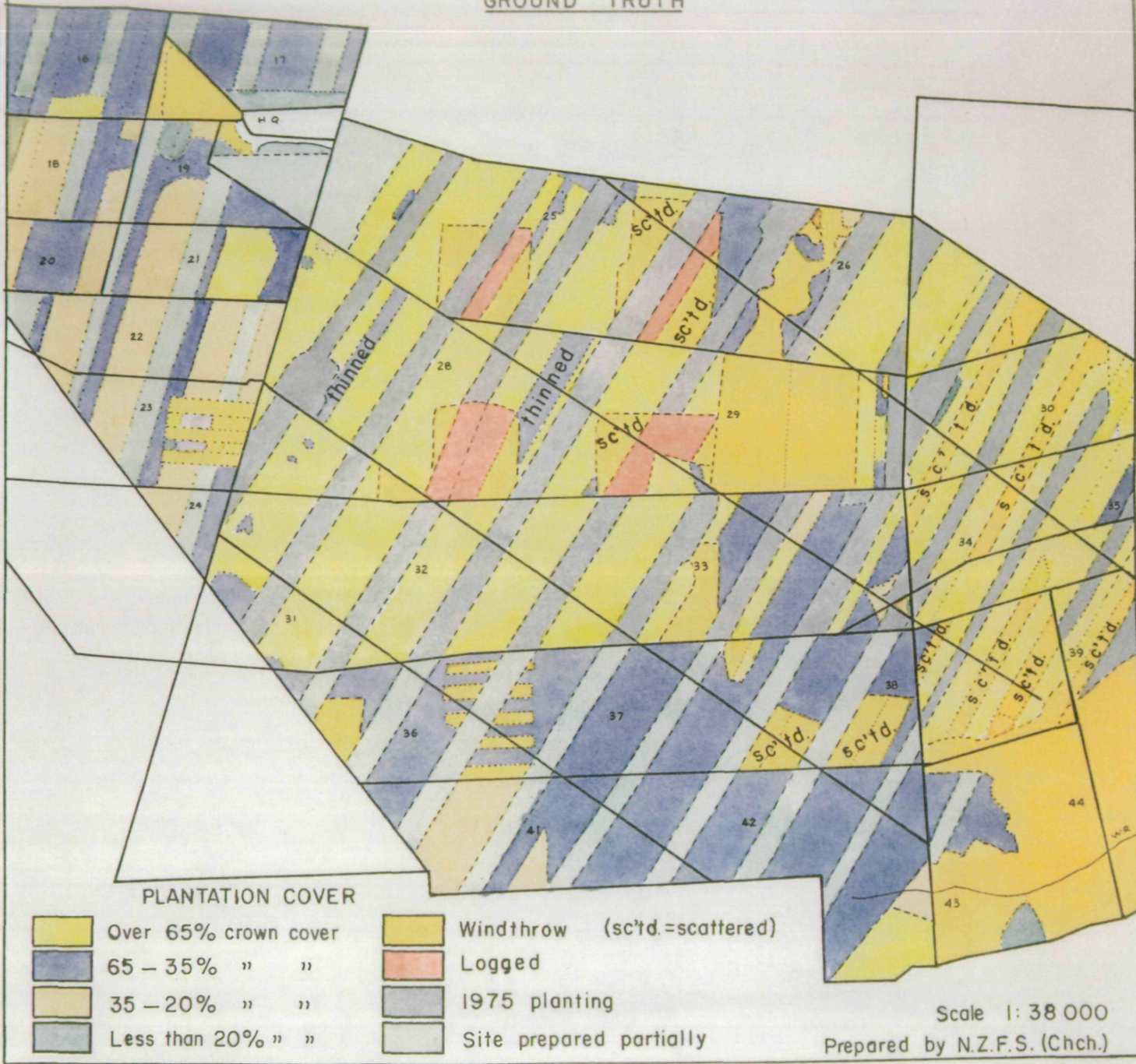
Prepared by N.Z.F.S. (Chch.)

Figure 1   Ground truth map of Eyrewell State Forest
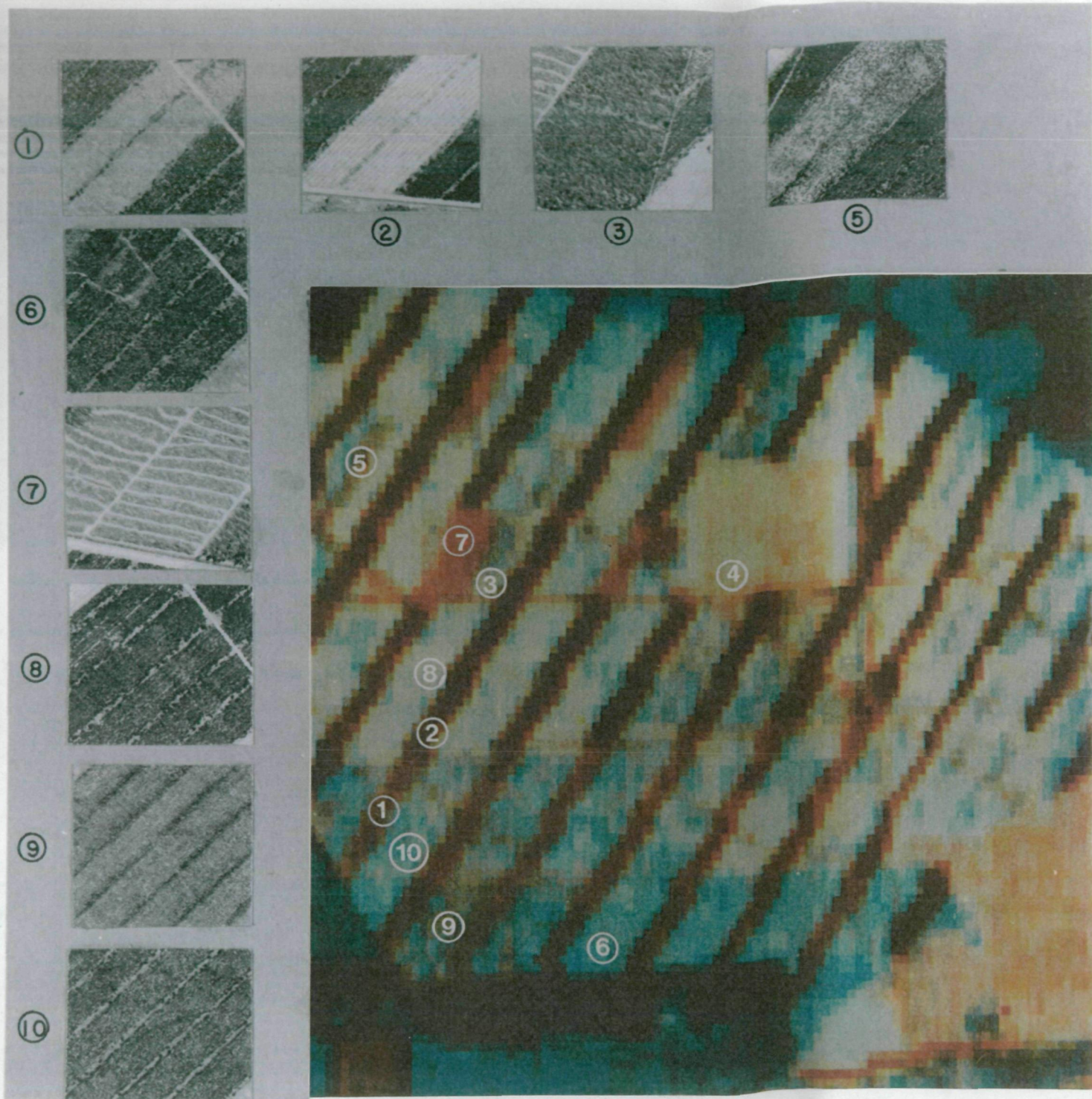applicable to scene no. 2282–21254.

Figure 2   Relation between the colour coded LANDSAT composite
of scene 2282-21254 and panchromatic aerial imagery
of various regions in Eyrewell State Forest. (For
Interpretation Key see text.)

Part EYREWELL STATE FOREST
Windthrow interpretation

Windthrown areas certainly identified
Windthrown areas uncertainly identified
Scattered windthrow showing up as a low crown density cover
Scattered windthrow not picked up on prints
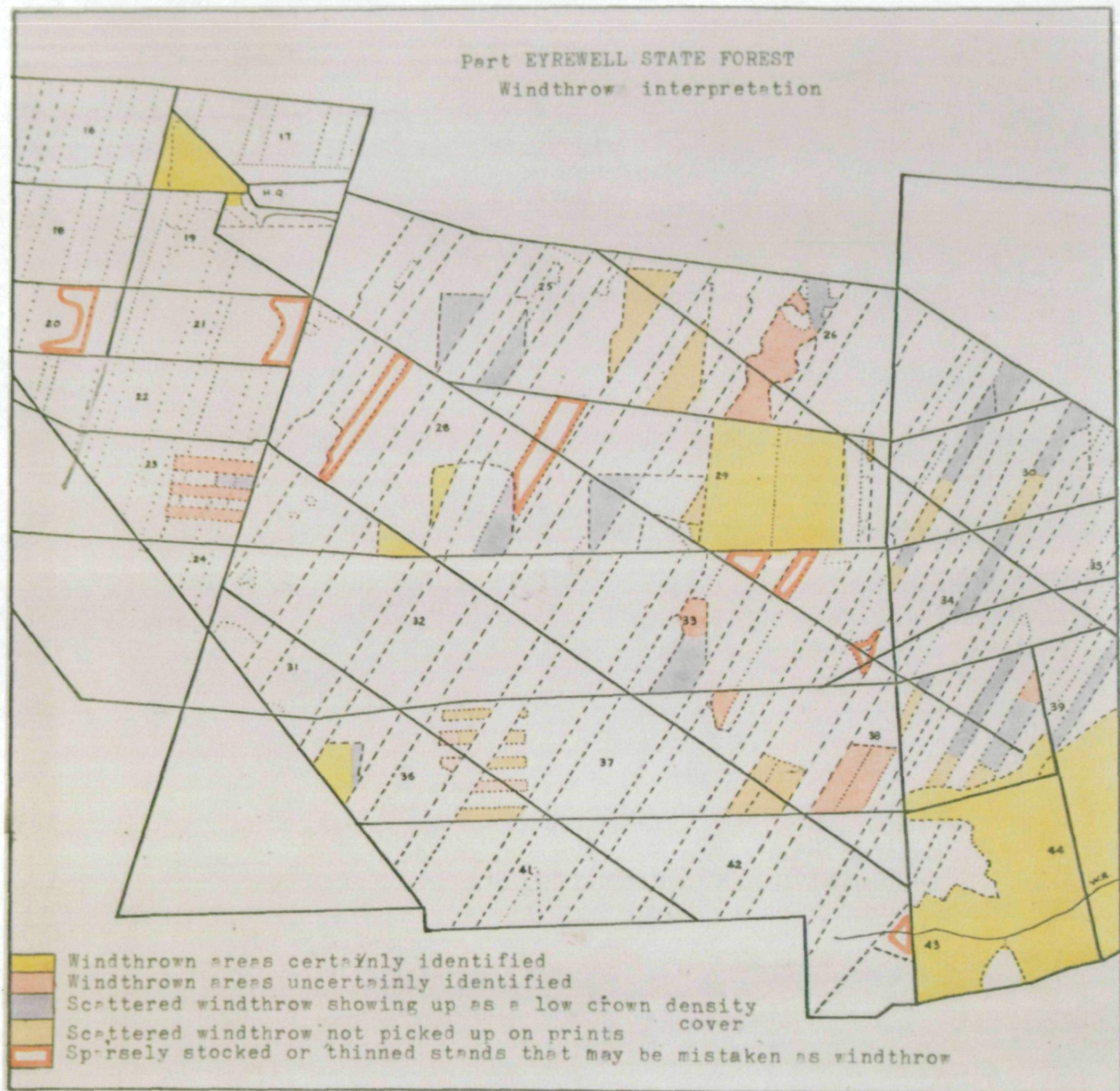Sparsely stocked or thinned stands that may be mistaken as windthrow

Figure 3   Eyrewell Forest windthrow interpretation
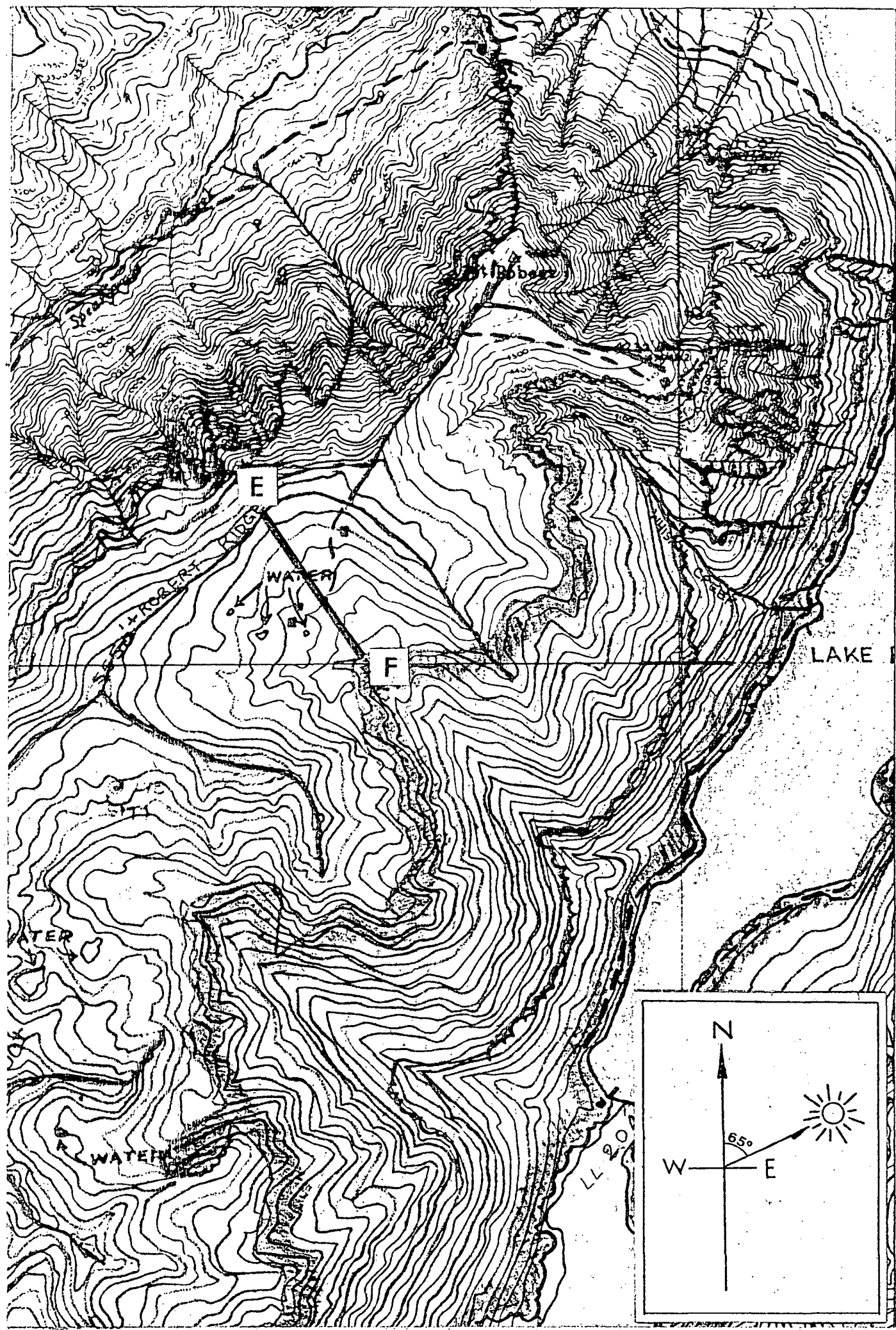obtained from LANDSAT scene no. 2282-21254.

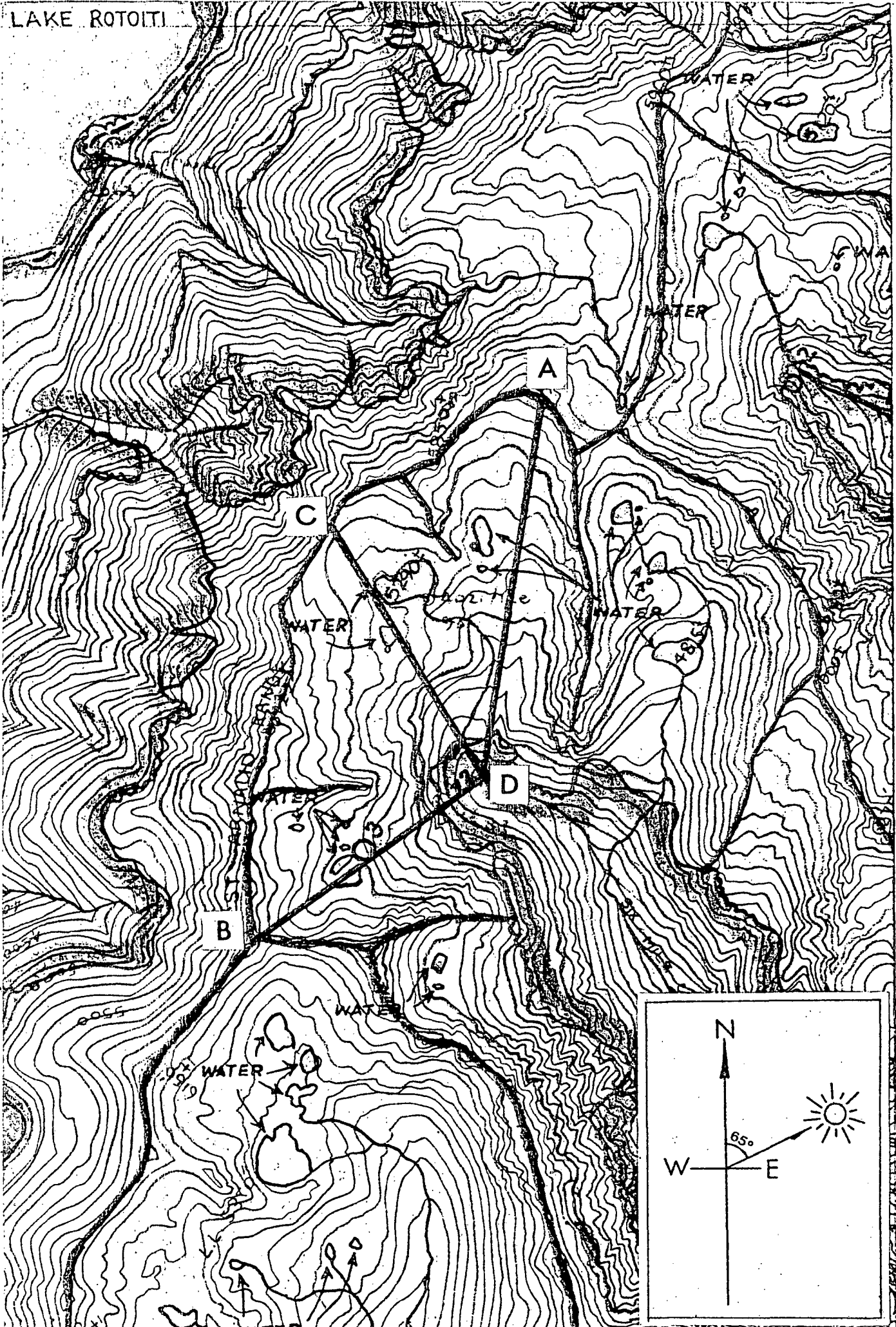Fig. 4a   Transect line for CCT radiance comparisons on Mt. Robert.

Fig. 4b CCT radiance transect lines at the head of Six Mile Creek Basin on the St. Arnaud Range.
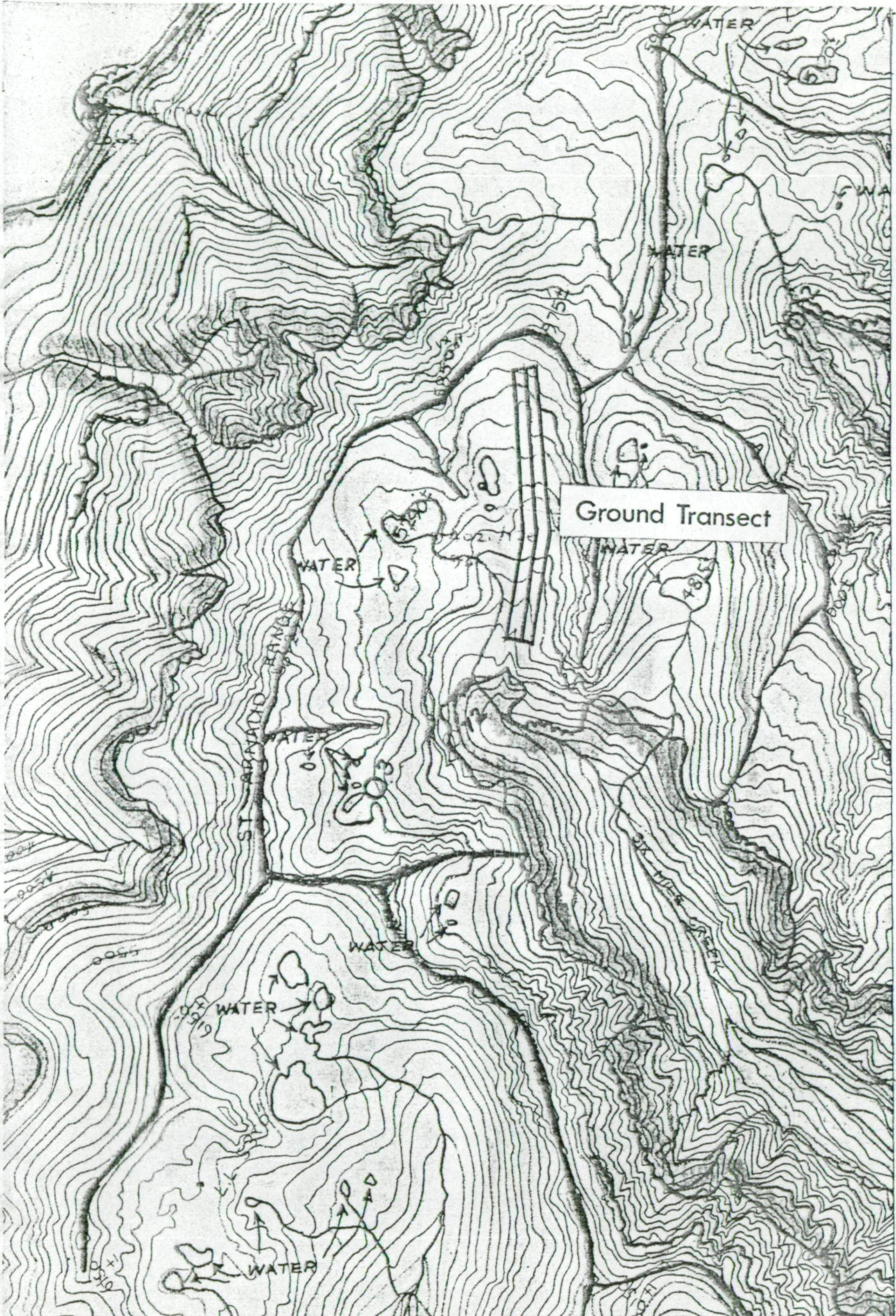
Ground Transect

Fig. 4c   Ground sampling transect line.

13

Part VI

Vegetation Map and Landform Map of

Aupouri Peninsula, Northland

Agency: Ministry of Works and Development
                            Water and Soil Division

Address: P.O. Box 12-041
                            Wellington North
                            New Zealand

Telephone No.:   Wellington 729-929

                            Extension 596

Author: Mr Douglas L. Hicks

FIGURE   CAPTIONS

Figure 1   Vegetation map of Aupouri Peninsula, Northland.

Figure 2   Landform map of Aupouri Peninsula, Northland.

———

1.   INTRODUCTION

These maps were drawn to assess the accuracy with which the
boundaries (a) of major vegetation types, and (b) of major landform
types on sand dune terrain can be mapped from LANDSAT imagery, for
the purpose of catchment condition survey work in the coastal sand
dune country of New Zealand.

2.   TECHNIQUE

Overlay maps were traced directly from a 1:1,000,000 colour
composite print of bands 4, 5 and 7.   (LANDSAT I.   ID No: 1648-21240
2 MAY 1974)

3.   VEGETATION MAP   (Figure 1)

Boundaries of major vegetation types were easily located, due
to clear colour contrasts on the print.   The principal limit to
accuracy was the 1:1,000,000 scale of the print;   much more detailed
boundaries could have been mapped had a 1:250,000 enlargement been
available.

Peat swamps, due to their complete absorbtion of near I.R.
radiation (band 7), could not be distinguished from lakes, nor
could manuka scrub dominant peat swamp be distinguished from sedge
dominant peat swamp.

Subtle contrasts in red hue within the pine forest areas
distinguished young (< 12 year old) pine plantations from isolated
older stands of mature trees planted in the 1940s.

Subtle differences in the red hue of pasture areas could be
matched with either increasing vegetation stress or decreasing soil
moisture, in a dark - pale sequence from pasture on clay soils,
through pasture on swampy interdune flats, to pasture on dune ridges.

Since the LANDSAT map shows large areas of recently planted
marram grass and pine trees, together with areas of new pasture on
recently developed Crown Land farm settlement blocks, it is
considerably more accurate than the most recent 1:250,000 topographic
map of the peninsula (1963).   Apart from the failure to distinguish
peat swamp vegetation, or to differentiate small patches of indigenous
forest in a matrix of scrub, the level of accuracy approximates the
current 1:63,360 topographic coverage (1971 - 75).

4.   LANDFORM MAP   (Figure 2)

Boundaries between transverse dunefields, parabolic dunefields
and foredunes were mapped except where obscured by pine plantations.
Boundaries between dunefields and solid rock were detected where
covered by pasture, but not where covered by scrub.   It was not

possible to detect boundaries between parabolic dunes of different ages (three parabolic dunefields are present), or between foredunes of different ages (two foredune belts are present). In some places, a known correspondence between a scrub-pasture boundary and a geomorphic boundary enabled the latter to be mapped, even though there was no obvious change in terrain.

Clear dune ridge patterns were visible in all three types of dunefield, and could have been mapped had a 1:250,000 enlargement been available.

The accuracy of the LANDSAT map, in detecting major landform boundaries, is not as great as either the 1961 1:250,000 New Zealand Geological Survey map, nor the author's unpublished 1:50,000 geomorphological map. This is due to the failure of the LANDSAT image to detect changes in drainage patterns, dune shapes and soil types, which are crucial for delineating dunefields of different ages.

5. CONCLUSIONS

LANDSAT imagery enables accurate mapping of all the vegetation types shown on the 1:250,000 and 1:63,360 topographic coverage of the Aupouri Peninsula, with the exception of peat swamp vegetation. The detail and accuracy of the map exceeds that of 1:250,000 coverage and approaches that of 1:63,360 coverage.

LANDSAT imagery can differentiate pine plantations on sand country into at least two age classes. It can also differentiate pasture on the basis of stress induced by soil moisture variations, from wet inter-dune hollows to dry ridges.

LANDSAT imagery is unsuitable for geomorphological mapping in sand dune country, since while it can detect major differences in terrain (e.g. dune ridge patterns), it cannot detect less obvious variations in dune characteristics, such as soil type. It does have some geomorphological application, as a means of mapping dune ridge patterns, and as a means of detecting long term change in the position and vegetation cover of active dunes.

It is unlikely that LANDSAT imagery, in its present form, can be used for initial catchment condition survey work in sand dune country on the New Zealand coastline. This is due to its inability to detect subtle parameters of dune conditions, e.g. variations in soil type, and individual erosion scars. However, should subsequent re-survey be required, to establish catchment trend, comparative LANDSAT imagery for the two survey dates would enable assessment of changes in position and vegetation cover of active dunes. It would also enable assessment of changes in vegetation and land use on stable dune country. In both cases, field checks would be necessary to obtain more detailed information about the changes depicted by the imagery.

3

Figure 1.

Vegetation Map of Aupouri Peninsula, Northland.
Drawn from Landsat I Image 1648-21420.

Key

1. Bare sand dunes
2. Marram Grass Plantings
3. Pine Plantations
4. Sown Pasture
5. Sown Pasture, reverting to scrub.
6. Scrub (Manuka dom.)
7. Peat Swamps and Lakes.

N

0 10 20 30 40 km

Scale 1:1,000,000
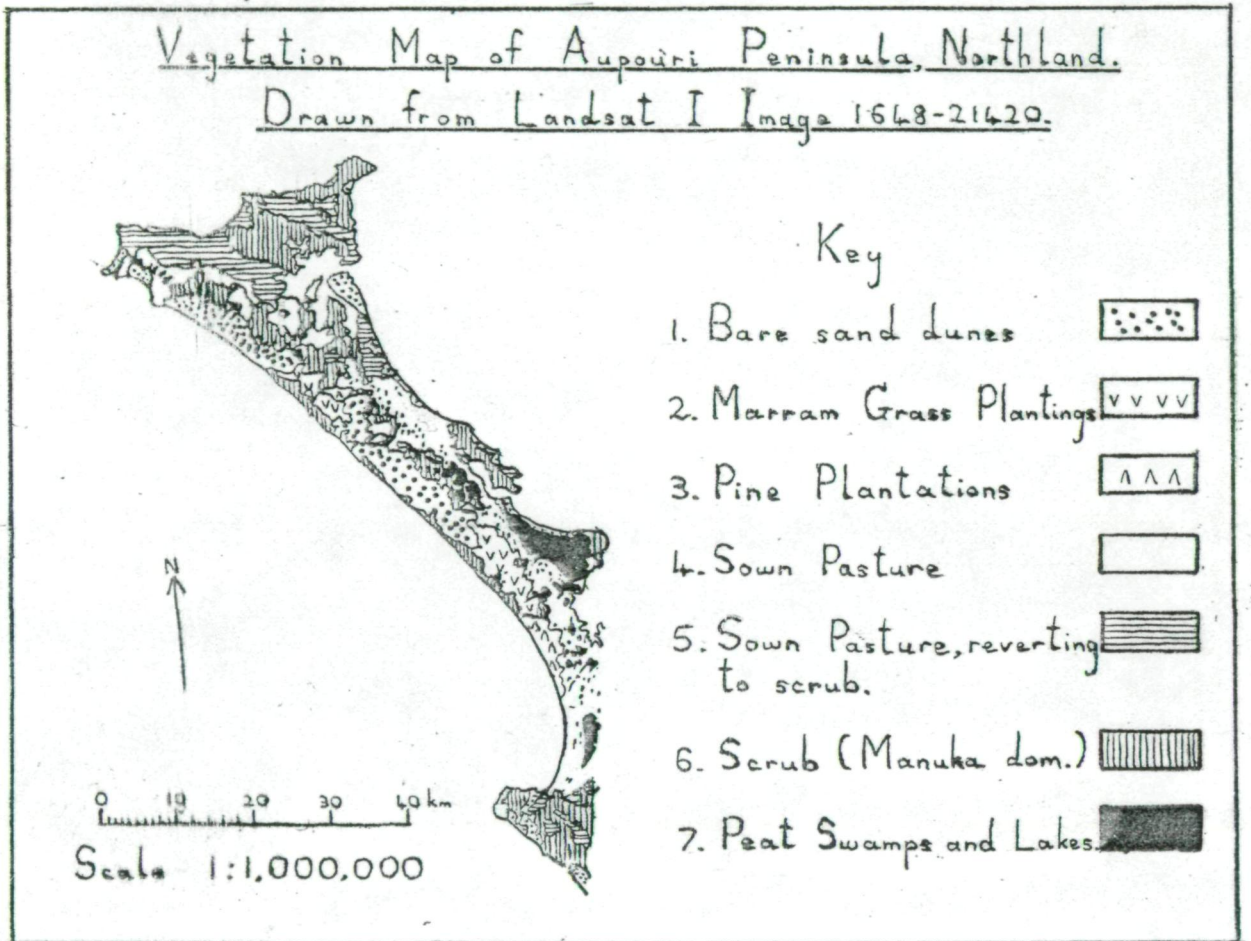
Figure 1   Vegetation map of Aupouri Peninsula, Northland.

4

Figure 2.

Landform Map of Aupouri Peninsula, Northland.
Drawn from Landsat I Image 1648-21420.

Key

1. Coastal Deflation Zone
2. Transverse Dunes
3. Parabolic Dunes
4. Foredunes
5. River floodplain and deltaic deposits
6. Lakes
7. Fluvially dissected hill country, formed on solid rock.
8. Terraced sand deposits.

N

0 10 20 30 40 km.

Scale 1:1,000,000.

Boundary identifiable on image
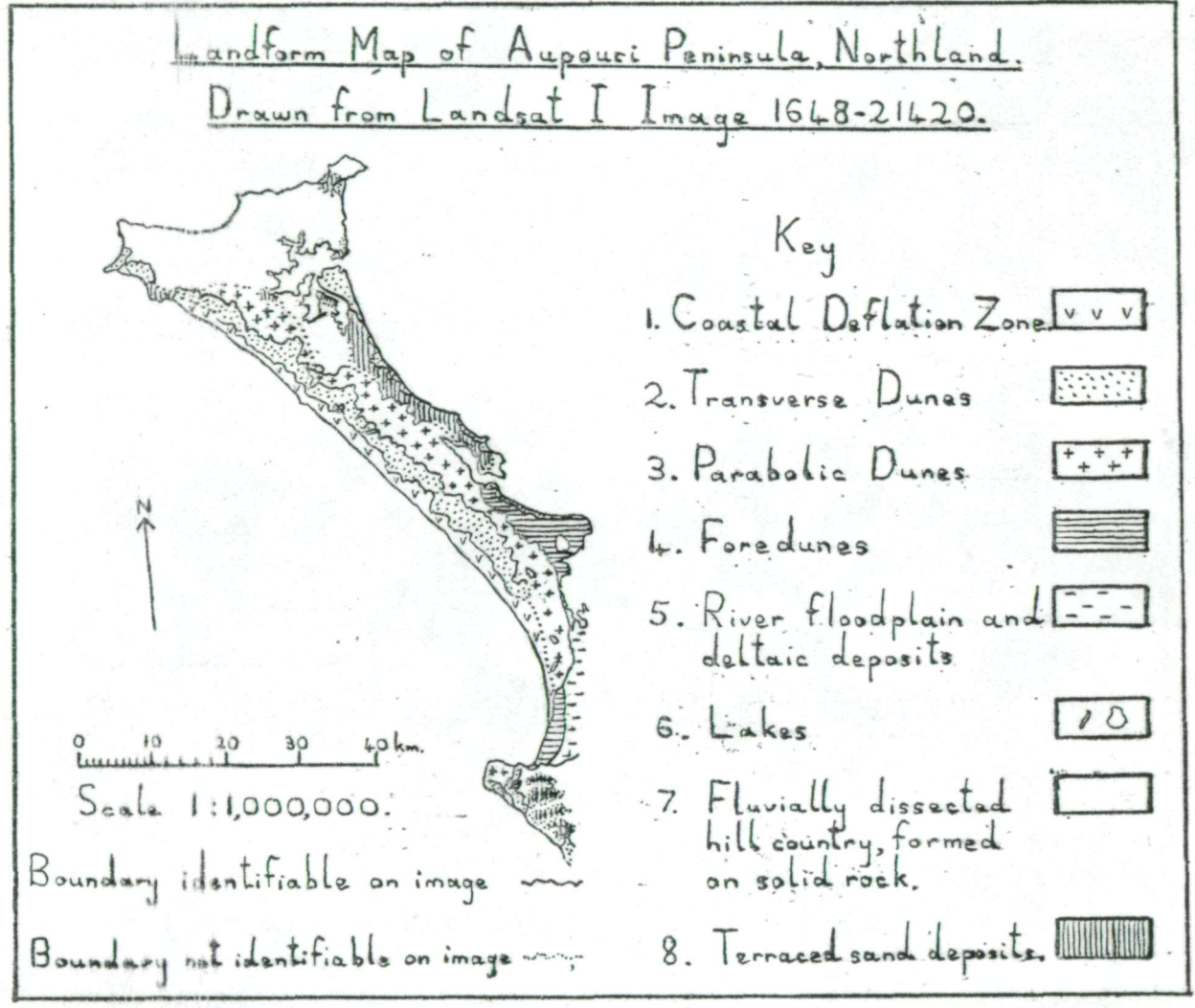
Boundary not identifiable on image

Figure 2   Landform map of Aupouri Peninsula, Northland.

PART VII

GEOGRAPHICAL APPLICATION IN LANDSAT MAPPING:

LANDUSE AND ENVIRONMENTAL STUDIES USING SATELLITE

IMAGERY, ELECTRONICALLY ENHANCED IMAGERY, AND

COMPUTER PROCESSING TECHNIQUES

Investigator: Professor G. Ross Cochrane

Agency: Department of Geography
                     University of Auckland

Address: Private Bag
                     Auckland
                     NEW ZEALAND

Telephone No.:   Auckland 74-740

Author: G. Ross Cochrane

———

1.   INTRODUCTION

The Department of Geography of the University of Auckland is continuing its analysis of a range of LANDSAT single band and colour composite imagery made available by P.E.L. The use of facilities for image interpretation at P.E.L. remote sensing unit is gratefully acknowledged.

Major interest is focussed upon:

1. Landuse mapping

2. Vegetation classification

3. Pasture change and seasonal productivity

4. Hydrology

5. Geologic-geomorphic mapping

6. Coastal processes

2.   TECHNIQUES

2.1 Photographic Interpretation

Standard photo interpretation techniques are being used on selected LANDSAT single band and colour composites at 1:1,000,000 and larger scales and on Photowrite enlargements of bands 4, 5 and 7 of an area of central North Island. Substage sampling has used large scale aerial photos and maps supported by some field checking.

2.2 Enhanced Processes

These have included optical enhancement with a colour additive viewer and electronic enhancement (density slicing and colour enhancement) of selected areas on various bands to provide additional detail for comparison with photo images.

2.3 Computer Processes

Line printout maps of selected areas showing radiance values have been provided by P.E.L. for comparative mapping analyses.

3.   APPLICATION OF LANDSAT DATA

The following specific investigations have been carried out by the author and graduate students of the Department of Geography at the University of Auckland. Some of these are a continuation

of studies recorded in P.E.L., DSIR September 1976 Quarterly
Report, others are new investigations.

1. Analysis of suspended sediment patterns in the
    Firth of Thames.

2. Lake Taupo suspended sediment study: a
    preliminary report.

3. Regional and seasonal patterns of sediments
    in New Zealand coastal waters.

4. Coastal geomorphology. Analysis of sand dunes,
    Aotea Harbour, west coast North Island.

5. Applications of LANDSAT imagery for mapping
    regional geology -

    (a) Marlborough
    (b) Rotorua-Taupo

6. Comparative evaluation of enlarged Photowrite
    bands 4, 5, and 7 for landuse and land cover
    mapping.

7. Thematic mapping: Large scale mapping of vegetation
    from a LANDSAT-II image of East Taupo.

8. Thematic mapping: Landuse mapping of the Aupouri
    Peninsula, Northland from LANDSAT.

9. Thematic mapping: Vegetation mapping in Westland,
    South Island, from LANDSAT colour composites.

10. Thematic mapping: Usefulness of LANDSAT data for
    monitoring range conditions in Marlborough.

4. DISCUSSION

   As full detailed statements of each of these investigations
will be presented in the next quarterly report some general
observations only will be outlined here.

5. DIGITAL PROCESSING

   In addition to using photo interpretation and enhancement
techniques in these analyses, increasing emphasis has been placed on
evaluating detailed large scale sample patterns of selected areas
using computer printout data from LANDSAT CCTs.   Generally, the
greatly increased detail and larger scales of computer printout data
have facilitated detailed mapping in such diverse investigations
as lake sediments; stream plumes; ocean currents and thermal
fronts; exotic forest types by species and age; pasture and
lucerne; scrub types; and categories of natural vegetation.

6.   COLOUR COMPOSITES

These investigations using LANDSAT colour composite imagery, even at scales of 1:1,000,000 have demonstrated that landuse and land cover data can be obtained efficiently over large areas. Many equivalent Category II land cover classes to those outlined by Anderson et al. 1976 (U.S.G.S. Prof. Paper 364) have been recognised in widely diverse areas of New Zealand. Such imagery is even more valuable at enlarged scales especially for rapidly and efficiently updating information with a high degree of accuracy.

Unfortunately, because of the heavy demands placed upon P.E.L. in providing user-services we have not been able to have as much colour composite enlargement imagery as we would like in order to carry out a wider range of comparative evaluation.

Investigation have also indicated that ready availability of colour composite positive transparencies would provide a more useful tool for land cover and landuse mapping than either the standard colour composite positive prints or enlargements.

Our surveys suggest that the use of colour composite imagery is a relatively inexpensive technique that is highly flexible in application.

In addition to its value for mapping of agricultural landuse the utility of LANDSAT colour composite imagery enlargements for mapping vegetation is very encouraging. Many major plant associations can be recognised by their distinctive tonal signatures. Equal success has been achieved in studies from LANDSAT colour composites of Westland, Volcanic Plateau and Northland.

7.   DENSITY SLICING AND COLOUR ENHANCEMENT

These techniques have facilitated geomorphic studies greatly increasing the ability to detect (a) some differences in sand dune geomorphology and (b) to identify linears in the Marlborough region and in the Volcanic Plateau. The use of sequential imagery has been employed in the Marlborough area but not in the Taupo area as to date only one image has been available. Seasonal differences in vegetation often help demark lineaments.

A range of techniques have been employed in our suspended sediment analyses as was reported in the 1976 September Quarterly Report. These analytical procedures have been employed in new areas including studies of sedimentation in Lake Taupo, New Zealand's largest freshwater lake.